Unclassified
Security Classification

DOCUMENT CONTROL DATA - R&D

(Security classification of title, body of abstract and indexing annotation must be entered when the overall report is classified)

1. ORIGINATING ACTIVITY *(Corporate author)*
Air Force Cambridge Research Laboratories (LI)
L. G. Hanscom Field
Bedford, Massachusetts 01730

2a. REPORT SECURITY CLASSIFICATION
Unclassified

2b. GROUP

3. REPORT TITLE
A SURVEY OF SCINTILLATION DATA AND ITS RELATIONSHIP TO SATELLITE COMMUNICATIONS

4. DESCRIPTIVE NOTES *(Type of report and inclusive dates)*
Scientific. Interim.

5. AUTHOR(S) *(First name, middle initial, last name)*
Jules Aarons, Editor

6. REPORT DATE	7a. TOTAL NO. OF PAGES	7b. NO. OF REFS
January 1970	117	251

8a. CONTRACT OR GRANT NO.		9a. ORIGINATOR'S REPORT NUMBER(S)
b. PROJECT, TASK, WORK UNIT NOS.	4643-01-01	AFCRL-70-0053
c. DOD ELEMENT	62101F	9b. OTHER REPORT NO(S) *(Any other numbers that may be assigned this report)*
d. DOD SUBELEMENT	681000	Special Reports, No. 106

10. DISTRIBUTION STATEMENT
1—This document has been approved for public release and sale; its distribution is unlimited.

11. SUPPLEMENTARY NOTES	12. SPONSORING MILITARY ACTIVITY
TECH, OTHER	Air Force Cambridge Research Laboratories (LI) L. G. Hanscom Field Bedford, Massachusetts 01730

13. ABSTRACT

In order to provide a state-of-the-art survey of amplitude fluctuations produced by irregularities at F-layer heights in the ionosphere, a survey and review of scintillation phenomena has been produced. The survey starts with a definition of scintillation index and a means of characterizing the effect of the amplitude fluctuations on transmissions from a satellite beacon. Various mechanisms proposed for the origin of the irregularity structure are reviewed in light of the observations. The translation of the geophysical information into engineering terms is made so that both depth of fade as a function of latitude and fading rate can be determined; these in turn are used to determine percentage of time scintillations will be a problem at various locations. Characteristics of scintillation dictate modulation systems to be specified for communication and navigation systems employing synchronous satellite beacons at VHF and UHF. Specific problems are addressed. These include low angle or tropospheric scintillations, polar observations, and equatorial irregularities. Variations of scintillation index with magnetic index, angle of elevation, and frequency in these regions as well as middle latitude areas are given. Another atmospheric effect on satellite transmissions is discussed in the final chapter, that is, propagation delays of VHF waves produced by the time delay of radio waves traversing the ionosphere.

DD FORM 1 NOV 65 1473

Unclassified
Security Classification

14. KEY WORDS	LINK A		LINK B		LINK C	
	ROLE	WT	ROLE	WT	ROLE	WT
Satellite communications Air traffic control VHF/UHF communication Scintillation Low latitude nocturnal fading Auroral propagation Transionospheric radar range errors						

AFCRL-70-0053
JANUARY 1970
SPECIAL REPORTS, NO. 106

AIR FORCE CAMBRIDGE RESEARCH LABORATORIES
L. G. HANSCOM FIELD, BEDFORD, MASSACHUSETTS

A Survey of Scintillation Data and Its Relationship to Satellite Communications

Editor
JULES AARONS

United States Air Force

AFCRL-70-0053
JANUARY 1970
SPECIAL REPORTS, NO. 106

IONOSPHERIC PHYSICS LABORATORY PROJECT 4643

AIR FORCE CAMBRIDGE RESEARCH LABORATORIES

L. G. HANSCOM FIELD, BEDFORD, MASSACHUSETTS

A Survey of Scintillation Data and Its Relationship to Satellite Communications

Editor

JULES AARONS

These papers were originally published by North Atlantic Treaty Organization Advisory Group for Aerospace Research and Development as AGARD Report 571, August 1969.

United States Air Force

Abstract

In order to provide a state-of-the-art survey of amplitude fluctuations produced by irregularities at F-layer heights in the ionosphere, a survey and review of scintillation phenomena has been produced. The survey starts with a definition of scintillation index and a means of characterizing the effect of the amplitude fluctuations on transmissions from a satellite beacon. Various mechanisms proposed for the origin of the irregularity structure are reviewed in light of the observations. The translation of the geophysical information into engineering terms is made so that both depth of fade as a function of latitude and fading rate can be determined; these in turn are used to determine percentage of time scintillations will be a problem at various locations. Characteristics of scintillation dictate modulation systems to be specified for communication and navigation systems employing synchronous satellite beacons at VHF and UHF. Specific problems are addressed. These include low angle or tropospheric scintillations, polar observations, and equatorial irregularities. Variations of scintillation index with magnetic index, angle of elevation, and frequency in these regions as well as middle latitude areas are given. Another atmospheric effect on satellite transmissions is discussed in the final chapter, that is, propagation delays of VHF waves produced by the time delay of radio waves traversing the ionosphere.

Contents

A SURVEY OF SCINTILLATION DATA AND ITS RELATIONSHIP TO SATELLITE COMMUNICATIONS

VHF Atmospheric Studies and Communications and Navigation Systems

John P. Mullen

1. INTRODUCTION

The first observations made of radio stars in Great Britain showed that the discrete sources fluctuated in amplitude. In order to determine whether the source amplitude changed, or the intervening atmosphere modulated the signal, an experiment was set up to correlate the fluctuations at greatly distant observatories. The fluctuations were not correlated and therefore the atmosphere was assumed to be the modulating source.

Atmospheric physicists have been studying ionospheric and tropospheric irregularities with the trans-atmospheric technique since World War II. The first studies used radio stars; subsequent studies used low altitude satellites ranging from Sputniks to the S-66; the present studies have added synchronous satellites to their observational objects.

Scintillation studies oriented towards applications expect to provide information of trans-ionospheric propagation that is of direct and immediate use to designers of aircraft systems which are to be operational in the early and mid-1970 period. While the emphasis has been primarily on commercial air transportation, the work is equally applicable to military systems, which normally advance in parallel channels.

(Received for publication 5 January 1970)

2. SATELLITE COMMUNICATION (VHF)

Perhaps the most representative aircraft control problem today is the transatlantic passenger and freight system. Between 1968 and 1971, the number of passengers crossing the North Atlantic will approximately double. Assuming the same logarithmic growth rate to continue, one observes that it will do so again by 1974. The advent of the supersonic aircraft and the giant air bus is likely to increase the growth rate in a quantitatively unpredictable manner. In any event, the number of transatlantic passengers will continue to increase, and the number of aircraft using the finite airspace will likewise.

At the present time, transatlantic aircraft fly along four or five tracks which are separated by 120 nautical miles. Along a track, aircraft are spaced 15 to 20 minutes apart, and 2000 feet in altitude between 29,000 and 41,000 feet. Navigation is accomplished by on-board devices, aided by high-frequency radio when out of line of sight, and VHF or UHF radio when within range of a traffic control station. Approximately a half dozen position reports are required during the transatlantic flight. This system is operable today and works satisfactorily at today's loads. However, it is clearly obsolescent and estimates of its breaking point vary.

Several satellite-based air traffic control systems are now in advanced design. These use VHF or UHF, or combinations of the two. While there is little question of the technical superiority of UHF systems over VHF systems, at least insofar as ionospheric propagation is concerned, there is a huge investment in VHF equipment. It is for this reason that the study of VHF trans-ionospheric propagation has great practical impact on the air traffic control operation in the early 1970 time period.

Considering briefly the propagation problems of a VHF satellite aircraft communications systems, one can group them into the single over-all category of signal fading, and this into two general subgroups: fading caused by polarization rotation and fading caused by irregular diffraction. The first can be alleviated by the use of circular polarization, whereas the second requires increased power and redundancy. Furthermore, transmission or reception of circular polarization over a wide angle is not always easy to accomplish, since true circular polarization exists only along the pointing axis of the circularly polarized antennas.

Both of these fading mechanisms produce reduction of signal level and thus reduce communications efficiency. The depth of fading has been observed to be as high as 20 decibels, and the fading rate up to 20 fades per minute. The two geographic regions most subject to scintillation are the polar and equatorial areas, both sharing the concurrent appearance of maximum depth and rate of fading.

3. SATELLITE NAVIGATION

At present, all navigation is performed on board, with an occasional radar fix from a surface ship. Currently accepted statistics, used to generate a tolerable collision probability of 10^{-7}, are based upon a deviation from planned position of 45 nautical miles 0.5 percent of the time and 60 nautical miles 0.05 percent of the time, using a track separation of 120 nautical miles. If on-board navigation were improved or supplemented by other methods, the same collision probability would be obtained with a smaller track separation. Not only would this increase capacity by adding tracks, but it would also tend to permit more nearly optimal tracks, since only one of the present tracks is optimal from the point of view of fuel consumption. The other three or four pay a fuel penalty of an estimated $200 for each additional 120-mile offset from the optimal.

One system, based upon VHF tone ranging using geostationary satellites (Anderson, 1968) would provide 90-mile spacing. Here another ionospheric phenomenon becomes important, namely, the large variation in total electron content which results in variations in the group velocity of a transmitted signal. These provide range uncertainties up to about a mile, depending on zenith angle and time of day. This error is not inconsiderable when added to the other uncertainties inherent in a trans-ionospheric ranging system.

References

Anderson, E. (1968) Transatlantic air traffic control using satellites, IEEE, Eastcon 1968 Record.

The Definition of Scintillation Index and Its Use for Characterizing Ionospheric Effects

Herbert E. Whitney

1. INTRODUCTION

Studying the effects of ionospheric irregularities often involves measuring the amplitude and phase variations imposed on a signal as it traverses the ionosphere. Many workers have used signals from radio stars and satellites to record the changes in amplitude known as scintillations. Several measures are used to characterize the depth of scintillations; each of the measures is called a scintillation index (SI).

At the 1966 COSPAR Meeting, the Radio Astronomy Branch of AFCRL was requested to propose an index for measuring ionospheric scintillations. A proposed index, together with the results of an experimental study on the determination and use of this index, was reported at the 1967 and 1968 COSPAR Meetings. The results of this effort are summarized in the following report.

One measure for a scintillation index is the use of a scale from 0 to 5. By visual inspection, without actual measurement, a value is assigned to the record. Other ways involve scaling the deviation of the signal amplitude from the mean amplitude. Four measures are thus possible, depending on whether mean deviation or root-mean-square deviation is used and whether the record is proportional to voltage or power. If the probability distribution of the amplitude deviation is known, it is possible to relate the four measures of scintillation index (Briggs and Parkin, 1963).

While it is difficult to relate these measures theoretically because the probability distribution of the amplitude deviation is not in general known, experimental comparisons show that they are proportional to each other and empirical relations of the various possible indices are shown in Table 1. The relationships and additional considerations are given in the cited reference.

Table 1. Definition of Scintillation Indices*

$S_1 = \frac{1}{\bar{R}} \overline{(R-\bar{R})}$	$S_2 = \frac{1}{\bar{R}} \left[\overline{(R-\bar{R})^2}\right]^{\frac{1}{2}}$	$S_3 = \frac{1}{\bar{R}^2} \left(\overline{R^2-\bar{R}^2}\right)$	$S_4 = \frac{1}{\bar{R}^2} \left[\overline{\left(R^2-\bar{R}^2\right)^2}\right]^{\frac{1}{2}}$
$= 0.42\ S_4$	$= 0.52\ S_4$	$= 0.73\ S_4$	

*R is the instantaneous amplitude of the wave [after Briggs and Parkin, J. Atmos. Terr. Phys. 25, 339 (1963)].

However, in most cases, only a relative measure of scintillation index is required. For a statistical analysis that involves a long period of time, such as a study of the seasonal dependence of scintillations, it is important that a standard method of data scaling be used. The notation that has been adopted by AFCRL and the JSSG (Joint Satellite Studies Group) is:

$$\text{Scintillation Index} = \frac{P_{max} - P_{min}}{P_{max} + P_{min}} .$$

This relationship was developed specifically for scaling from strip chart records. An arbitrary rule is used for the selection of P_{max} and P_{min}, that is, P_{max} is the power amplitude of the third peak down from the maximum excursion, and P_{min} is the power amplitude of the third level up from the minimum excursion. It is realized that this definition offers little help toward understanding the relationship between properties of irregularities and effects on wave propagation, but it does result in a standard method of scaling which will help comparison of scintillation analysis between various workers.

The use of this expression is demonstrated in Figure 1. The chart record is calibrated in dBm which is converted to relative power levels for calculation of SI. Over the period 1345 to 1350 UT, an index of 94 percent is obtained.

However, even though only relative values are usually required in a study of ionospheric scintillations, problems do arise in the comparison of data taken by various workers. Some measures of SI may have been scaled from chart divisions rather than by use of an accurate calibration. The SI scaled from the chart divisions under an assumption that the chart display is either linear in power or voltage

can lead to errors; in reality the chart amplitude could be somewhere in between, because it depends on the law of the receiver detector. Also, statistics on satellite scintillations may be in the form of a voltage-index distribution based on a voltage calibration.

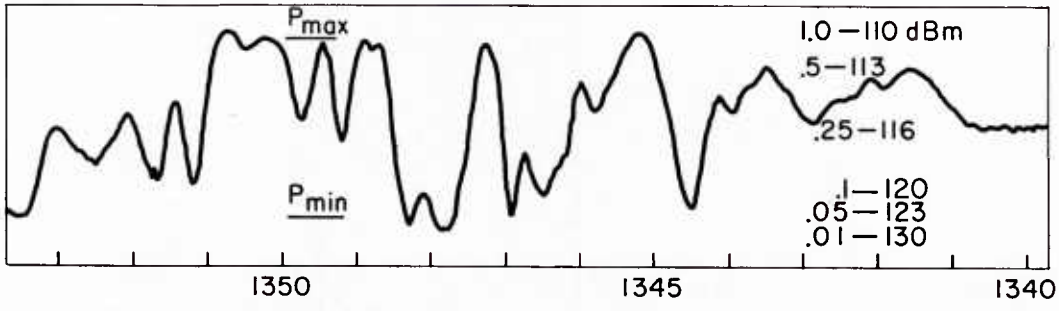

Figure 1. 136-MHz Scintillations From the Canary Bird Synchronous Satellite - 12 July 1967

$$SI = \frac{P_{max} - P_{min}}{P_{max} + P_{min}} = 94\%.$$

For comparison of data, it is useful to have a conversion relationship between power index, $SI_{(p)}$, and voltage index, $SI_{(v)}$. If data were obtained from a receiver with AGC and the slope of the detector curve is known, scintillation index values based on chart divisions can be converted for comparison on a $SI_{(p)}$ basis.

Because of the emphasis on relating statistics on ionospheric scintillations to the problems of communication engineers, the following method was developed for converting data to a common base, $SI_{(p)}$. The amount that a signal fades, important to communication engineers, is related to scintillation index by the following:

$$\text{Signal fades (dB)} = 10 \log \left[1 - SI_{(p)}\right] = 20 \log \left[1 - SI_{(v)}\right].$$

For example, if $SI_{(p)} = 0.5 = 50$ percent, then the signal fade is 3 dB.

Since the signal fade in dB would be the same on either a linear power or linear voltage display, the relationship is formed:

$$SI_{(p)} = 2\, SI_{(v)} - SI_{(v)}^2 .$$

This conversion method can be extended to cover receivers that are not linear with input power or voltage, such as a receiver with AGC, but do have a constant slope to the detector curve over the fading range, by the following:

$$SI_{(p)} = 1 - \left[1 - SI_{(x)}\right]^{x},$$

where $SI_{(x)}$ is the scintillation index measured in chart divisions with a receiver that has a detector law exponent of x.

2. EXPERIMENTAL RESULTS

To determine the accuracy of the described method for converting SI values to a common base, the following experiment was made. Three R-390 Collins receivers were gain adjusted so that a 40-MHz satellite signal received on a common antenna and a common frequency converter, whose output had been equally divided into three parts, would detect the identical signal in three different modes: linear power mode, linear voltage mode, and the AGC mode, corresponding to square law detection, linear detection, and logarithmic detection with a law of 4.5. As shown in Figure 2, the detector characteristics of each receiver had been carefully measured to determine over what signal range the receivers would be essentially linear with power, or voltage, or maintain a constant detector law.

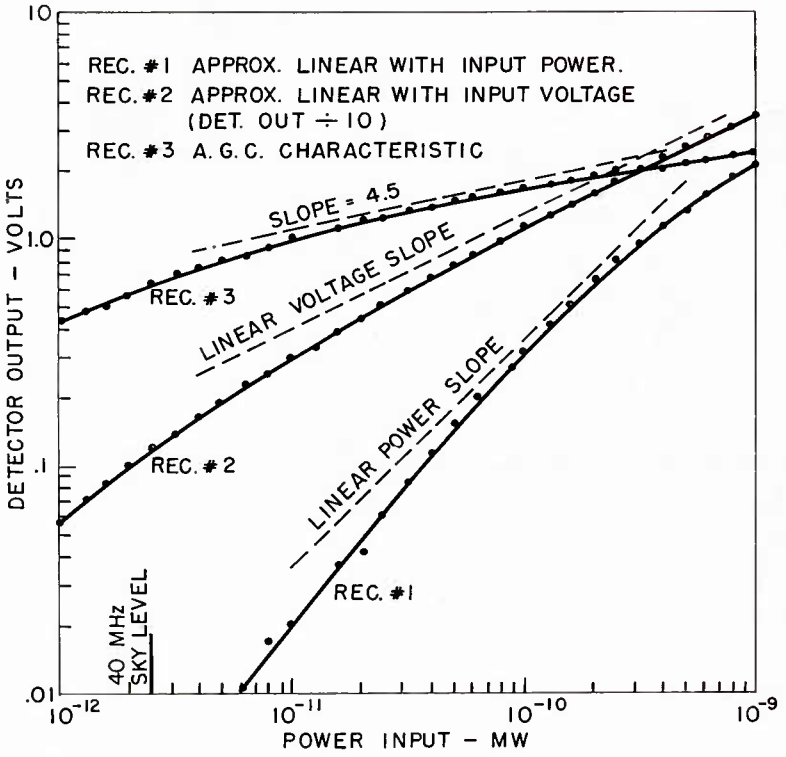

Figure 2. Detector Characteristic of 3 R-390 Receivers

Scintillation index was measured from the chart display using corresponding signal excursions for each of the three modes of receiver detection. Scintillation index was computed based on an accurate power calibration and also scaled from the deflections measured in chart divisions. When SI was measured by means of the signal generator power calibration, values for all three modes had a linear relationship to each other and agreed within 5 percent. Scaling SI from chart divisions resulted in the comparisons shown in Figures 3 and 4. The solid curves represent the

relationship $SI_{(p)} = 2\,SI_{(v)} - SI^2_{(v)}$ for the linear voltage comparison and $SI_{(p)} = 1 - \left[1 - SI_{(AGC)}\right]^{4,5}$ for the AGC comparison; the experimental points follow quite closely the stated relationships.

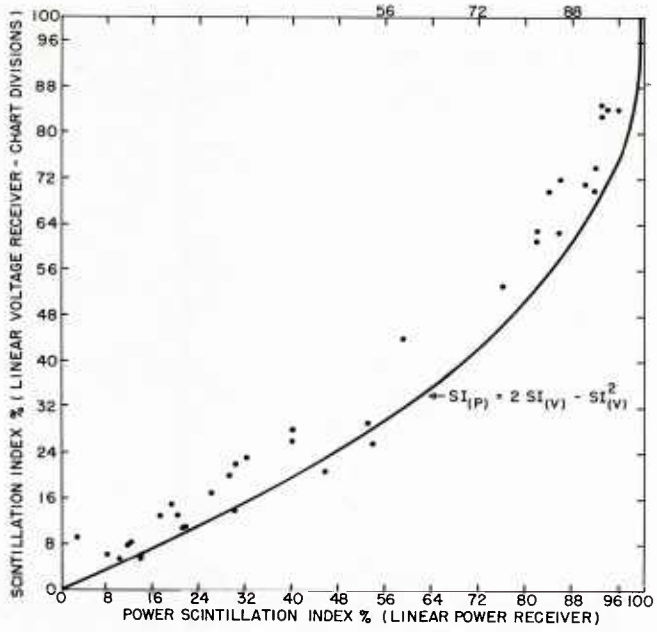

Figure 3. Measured Values of Scintillation Index From Linear Voltage Receiver vs Measured Values of Scintillation Index From Linear Power Receiver. Chart division calibration for linear voltage receiver. Power calibration for linear power receiver

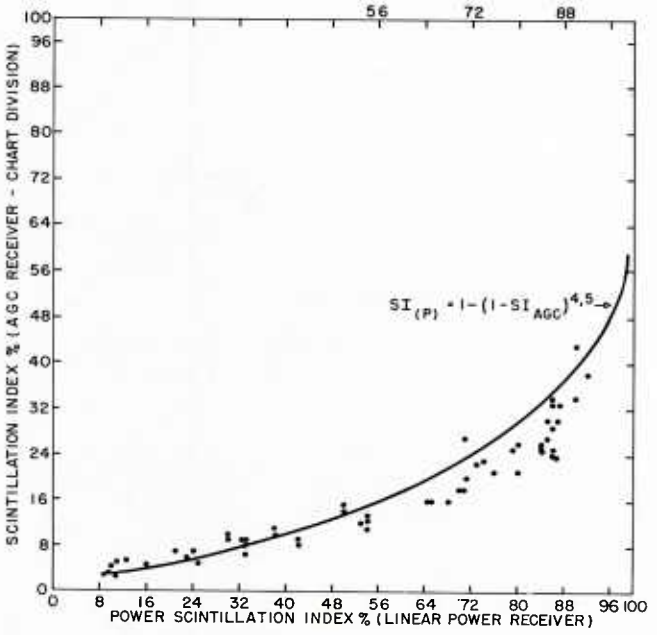

Figure 4. Measured Values of Scintillation Index From Receiver With AGC Characteristic vs Measured Values of Scintillation Index From Linear Power Receiver. Chart division calibration for AGC receiver. Power calibration for linear power receiver

3. SIMPLIFIED METHOD OF SCALING SCINTILLATION INDEX

Because statistical studies involve the scaling of many readings of SI, a conversion between $P_{max} - P_{min}$ and SI was computed. Figure 5 shows the relationship that can be used for simplifying the measurement of SI when a calibration of the chart is made in relative decibel levels. The conversion graph was determined by assuming equal percentage changes of P_{max} and P_{min} from the average level, changing these values to a decibel change and then summing them for the total decibel change.

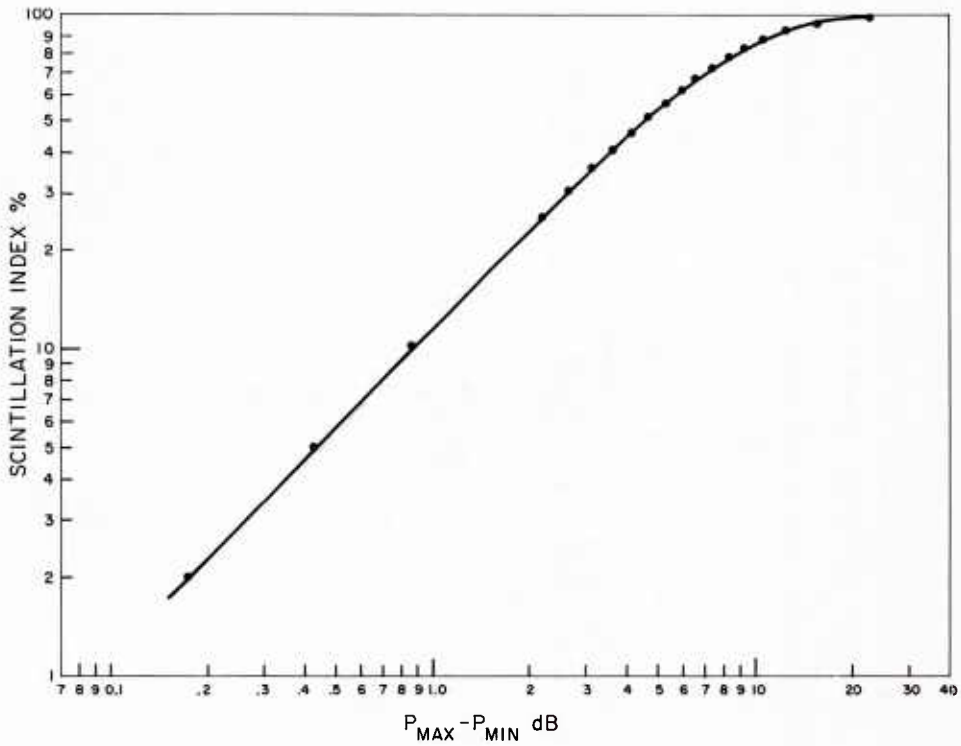

Figure 5. Graph for the Conversion of $P_{max} - P_{min}$ to Scintillation Index. $P_{max} - P_{min}$ is the peak-to-peak excursion of a scintillating signal, and is measured in decibels based on an amplitude calibration of the chart record

The accuracy of the simplified method was checked against a machine computation of SI using a chart record of S-66. Figure 6 shows that adequate accuracy is obtained when using the conversion relationship from Figure 5. The method was also checked at smaller and greater average signal levels with the same results.

If the simplified method is to be applied for analysis where there is a small signal-to-noise ratio and the deflection on the chart due to the sky background temperature is appreciable compared to the signal, then the receiver calibration must be correctly applied so that only the deflections from the signal are being measured.

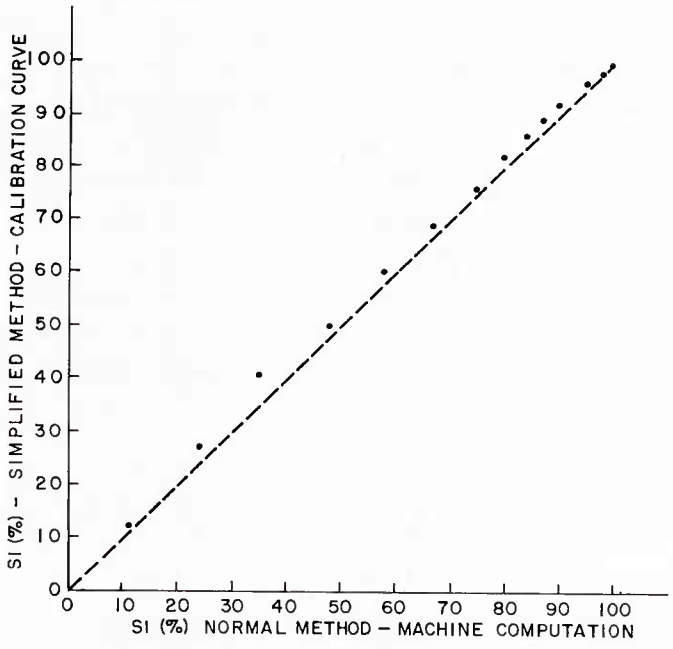

Figure 6. Comparison of Scintillation Index Measurements. SI measured directly from calibration and conversion curve vs SI measured with machine computation of $\frac{P_{max} - P_{min}}{P_{max} + P_{min}}$ (Medium signal case-average level approximately $\frac{1}{2}$ chart width 20-30 mm)

4. CONCLUSIONS

In summary, it is felt that only a relative measure of scintillation index is necessary to describe amplitude fluctuations caused by ionospheric irregularities, and that the simple measure

$$SI = \frac{P_{max} - P_{min}}{P_{max} + P_{min}}$$

defined earlier, should be used. To obtain the best accuracy when comparing scintillation data, the records should be precisely calibrated on a power base. If scintillation index is scaled from chart divisions and the law of the detector is known, the index values can be converted to a power base with a small decrease in accuracy as compared to scaling from a signal generator calibration. Comparison of data without the benefit of a calibration or knowledge of the detector characteristic can lead to errors of a factor of 2 or more. The simplified method of scaling SI using a conversion of $P_{max} - P_{min}$ (dB) to SI gives adequate accuracy for statistical studies.

Since communication engineers are concerned with the percentage of time that the signal drops below the average level, a simple empirical index is not sufficient to characterize the fading of the signal and determine the reliability of a communications system. In lieu of the simple empirical index for characterizing ionospheric scintillations as described, a detailed analysis by computer can be accomplished to

obtain an amplitude distribution as was done by the Communications Satellite Corporation (COMSAT). Canary Bird strip chart data which covered 1745 hours during the period May to August 1967 were provided to COMSAT for this type of analysis. The strip charts were digitized at about a one-second sampling rate which is sufficiently high for reproduction of the fastest scintillations. The resulting IBM cards (or magnetic tape) were then processed to give the amplitude distribution as shown in Figure 7. It shows that about 1 percent of the total time the signal was more than 4 dB below the normal level. Figure 8 is the distribution of the duration of fades due to ionospheric scintillation. In the period of May 11 to August 9, 1967, 6155 cases of 3 dB and 2507 cases of 6 dB fades were counted. Forty percent of the 3 dB and 65 percent of the 6 dB fades lasted for less than 10 seconds.

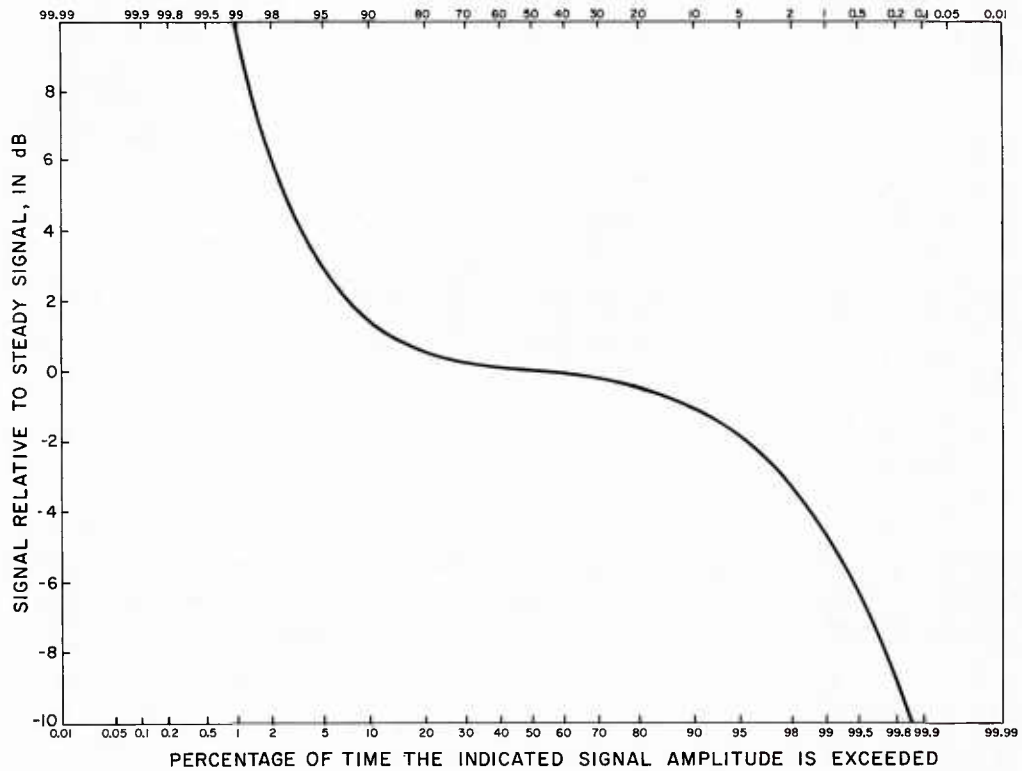

Figure 7. Ionospheric Scintillation of Intelsat II, F-3, VHF Signal, Representing 1745 Hours of All Data From May 11, 1967 to August 9, 1967

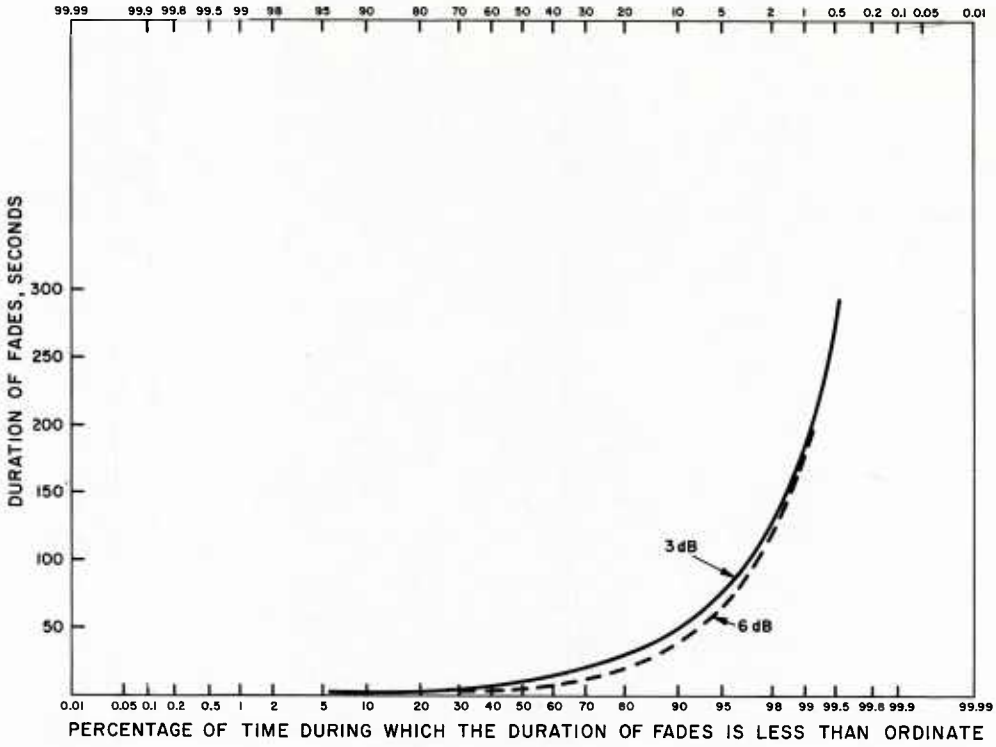

Figure 8. Distribution of Duration of 3 dB and 6 dB Fades Due to Ionospheric Scintillation of Intelsat II, F-3, VHF Signal From May 11, 1967 to August 9, 1967. Fades recorded: 6155 of 3 dB and 2507 of 6 dB

References

Briggs, B.H. and Parkin, I.A. (1963) On the variation of radio star and satellite scintillation with zenith angle, J. Atmos. Terr. Phys. 25:339-365.

Appendix A

Proposal For a Logarithmic Scintillation Index to be Applied to Satellite Radio Signals*

The Real Time Telemetry Panel of COSPAR WGII at its Tokyo meeting considered four papers in which methods are described to determine scintillation indices, their relevant merits and practical use. After discussion the panel came to the following conclusions:

(1) One should have a basic strict definition which compares easily with the known parameters of possible statistical distributions.

(2) The definition to be adopted should cover amplitude as well as power measurements. If different from indices used before this time, the new index system should be clearly distinguished from the older one.

(3) On a trial basis a logarithmic system indicating decibels below a level of maximum scintillation is proposed. It uses, essentially, the ratio of a standard deviation, σ, to the mean value, m, for a given sample, or the sum of several samples, covering an appropriate time interval. The defining formulae are (the bar indicating a mean):

$$S_L = -20 \log_{10} (\sigma/m)_{|\overline{A}|}$$

*The matter of defining a scintillation index was the subject of discussion of the RTT Panel at the 1968 COSPAR Meeting. This proposal is cited from URSI Information Bulletin No. 168, September 1968.

with

$$(\sigma/m)^2_{|\overline{A}|} = \overline{(A - \overline{A})^2}/\overline{A^2} ,$$

A being the instantaneous amplitude value (proportional to the field strength at the antenna).

(4) Experimental procedures to be applied should try to satisfy the above definition to a reasonable approximation, so that it can easily be used at stations. It is understood that, in this regard, one may replace

$$(\sigma/m)^2_{|\overline{A}|} \text{ by } \left(\overline{A}^2/\overline{A}^2\right) - 1$$

in case of amplitude determination, or by

$$\left(\overline{P}/\overline{p^{\frac{1}{2}}}^2\right) - 1$$

in case of power determination where $p = P^{\frac{1}{2}}$.

(5) The total sampling time should, on the one hand, be long enough so that the index is stationary but, on the other hand, practical limitations may preclude an upper limit, for example in the presence of Faraday fading.

(6) Standard, artificially produced scintillation records should be procured, exactly calibrated, and made available to all interested stations by the undersigned.

Professor K. Rawer

References

The papers by K. Bischoff and B. Chytil; Ch. Munther; V. Cappelini, P. Checcacci, and M. deGiorgio; H. Whitney, C. Malik, and J. Aarons are to be published in Planetary and Space Science, 1969, Vol. 1.

Appendix B

Definition of Scintillation Index*

In a recent discussion (COSPAR, 1968) the need arose of defining a scintillation index. This definition must be rigorous and unique so that no ambiguity exists in the computation of this index by different experimenters using amplitude or power measurements of the incoming signal.

A scintillated received signal resulting in crossing a time varying medium by a wave of constant amplitude possesses over a certain time interval Δt a mean power $<P>$, and a mean average amplitude $<a>$ being P and a the instantaneous power or amplitude and $<>$ indicating an averaging over the interval Δt. We wish to point out that the average power $<P>$ does not coincide in general with the received power in the absence of scintillation. An averaged power proportional to $<a>^2$ corresponds to the received average amplitude $<a>$ and can be thought as the power associated to an imperturbated signal. Hence $<P> - <a>^2$ will represent the power associated to a random noise-like signal due to the scintillation superimposed to the constant amplitude signal $<a>$.

In view of this statement the SI can be derived from the N/S power ratio where the noise power is represented by the power of the random signal $<a^2> - <a>^2$ and the signal power by $<a>^2$. Hence

---

*URSI Information Bulletin No. 168

$$SI = \frac{\langle a^2 \rangle - \langle a \rangle^2}{\langle a \rangle^2} = \frac{\langle (a - \langle a \rangle)^2 \rangle}{\langle a \rangle^2} = \frac{\langle P \rangle - \langle P^{\frac{1}{2}} \rangle^2}{\langle P^{\frac{1}{2}} \rangle^2} .$$

This scintillation index corresponds to the square of S_2 as defined by Briggs and Parkin (1963) and gives a unique value of SI whichever be the used power or amplitude measurements for the computations.

dB units can also be used by putting

$$20 \lg \frac{\left(\langle a^2 \rangle - \langle a \rangle^2\right)^{\frac{1}{2}}}{\langle a \rangle} = 20 \lg S_2$$

$$SI = 10 \lg \frac{\langle P \rangle - \langle P^{\frac{1}{2}} \rangle^2}{\langle P^{\frac{1}{2}} \rangle^2} = 10 \lg S_2^{\,2} .$$

In these units - ∞ dB correspond to the absence of scintillation and 0 dB corresponds to complete scintillation. Due to their physical meaning (N/S power ratio) the above definitions are most significant both for the study of the medium properties as well as for the communication engineering. However, the definition must specify also the interval Δt. This is especially true for a short time interval Δt.

P.F. Checcacci
Centro Microonde del C.N.R.
Florence, Italy

References

Open Meeting of the Real Time Transmission Panel of W.G. No. 2, COSPAR Meeting, Tokyo, May 1968.

Briggs, B.H. and Parkin, I.A. (1963) J. Atmos. Terr. Phys. 29:1175.

Summary of Properties of F-Region Irregularities

Terence J. Elkins

1. INTRODUCTION

The subject of F-region irregularities has always been of great interest in ionospheric research, both from a practical and a theoretical viewpoint. An understanding of the irregularity morphology is essential to the efficient use of the F-region as a communications medium, a factor which has led to a long and sustained study of the phenomenon of spread-F and other manifestations of irregular F-region structure. On the theoretical side, the presence of inhomogeneities in the F-region poses several fundamental problems. The kinematic viscosity of the ionosphere is sufficiently great to inhibit strongly the type of irregularity structure found in the lower atmosphere. Furthermore, the earth's magnetic field, acting on the ionized constituents of the F-region, introduces an additional strong damping effect, so that dynamic irregularities, in the conventional fluid dynamics sense, cannot form in this region.

Yet a great variety of observational evidence exists, which shows that strong density irregularities actually are present in the F-region, over a wide range of spatial and temporal scales. The explanation for their formation and their dynamic characteristics is largely unfamiliar to the classical fluid-dynamicist, or meteorologist, and is to be found in terms of electrodynamics and plasma physics. The upper ionosphere is dominated by electrodynamic forces and ambipolar diffusion,

whereas electrochemical processes exercise an important control over the spatial and temporal variations of its constituents. Many or most of the properties of F-region inhomogeneity can be understood in the light of these few remarks.

In this chapter, a summary will be presented of the present knowledge of the morphology of F-region irregularities, and of the various theories which have been proposed to account for it. Emphasis is placed on the fact that one cannot study irregularities in isolation, that is, without consideration for the properties of the background F-region itself. This observation helps to create some degree of order, in classifying the properties of irregularities, and provides useful clues in the search for likely generation mechanisms. Thus begins a very brief review of the dynamics of the F-region itself, that is, to the extent that this subject is presently understood.

2. GENERAL CHARACTERISTICS OF IONOSPHERIC STRUCTURE

A great many ionospheric and geomagnetic parameters display geographical characteristics that suggest the division of the earth into three main latitude zones. Although such a division may appear somewhat arbitrary, it does have some physical significance, especially in regard to the dominant physical processes at work in the ionospheric dynamics. For most purposes, the geomagnetic latitudes ± 20° will be taken as defining the boundaries of the equatorial zone, whereas the polar zones lie between ± 65° and the respective magnetic pole. The intervening zones, between 20° and 65°, will be referred to simply as the medium latitude or temperate zone. We note that, if the top of the ionosphere is somewhat arbitrarily set at one-tenth of the earth's radius, the boundaries of the equatorial zone define the region in which magnetic field lines are confined within the ionosphere. The temperate region is characterized by interconnection, through the magnetosphere, of conjugate magnetic points on the earth's surface. In the polar regions, the magnetic field lines extend into the magnetospheric tail, and may be connected into the interplanetary magnetic field. This behavior of the magnetic field is, to a large extent, responsible for the rather profound differences in the ionospheric properties between the various regions.

3. EQUATORIAL REGION

The equatorial ionosphere appears to be dominated by electromagnetic drift, driven by the S_q current system, which, in turn is set up by the thermal and gravitational atmospheric tides. That electromagnetic forces are predominant is clearly indicated by the fact that many ionospheric parameters, such as the equatorial

anomaly (Appleton, 1946; Rastogi, 1959) and spread-F (Singleton, 1960) are functions of geomagnetic, rather than geographic latitude. The study of the effects of lunar tidal perturbations upon the F-region (Rastogi, 1963; Kotadia, 1962) shows clear evidence that tidal motions in the lower, denser atmosphere have an important influence on the upper levels, even though direct tidal motions are to all appearances strongly damped there. Bramley and Peart (1965) put forward a theory of ionization balance, in the equatorial F-region, which accounted for the equatorial anomaly -- the persistent minimum in F-region electron density (King, 1968) observed between $\pm 20°$ geomagnetic latitude. In this model, electromagnetic drift forces electrons upwards above the equator, and they subsequently diffuse downwards along the magnetic field lines, which terminate at higher latitudes. These electromagnetic forces are at a maximum during the daytime, when the equatorial electrojet is at its maximum intensity. At night, this highly concentrated current system is greatly diminished, and the equatorial anomaly is far less in evidence. As a result of the more rapid attachment processes at the lower levels, the F-layer appears to drift upwards, and to some extent coincident with this, irregularities are observed by means of bottomside soundings.

Martyn (1959) was the first to put forward a mechanism of irregularity enhancement accompanying this upward drift; this theory has received considerable attention in subsequent years (Clemmow and Johnson, 1959; Piddington, 1964). Regardless of the precise details of this enhancement process, the theory encounters considerable difficulties from a purely observational standpoint. In the first place, the advent of topside satellite soundings showed that irregularities were present above the F_2 peak, whether the layer was moving upwards or downwards (Calvert and Schmid, 1964; Lockwood and Petrie, 1963). These irregularities apparently consist of field aligned ducts or sheets of ionization, and are also observed in total electron content measurements during the day (Mass and Houminer, 1967). Furthermore, Rao (1966) determined, from bottomside soundings, that there is a delay of 1 to 3 hours between the upward layer movement, and the onset of spread-F, whereas the spread-F persists for several hours after the layer has begun to descend. Thus, it is apparent that, whatever the merits of Martyn's proposed amplification theory, it does not answer the questions relating to the origin of the irregularities. It seems more likely that the irregular structure exists continuously at the upper levels, where diffusive equilibrium prevails, and that, at lower levels, production and attachment terms dominate the continuity equation. As Piddington (1964) shows, the flux divergence in the F-region is determined by the electron density gradient in the direction of the drift velocity. If such gradients are small, as for a Chapman-like layer (horizontally stratified), no appreciable irregularity formation will take place. When the layer moves upwards after sunset, the already existing field aligned structure is rendered accessible to bottomside sounders.

Geomagnetic activity is known to inhibit upward layer movement, and consequently, spread-F observations, in the equatorial region (Goldberg et al., 1963; Lyon et al., 1960). This again is apparently a manifestation of electrodynamic forces, probably of magnetospheric origin, which oppose the layer motion. However, it may also be related to an electron production at lower levels, possibly caused by direct precipitation from the magnetosphere. There seems to be indirect evidence for this process in the red line airglow observations of various workers. Dalgarno and Walker (1964) have presented arguments to indicate that the 6300 Å emission line could be at least partly due to hot electron excitation, or impact ionization by fast electrons. Observations do not explain all of the red line intensity as being due to dissociation and recombination. For example, Carman and Kilfoyle (1963) have shown a correlation between red line intensity and charged particle influx, as well as a positive correlation between f_oF_2 and red line intensity, instead of the negative correlation required by the recombination hypothesis. Van Zandt et al. (1965) observed "fingers" of airglow enhancement extending across the equator, with a lifetime of 2 to 3 hours, and spaced ~ 200 km apart. Greenspan (1966), and Davis and Smith (1965) observed a latitude variation of red line intensity which maximized at ± 20° geomagnetic latitude, with peak intensities before midnight. These observations may indicate the presence of an electron flux which, due to enhancement during a magnetic disturbance, can effectively inhibit the rise of the F-layer. The 2 to 3-hour lifetime of the red arcs reported by Van Zandt et al. seems significant. Duncan (1960) showed that the ionization which is lifted above the equator would take about two hours to diffuse downwards to the transition zone at 20° latitude. Rao (1966) experimentally verified that there is a two-hour delay between upward layer motions at the equator, and F-regions electron density enhancements in the transition zone. Thus it seems likely that this electron transfer takes place along field aligned striations, with a typical longitudinal separation of some 200 km.

4. MEDIUM LATITUDE REGION

The ionosphere at medium latitudes is very stable by comparison with both the equatorial and polar regions. Although electrodynamic forces still play an important role in the F-region morphology in temperate regions, the overwhelming influence of the electrojets is not in evidence, nor are the tidal driving forces anywhere near as important as in the equatorial region. In contrast to the situation at high latitudes, the interconnection, through the magnetosphere, of magnetically conjugate regions is of great importance, although its role is different to that at low latitudes. In many ways, despite the relative stability of the temperate regions, the F-region behavior in these parts is probably more complex than at high or low latitudes. This is due to the substantial weakening of electrodynamic forces, which,

as a result, become comparable to the direct solar effect. This is clearly illustrated, for example, in the topside sounder data of Nelms (1966) which showed a stable F-region plateau, in the summer hemisphere, the latitude extent of which bears a direct relationship to the latitude differences between the geomagnetic equator and the subsolar latitude.

Eyfrig (1963) showed that a strong magnetic declination influence is present at medium latitudes, and Sayers (1965) has derived a rather complex spatial distribution of ionization in the topside ionosphere. These longitudinal effects are compounded by other latitudinal effects which increase in importance as the transition regions with the other two zones are approached. Despite the complexity of this region, some features exhibit reasonable symmetry in geomagnetic coordinates. One of these is precipitation, from the magnetosphere, of low energy electrons, which appears to be an important source of ionization in the temperate F-region, as elsewhere. There exists considerable evidence to support the view that this precipitation is brought about by the influence of those electric fields, in the highly conducting E-region, which drive the world-wide S_q and DS current systems.

Martyn (1955) deduced that a meridional electric field is set up by dynamo action, causing a horizontal ionization drift in the F-region, which is a function of both latitude and longitude. For the magnitude of the zonal drift velocity, Martyn gave

$$V = \frac{27}{H_z} \sin\theta\,(1 - 3\cos^2\theta)\cos\phi\,,$$

where V is measured in meters per second, θ is the colatitude, ϕ the longitude, measured Eastwards from the midnight meridian, and H_z the vertical component of the magnetic field intensity. This velocity distribution shows maximum values at low latitudes, and at 60° latitude, with a reversal at 35° latitude. However, if the real world-wide current system is considered, there is considerable asymmetry between magnetically conjugate regions, with the result that an electrostatic potential difference may be set up along a field line. Catchpoole (1967) has computed the effect of such dynamo-established potential differences in causing electron precipitation from the magnetosphere. His calculations show that there are zones of enhanced electron precipitation probability, for low energy electrons ($\lesssim$ 100 eV), located at about 35° magnetic latitude, and varying with local time because of the time varying wind field. The satellite observations of Sayers (1965) and of Reddy et al. (1967) indicated regions of excess F-region ionization which could well be caused by such a process of electron precipitation. Also, Paulikas and Freden (1964), in mapping world-wide precipitation of electrons with >0.9 MeV, found regions of precipitation, on magnetic shells $L \sim 1.2$ and $L \sim 2$, which coincide

quite well with Sayers' zones of enhancement. Knudsen and Sharp (1968) observed enhancements of electron concentration at L = 1.1 and L = 1.7. Interestingly, Mariani (1963) indicated that a corpuscular ionizing flux should be present at L = 1.7, which, however, is of secondary importance to another at L = 3.5. Vaisberg (1966) observed diurnal and semidiurnal variations in the height of mirror points of trapped electrons, plus sporadic variations of comparable magnitude. He concluded that his observations, which indicated minimum mirror altitudes at 0800 and 1900 local time, were consistent with the action of the dynamo-induced electric field.

As the auroral zones are approached, the character of the average ionosphere properties changes markedly. A number of aeronomic parameters display pronounced activity in the range 50° to 60° geomagnetic latitude. Briefly, these are:

1. Radio star and satellite scintillation increases sharply Northward of 55° (Bol'shoi, 1966; Yeroukhimov et al., 1968; Aarons et al., 1969).
2. Electron precipitation (low energy) maximizes at 55° (Mariani, 1963).
3. Incidence of red arcs maximizes at 53° (Marovich and Roach, 1963).
4. VLF lower hybrid resonance incidence maximizes at 55° (McEwan and Barrington, 1967).
5. Effective mean molecular weight in the F-region increases sharply above 55° (Barrington and McEwan, 1967; Barrington et al., 1966).
6. The plasmapause is located in the range L = 3.5, corresponding to a range of geomagnetic latitudes of roughly 54° to 63° (Carpenter, 1966; 1967).

It seems that a narrow belt of geomagnetic latitudes near 55° is, in some respects, rather unique. Polewards of this latitude range occurs the main F-region trough, observed in topside soundings (Muldrew, 1965; Nelms, 1966; Hagg, 1967), and further polewards lies the more highly active auroral zone. It may be significant that Nelms (1966) finds a remarkably stable world-wide height interval between 400 and 600 km, whereas above 600 km, strong electron distribution processes take place. It might reasonably be assumed that the electron energy is sufficient to allow penetration into the ionosphere only to the 600-km level, implying energies of $\lesssim$ 100 eV.

King et al. (1967), using topside sounder data, found no evidence for electron precipitation at heights of 400 to 500 km, except near the South Atlantic anomaly, during geomagnetic disturbances. This is not in conflict with the observations of Nelms, since the height interval is precisely that which the latter indicates as being the most stable. Thus, while the reason for the enhanced disturbance characteristics near 55° magnetic latitude is not precisely clear, there does seem to be considerable evidence for low energy electron precipitation in this region, and this precipitation is intimately associated with certain phenomena in the magnetosphere.

5. POLAR REGION

Above about 65° geomagnetic latitude, the earth's magnetic field lines become very distorted, due to interaction with the highly conducting solar wind, and no longer rotate synchronously with the earth. This causes extremely complicated convective motions in the magnetospheric plasma, whose nature is poorly understood at present. Although the physical processes at work in the magnetosphere have, thus far, defied explanation, nevertheless, from a phenomenological viewpoint, their effects upon the ionosphere are now reasonably well understood. As in the case of the equatorial region, electromagnetic forces produced by an intense large scale current system -- the DS system -- play an important role in polar regions. Closely related to this current system is the precipitation, into the polar ionosphere, of energetic electrons which have been accelerated by some unknown mechanism, somewhere in the magnetosphere, or in the magnetic tail of the earth.

There are a number of unsolved problems connected with the behavior of the polar ionosphere, and thus also with the understanding of irregularity formation in these regions. Perhaps the most outstanding of these is the evaluation of the role of the aurora and its effects on polar ionospheric dynamics. Another important question is the mechanism by which the ionization is maintained during the long polar night. Both of these problems are related to particle influx from outside the ionosphere, and satellite observations, in recent years, have begun to clarify the complex processes involved in such precipitation. Hartz and Brice (1967) summarized a large number of observations of different sorts, and concluded that two distinct precipitation mechanisms operate in the auroral zone. The disturbance events observed on the night side of the earth are consistent with a flux of low energy electrons (< 1 keV), whereas those on the morning side may be attributed to higher energy electrons (> 40 keV). For purposes of comparison, and for the following discussion, it might be noted (Rees, 1964) that 1-keV electrons penetrate approximately to the 150-km level, while 40-keV electrons produce maximum ionization at about the 110-km level.

In the study of the morphology of polar disturbances, a very significant fact emerges, which seems to be of far-reaching importance. This is the shape and movement of the auroral oval and other related parameters. Gustaffson (1967), and Feldshtein et al. (1966) have found that the orientation of auroral arcs lies along the direction of the tangent to an oval on the earth's surface, located asymmetrically with respect to the axis of rotation. According to these authors, the oval lies closer to the pole at midday than at midnight, the asymmetry apparently being due to the drag interaction between the magnetic field-entrapped plasma, and the solar wind. This oval locus, which is also the locus of maximum auroral occurrence, agrees well with the results of morphological studies of other parameters.

Hartz and Brice (1967) arrived at a locus of low energy electron precipitation very similar to the auroral oval. Hagg (1967) found that a "trough" or region of low electron density exists at L ~ 6, at an altitude of 1500 to 3000 km, and that at a particular longitude, it moved North to South by 8 degrees diurnally, being farthest North at local noon. O'Brien (1963) has observed a diurnal variation of the highest latitude at which electrons ($\gtrsim$ 40 keV) are trapped at 1000 km in the North American longitude zone. The trapping zone terminates at L ~ 8 by day and at L ~ 16 at night, corresponding to a diurnal variation of ~ 10°. Figure 1 shows the results of Frank et al. (1964) for the locus of precipitation of electrons of 40 keV or greater. If the very intense flux (by an order of magnitude) at 64° to 68° latitude and 0800 to 1200 local time, is temporarily ignored, the remainder of the precipitation locus closely resembles the auroral oval in shape. There is a diurnal variation of position of about 8°, and possibly even a slight tilting so as to produce reflection symmetry about the line from the 1000 to the 2200 meridian. This small tilting effect is observed in several studies; it is attributed (Walters, 1964) to the combined effects of the oblique interplanetary magnetic field and the earth's orbital velocity, relative to the solar wind. The intense flux at ~ 1000 local time is apparently the second, more energetic effect deduced by Hartz and Brice.

The diurnal movement, in the rotating terrestrial coordinate system, is also to be seen in the behavior of certain midlatitude phenomena. This correspondence is also apparent when the magnetic activity correlation of these same phenomena is studied. It seems to be a general rule that the oval locus of high latitude disturbances moves equatorwards with increasing magnetic disturbance and also, on a much slower scale, with increasing sunspot number. Malko (1966) and Feldshtein et al. (1966) have noted these characteristics for the auroral oval. Muldrew (1965) observed that the midlatitude F-region trough moved towards the equator with increasing magnetic disturbance, and furthermore, exhibited a seasonal latitude movement, being closest to the equator in winter. Similarly, King et al. (1967) have reported that the low latitude boundary of the zone of high latitude topside spread-F, which according to them is very sharply defined, has a diurnal movement of 12°.

Of the many authors whose observations have contributed to an understanding of high latitude particle precipitation, the work of Maehlum and O'Brien (1963) and McDiarmid and Burrows (1964) is particularly valuable in elucidating the diurnal variation of the flux of precipitating electrons. While it is clear that the precipitation mechanism is, more or less, closely associated with the DS current system, it is also known that the acceleration process is not a simple one. Cummings et al. (1966) have noted that, at times of electron precipitation, the entire pitch angle distribution of the magnetically trapped electrons is altered, and that the flux of trapped electrons, in a given energy range, actually increases, rather than decreases during

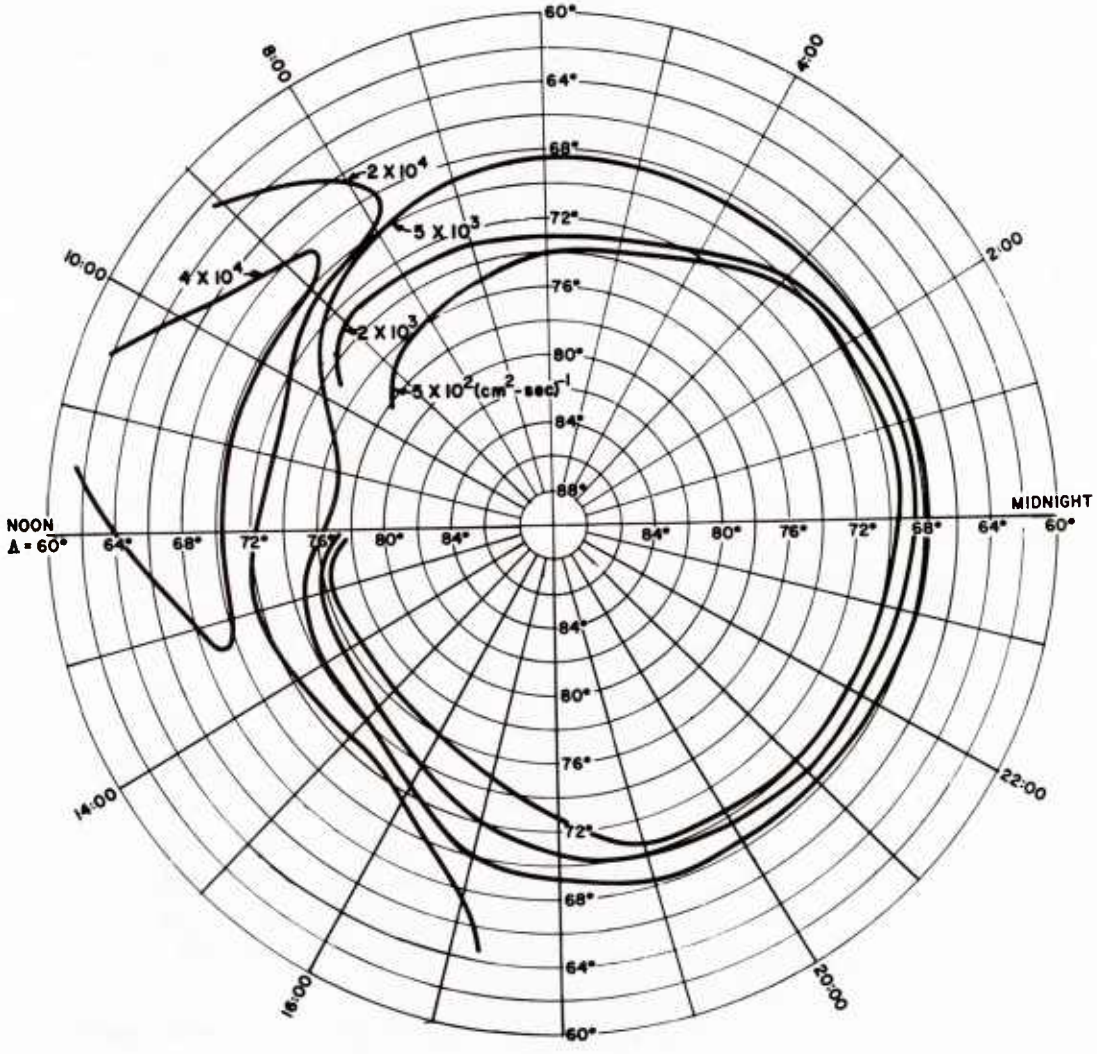

Figure 1. Locus of the Zone of Precipitation of Electrons (> 40 keV) in the Polar Regions. Coordinates are geomagnetic latitude and local time

electron "dumping." Kim and Wang (1967), however, deduced that the current inside the auroral zone is directed along the auroral arcs, and Taylor and Hones (1965), using the previously measured mean DS current system, calculated the electrostatic potential field necessary to drive these currents. This potential field is reproduced in Figure 2, and comparison with the orientation of auroral arcs shows that the potential lines are closely normal to the arcs, and thus to the auroral zone currents. This is to be expected, since the induced currents are Hall currents. The origin of the DS potential system is not clear, but Taylor and Hones projected their potential distribution back into the magnetospheric tail, and showed that the resultant electrostatic fields could accelerate low energy electrons to energies in the range 1 to 40 keV, in a narrow range of equivalent latitudes, during local nighttime. The phenomena associated with the higher energy electron precipitation in the morning are even less clear, but may be related to the diurnally occurring compression of the magnetosphere by the solar wind.

6. MORPHOLOGY OF F-REGION IRREGULARITIES

Having briefly examined the principal factors which are thought to be of importance in F-region dynamics, we consider it now appropriate to explore the morphology of F-region irregularity, in the light of this knowledge. The division of the earth into three, more or less arbitrary zones of geomagnetic latitude will be retained, since it will be seen that the evidence justifies this procedure, also in this case. Because of the large body of data to be summarized, a tabular format will be used to present the result of almost two decades of research into the height, size, magnetic and solar activity dependences, geographic distribution and drift of F-region irregularities.

It should be borne in mind that many different techniques are represented in the observations presented in these tables. Different techniques are often most sensitive to different effects, and it has become clear, in recent years, that F-region inhomogeneity is manifested in a variety of ways, such as small magnetically elongated, diffusion dominated cylinders; sheets or ducts of ionization; large traveling disturbances, or acoustic-gravity waves. As a simple example of preferential sensitivity in observing technique, it might be pointed out that a backscatter radar is most sensitive to irregularities whose size is of the order of the radar wavelength. Again, a vertical sounder samples only a small range of heights near the altitude at which the operating wavelength equals the local plasma frequency. This effect is especially important in the measurement of ionospheric drifts by the pulse reflection technique. On the other hand, a technique such as radio star scintillation measurement produces a result which is some weighted average over the entire range of ionospheric altitudes. In the closely spaced receiver technique of drift

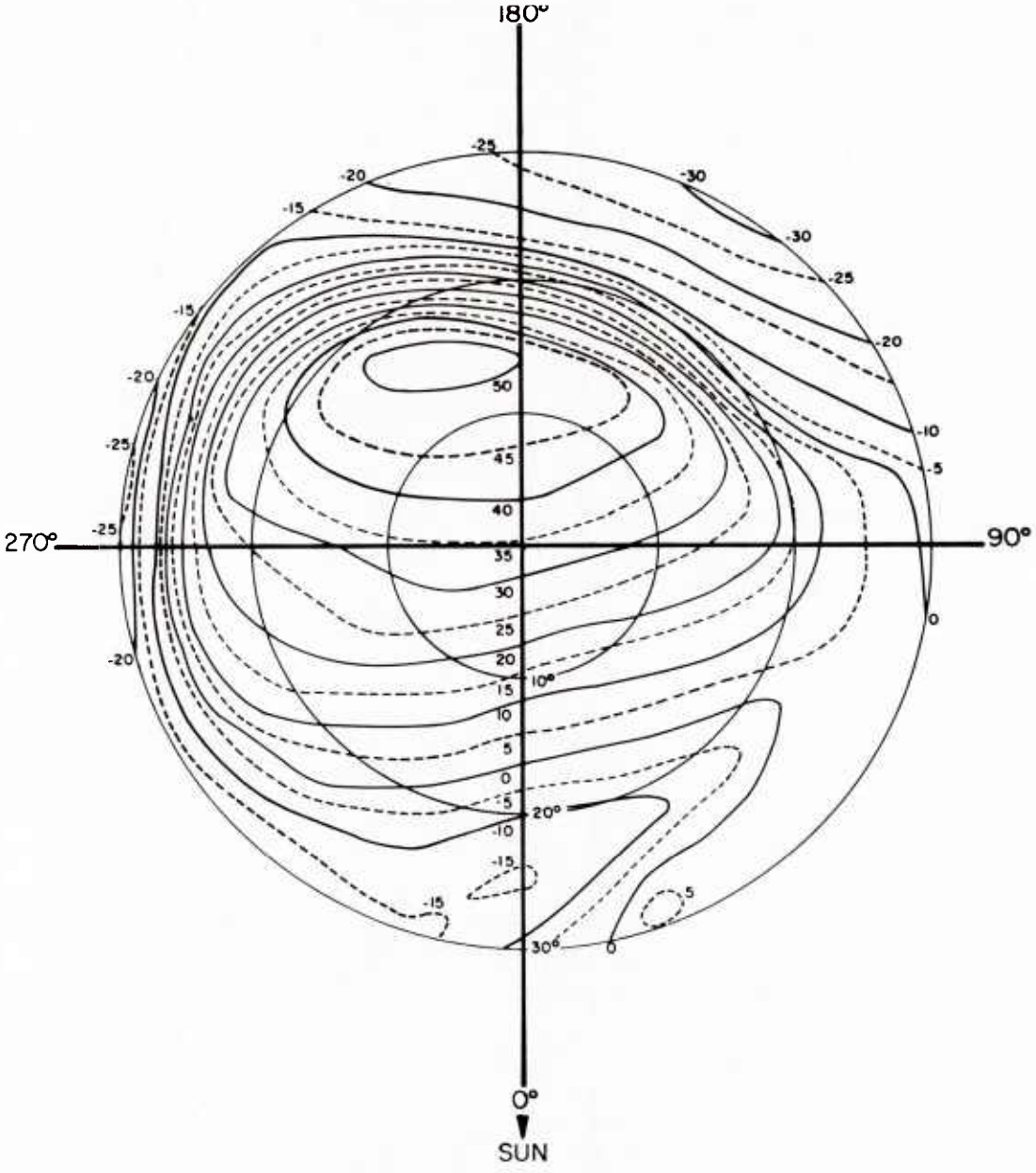

Figure 2. Magnetospheric Electrostatic Potential Field Required to Drive the Polar DS Current System

measurement, the drift of irregularities, the size of whose ground diffraction pattern approximates the receiver spacing, is preferentially measured. The widely spaced technique, as with spaced ionosondes, tends to discriminate against small irregularities in favor of larger traveling disturbances. These and other effects need to be borne in mind when comparing different results in the tables.

7. METHODS OF OBSERVATION

A variety of different experimental techniques has been applied to the study of F-region inhomogeneity. These may be briefly summarized as follows:

7.1 Vertical Incidence Ionosoundings

Over a period of thirty years, an enormous amount of data has been obtained by the world-wide network of vertical incidence ionosondes. The phenomenon of spread-F, which is indicative of F-region irregularities, has been reviewed by many authors (for example, Shimazaki, 1959; Herman, 1966; Penndorf, 1962, 1964; Singleton, 1962). Because of the world-wide distribution of stations, and the high sensitivity to irregularities, this technique has been very useful in morphological studies. However, since it can observe irregularities only below the F-layer maximum, its usefulness is considerably limited.

7.2 Topside Sounding

The advent of the satellite era allowed ionosondes to explore the topside of the ionosphere. Calvert and Schmid (1964) have published a study of the geographic variation of topside spread-F, obtained by this means. The technique has also allowed a more detailed study of the structure of the perturbed ionosphere, resulting specifically in the discovery of field aligned ducts and sheets of ionization. Of course, a major disadvantage is that the rapid motion of the satellite precludes the continuous study of a given region, although it does provide observations in otherwise inaccessible regions of the earth.

7.3 Radio Star and Satellite Scintillation

The study of the diffraction pattern, produced on the ground, when radio waves from a radio star or a satellite traverse the disturbed ionosphere, has been particularly useful for the measurement of irregularity heights and drifts, as well as for detailed analysis of the properties of individual irregularities. Satellites, in particular, can be observed with relatively simple equipment, allowing spatial coverage which is difficult, or even impossible to achieve, using other techniques. The main disadvantage of orbiting satellites, in this work, is their rapid motion which,

however, may be used to advantage in the measurement of irregularity heights. This disadvantage is eliminated when geo-stationary satellites are used; this latter technique combines the most useful features of the radio star and orbiting satellite methods.

7.4 Radio Wave Scattering

Forward and backscattering of HF and VHF signals is a valuable experimental tool for studies of F-region irregularities. In the case of VHF forward scatter, as Cohen and Bowles (1961) showed, the geometry of the propagation circuit can allow the height and the spatial distribution of the scattering irregularities to be determined. Backscatter observations are generally carried out at a frequency somewhat above the penetration frequency of the F-layer, although Leadabrand et al. (1965), in observing auroral backscatter, used frequencies well into the UHF range. Clemesha (1964), using a frequency of 18 MHz in the equatorial region, was able to deduce the height, size, and drift velocity of patches of irregularities, as well as the motions of individual irregularities within the patches.

7.5 Other Techniques

Among the miscellaneous, lesser-used observational techniques, one of the oldest is that of recording the oblique transmissions from distant transmitters, noting the amplitude and phase variations due to the time varying character of the ionospheric medium near the reflection point. This method is still used quite profitably on transequatorial paths (for example, Heritage and Fay, 1967) and auroral paths (Bates et al., 1966). Georges (1967) has observed phase fluctuations of the reflection from the F-region, of a vertically transmitted wave of very high frequency stability. He concluded that gravity wave propagation in the F-region produced the observed fluctuations. Thome (1964) studied perturbations of the incoherent backscatter from the F-region, and arrived at similar conclusions. Many variations of these techniques have been used, and new ideas are constantly being tried.

8. GENERAL DESCRIPTION OF F-REGION IRREGULARITIES

A great variety of physical pictures has been suggested for F-region irregularities, in order to account for the observations of various authors. As previously pointed out, the apparent discrepancies between these representations are often due to the use of different observing techniques. In particular, many observers using relatively short radio wavelengths, such as with the radio star or satellite methods, describe the irregularities as being cylindrical, with a diameter of the

order of a kilometer or so, and with the axis along the direction of the local magnetic field.

Others have concluded that the irregularities are sheets of ionization or ducts in the ionization profile, aligned along the magnetic field direction. Still others have reported that large traveling disturbances, with frontal dimensions of up to thousands of kilometers, are responsible for F-region fading of propagated signals and for irregular features on ionosonde records. Bramley (1953) associated such large disturbances with sunrise at F-region altitudes, while Munro (1950) examined the propagation of traveling ionospheric disturbances using a number of widely spaced transmitters. Bowman (1968) showed that some large disturbances are generated in polar regions, and propagate towards the equator. Bowman (1968) has also suggested a model for the irregularities responsible for spread-F, which consists of a wavy or corrugated structure, with a wavelength of typically 30 km.

Some authors (Wild and Roberts, 1956; Dagg, 1957; Warwick, 1964) have deduced that radio star scintillation results from the passage of large lens-shaped or wedge-shaped ionization formations through the ray path. It is clearly impossible to encompass all of the preceding models for irregularities in a general, all-purpose, mathematical formulation. The best that can be done is to choose that formulation which best appears to fit the observational technique. Thus the model of an "optically thin" phase changing screen, consisting of randomly arranged "blobs," has proved reasonably adequate to describe radio star or satellite scintillation. This is principally due to the fact that this particular technique tends to discriminate against very large irregularities, being most sensitive to irregularities having dimensions comparable to those of the first Fresnel diffraction zone (several kilometers, in typical cases).

In summarizing the present state of knowledge concerning irregularities in the ionospheric F-region, we consider it important to evaluate properly the relationship between the various observing techniques. This ultimately poses the question as to whether the transmission techniques (radio star and satellite scintillation) and reflection techniques (ionosoundings and so forth) observe the same type of F-region irregularity. This point is often taken for granted, but it is useful to examine the question more objectively. Following this, a brief but comprehensive survey of the literature, aimed at formulating an average description of the morphology of F-region irregularities, will be presented.

9. ASSOCIATION BETWEEN SCINTILLATION AND SPREAD-F

There seems little doubt that a close association exists between these two phenomena. However, it is important to note that, in view of the often localized nature of the irregularities, simultaneous observations of the same ionospheric

region using both techniques are necessary. Briggs (1958) has given a semi-quantitative relationship between the two, while Little (1951), Koster (1958), Yeh and Swenson (1959), Klemperer (1963), and Jesperson and Kamas (1964) are among those who have reported positive correlation between spred-F and scintillation activity. The observations of Klemperer, however, appear to be the only ones in which both sets of data refer to the same location in the F-region; it is significant that he reports a very high correlation. On the other hand, Chivers (1960) finds a strong negative correlation between spread-F and radio-star scintillation, which may well be attributable to the wide and variable separation of the regions observed by him in each case [cf Singleton (1961)].

Wild and Roberts (1956) mention a positive correlation between scintillation of radio stars and spread-F during the nighttime only, whereas the scintillations are correlated with sporadic-E during the day. This raises another point, which will be further considered later, concerning the height at which the irregularities occur. If it be tentatively admitted that the inhomogeneities at both E- and F-region altitudes can produce scintillation, and if the separate diurnal variations of sporadic E and spread-F are taken into account, then the observation of Wild and Roberts may be seen in better perspective. The relationship between spread-F and scintillation is not always clear, as shown by the work of Wells (1954). Although he finds the diurnal variations in scintillation and spread-F incidence to be similar, Wells finds no seasonal scintillation variation comparable to that of spread-F. Hartz (1955) reports only a weak correlation and Dueno (1955) finds none at all. Bolton et al. (1953) found a positive correlation only during the winter months at their Southern hemisphere station, while Mills and Thomas (1951) discovered no such correlation at a similar Southern latitude. Owren et al. (1964) in College, Alaska, discovered only very small scintillation - spread-F correlation.

A few workers, for example, Dueno (1955) and Dyce et al. (1959), have reported significant correlations between sporadic-E and scintillation activity, while others have found a relationship between occurrence of spread-F and retardation type sporadic-E in the auroral zone. However, Lawrence et al. (1961), in an experiment designed especially to detect such a relationship between scintillations and sporadic-E, arrived at a negative result.

It seems that one may confidently assume that if spread-F and ionospheric scintillations are not manifestations of a common physical event, they are at least very closely related. With this conclusion in mind, it becomes possible to extend many of the results of spread-F research to ionospheric scintillation as well. Good examples are the geographic and seasonal spread-F distributions obtained for the polar regions by Penndorf (1962, 1964) and those of Singleton (1962).

10. HEIGHT OF THE IRREGULARITIES

It is in general a difficult matter to establish at which height the perturbations are imposed on the downcoming radio waves; this point has occasionally been debated heatedly. The majority of workers agree that the F-region is the most likely location, although actual height estimates differ greatly, and some authors favor the E-region. Since such a large body of information relating to this subject is to be found in the literature, it seems most appropriate to present it in tabular form. Table 1, while still not pretending to be exhaustive, lists many of the height determinations referred to above, together with appropriate comments. For proper evaluation of the methods used and assumptions made, the reader is advised to consult the original publications.

The general consensus would appear to place the most frequently occurring height of the irregularities, as already noted, in the F-region. Regarding the relatively fewer E-region determinations, two factors might be remarked upon which will be considered in more detail in a later section of this paper:

1. Those of Liszka, and of Hook and Owren refer to locations in the highly disturbed auroral zone.
2. Those of Wild and Roberts, and of Jespersen and Kamas apparently refer to very large "traveling ionospheric disturbances," perhaps of a wavelike nature, and different character from the bulk of the other types considered. Chivers and Davies employed a frequency at which ionospheric effects are usually thought to be negligible, so that there has been a tendency to ascribe somewhat less weight to their E-region height determination. (Briggs and Parkin, 1963, however, taking their observations at face value, deduce an irregularity size of 300 meters.) Since it is reasonable to assume that consideration of this large selection of data, from many different sources, has to some extent nullified the inherent systematic errors involved in height-finding, the conclusions of this section might perhaps be accepted with some confidence.

11. SIZE AND SHAPE OF IRREGULARITIES

Once again, a large volume of sometimes controversial data exists on the subject of scale sizes of the irregularities. Table 2 summarizes a representative sample. Note that where the explanatory remark denotes "patches," the measurement refers to the size of large patches of much smaller irregularities. Attention is drawn to the possibility of a certain systematic observational bias, such as remarked in the introduction, namely, there appears to exist an inverse relationship

between observed scale size and the probing frequency. It may be significant, however, that this does not apply to the reflection type measurements made in the range 2.4 to 5.0 MHz, relating mainly to the F-region, when compared to the scintillation data taken below 100 MHz. This might be taken as evidence that the scale sizes of the order of a few kilometers occur mainly in the upper F-region, or else that there is some unsuspected difference between the two methods of observation. That the latter is unlikely, however, is illustrated by the work of Jones (1960).

There have been some suggestions that the UHF results, which give scale sizes of the electron mean free path, or less, are physically very improbable, since they imply irregularity lifetime less than the electron collision period. This criticism seems, however, to be not wholly justified. While the origin of such small irregularities is admittedly speculative, their geographic location (usually in the auroral zone) provides a clue. Perfectly admissible physical mechanisms, such as interacting shock waves, or plasma oscillations, could account for these observations. It is the author's contention that these should not be overlooked.

When one comes to consider the shape of the irregularities, there seems to be fairly general accord that the anisotropy introduced by the earth's magnetic field plays a dominant role. The effect of this anisotropy is to produce elongation along the direction of the magnetic field lines, at least for irregularities of moderate size. This effect was first noted by Spencer (1955) who deduced an elongation factor of 5 to 20. While some subsequent workers have derived widely different elongations, a figure of about 10 (Briggs and Parkin, 1963) corresponds roughly to the median value, although Flood (1964) finds no evidence for such anisotropy at all.

Some explanation for this wide variation in elongation is given by Jones (1960) who, in observing scintillations of Cassiopeia A, deduced a mean major axis of 7.5 km (ellipticity 12) at high elevations, but only 2.0 km (ellipticity 2.5) at low elevations. In deducing these dimensions, he made the assumption, following Hewish (1951), that the phase perturbations in the diffracted field did not exceed one radian. It seems likely, therefore, that this assumption is not valid at the frequency used (38 MHz) for the much longer, low elevation path through the ionosphere. Although this would cause the indicated size to be underestimated, it is not clear why the elongation should be altered, and the possibility of a latitude variation of size, as suggested by Jones, must also be considered. This suggestion is reinforced by Jones' observation of night to night variability in ellipticity.

For the larger inhomogeneities, sometimes known as traveling disturbances, no such elongation is apparent. Rather, they are often depicted as being prism-shaped (Wild and Roberts, 1956) or lens-shaped (Lawrence et al., 1961). Most observers consider these irregularities to be some form of distorted wave structure, perhaps of the kind suggested by Hines (1960), and that they impose purely refractive effects on the penetrating or reflecting radio waves. Claiming that the

standard methods of scale size measurement are not well adapted to these larger types, Gusev et al. (1958) developed a better method.

At the low end of the scale size spectrum, the situation seems less clear regarding the shape of these irregularities. One factor which is very apparent from the radar experiments, however, is that they have a very strong tendency to be field aligned. This is deduced from the extreme aspect sensitivity of the radar echoes, for example, Egeland (1964), Watkins (1960). Presnell et al. (1959) deduced an elongation of 35:1 from UHF auroral reflection measurements.

12. SPATIAL DISTRIBUTION OF IRREGULARITIES

A striking feature of the spatial distribution of irregularities is their different character in different zones of geomagnetic latitude. This predominance of one or the other type of ionospheric disturbance in different regions may provide important clues in the search for the relevant physical mechanisms. In the interest of brevity, Table 3 presents a representative survey of the literature pertaining to irregularity distributions in the three geographic zones defined in Section 2. As far as the high latitude zone is concerned, little information is available for geomagnetic latitudes above about 70°, so that the information in this category refers predominantly to the auroral zone. The "medium" zone, or temperate zone, is characterized by the large lens- or prism-shaped irregularities mentioned, and also by the fact that scintillations and spread-F are far more common in this zone than in either of the other two (Singleton, 1960). After perusal of Table 3, it might perhaps seem more accurate to say that the large irregularities, with size in the range 100 to 500 km or so, are observed at all latitudes, but that the smaller irregularities (several kilometers) are present mainly at low and at high latitudes. At low latitudes, however, the large patches appear to be elongated in the East-West direction, while at medium latitudes, the elongation is observed to be in the North-South direction. There is also evidence, at least in medium latitudes, of a diurnal variation in their shape. Gusev et al. (1958) who have conducted an experiment especially designed to study these large scale structures, have reported diurnal changes in the size, shape, and orientation of irregularities in the size range $\sim$ 100 to 200 km.

The geographic distribution, at high latitudes, of ionospheric irregularities probably is influenced strongly by the behavior of the aurora. Benson (1960), in fact, reports that the effect on scintillation records of visible auroral forms which pass through the radio line of sight, is directly observable. Little and Maxwell (1952) observed that the frequency of radio star scintillations was greater than normal during a visible aurora, and attributed this fact to greater ionospheric drift velocities. The observations of satellite scintillations, conducted by Aarons et al. (1963) have revealed that the irregularity structure responsible for the

scintillations undergoes a latitude displacement, during geomagnetic disturbances, which is similar to the movement of other auroral phenomena, such as auroral absorption. These authors show that the probability of occurrence and intensity index of scintillations at Sagamore Hill, located slightly south of the auroral zone, are markedly higher for northern than for southern observation points in the ionosphere. Similar observations at an observing point in the auroral zone (Little et al., 1962) show very little latitude dependence, which strengthens the hypothesis of strong dependence upon the aurora and related phenomena.

13. MOVEMENTS OF IRREGULARITIES

This section is merely a brief summary of reported observations. Table 5 summarizes many of the observations made over the preceding decade of the drift speed or irregularities. The table is self-explanatory, but in regard to the direction of the velocity vector, one important consideration needs to be kept in mind. Spencer (1955) has shown how the measured elongation of the ground pattern, or "shadow" of the irregularities may give rise to serious errors in the estimation of direction of drift. Specifically, for North-South elongation due to the magnetic field, he showed that small changes in orientation could be interpreted as large changes, or even reversals, and that there would exist a strong tendency to observe velocities in the East-West direction. A glance at Table 5 shows a strong predominance of East-West velocities, so that a suspicion of this effect must be held. It is not always clear from the published work of investigators who succeeded Spencer, whether or not the possibility of such experimental bias has been considered. Although it is inferred from magnetic and earth current observations that the ionospheric currents near the equator and auroral zones are predominantly in the East-West direction, it need not necessarily follow that the drift of irregularities will be the same. In fact, Cole (1962) shows that there will, in general, be a considerable difference, especially in the F-region. This point requires further study.

14. DIURNAL VARIATIONS IN IRREGULARITY OCCURRENCE

Table 6 summarizes observations of the diurnal variation of irregularity occurrence. Most of the observations refer to equatorial zone locations, and there appears to be some disagreement. This may be due, at least in part, to the following circumstances, which illustrate the complexity of the problem, while at the same time providing further clues toward its solution:

1. The work of Marasigan (1960) indicates that there is seasonal and sunspot cycle effect of the diurnal variation of spread-F, near the equator.
2. Skinner and Wright (1957), Kotadia (1956), Marasigan (1960), and others have shown that the local time of maximum spread-F occurrence is quite variable from one location to another in the equatorial zone, although it always occurs after sunset.

It is clear from the work of several authors that the occurrence of equatorial spread-F is closely connected with the diurnal variation of the equatorial electrojet, lending support to Martyn's theory of formation, which involves dynamo interaction between E- and F-region. The conclusions of Shimazaki (1959), Renau (1960), and Aarons et al. (1964) reinforce the somewhat arbitrary division of the earth into separate latitude zones for this purpose.

In addition to the diurnal variation of occurrence of small irregularities, there has been observed, for over 20 years, an effect due to tilts of the F-layer at about sunrise and sunset. Ross and Bramley (1947, 1949) appear to be the first to have observed this effect at sunrise, while apparently the same description fits the post-sunset observations of Osborne (1951). Somayajulu et al. (1953) observed similar traveling disturbances, with velocities in the 200 to 400 meter/sec range.

15. SEASONAL VARIATIONS

Not a great amount of information is available concerning the seasonal variation of irregularity occurrence (see Table 7). There seems to be fairly general accord that, in the equatorial zone at least, the seasonal peak occurs in the equinoxes, although Marasigan (1960) indicates that there is an effect of the sunspot cycle on this dependence. The situation at other latitudes is less clear, as is well illustrated by the conclusions of Shimazaki (1959) who, after an extensive study, could only suppose that the seasonal dependence itself varied with geographic location. At high latitudes there does seem to be evidence for a winter maximum, although it is not obvious whether this conclusion relates to the auroral zone itself. Several authors report strong positive correlation of spread-F amid scintillation activity, near the auroral zone, with magnetic activity. Since it is well known that maximum magnetic activity in the auroral zone occurs at the equinoxes, one might reasonably expect a similar variation in irregularity occurrence at these locations.

16. MAGNETIC AND SOLAR ACTIVITY DEPENDENCES

There are pronounced effects on the ionospheric irregularities associated with

the well-known variations in disturbance of the magnetic field, and ultimately of the sun, as reflected by the Wolf Sunspot Number. Table 4, again divided into three latitude zones, summarizes observations of this aspect of the study. A very significant difference between these three zones is apparent, when it is noted that spread-F is negatively correlated with magnetic activity in equatorial regions, but the correlation is positive at higher latitudes. This observation, puzzling at first, may provide an important clue in understanding the phenomenon. In Martyn's theory, the irregularities are formed on the underside of an upward drifting layer, but on the topside of a downward drifting layer. Since an increase in magnetic activity generally causes the equatorial F-region to decrease in height, the irregularities would be shielded, it is claimed by some, from the "view" of the ground-based ionosondes. This would not, however, explain the observations of Koster and Wright (1960) and others, who state that the magnetic dependence of radio-star scintillations is strongly negative at sunspot maximum, although somewhat indeterminate at sunspot minimum. The radio-star technique ought to be equally sensitive to irregularities on both upper and lower sides of the layer (providing it is symmetrical).

Allen et al. (1964) have made a thorough study of the magnetic dependence of scintillation at a subauroral location, following earlier work by Kidd et al. (1962), and Aarons et al. (1964). They demonstrate an important "inversion" effect of the theoretical frequency dependence of scintillation index, as magnetic activity increases, due to the root-mean-square phase perturbations in the diffracted field becoming excessive. This observation may explain some of the discrepancies between spread-F and scintillation observations, especially when the latter are conducted at low frequencies during years of high sunspot number.

17. SUMMARY OF OBSERVATIONS

Table 8 represents an attempt to summarize the essential features of the observations contained in Tables 1 to 7. It will be seen that several gaps appear to exist in our knowledge of this subject. These can be filled only by long-term observations at a greater number of strategically placed stations.

Table 1. Irregularity Height

Author	Height (km)	Remarks
Hewish (1952)	400	
Wild and Roberts (1956)	500	Some daytime E-region observations
Briggs (1958)	300	
Kent (1959)	270-320	Equatorial zone
Chivers and Greenhow (1959)	E-region	
Kent (1960)	E-region	
Frihagen and Troim (1960)	340; 365	One additional observation at 104 km
Little and Lawrence (1960)	230 upwards	Irregularities often in large patches
Frihagen and Troim (1961)	300-500	Auroral zone observations
Kent and Koster (1961)	380-425	Equatorial zone observations
Cohen and Bowles (1961)	Up to 450	Equatorial zone observations
Basler and deWitt (1962)	250-650	Auroral zone observations
Chivers and Davies (1962)	100	Very high frequency (1370 MHz) observations
Hook and Owren (1962)	100 upwards	Auroral zone observations
Wagner (1962)	300-400	Several different locations used
Munro (1963)	200-350	Temperate zone
Calvert et al. (1963)	400-1000	Topside sounder data; ducts observed
Yeh et al. (1963)	300-400	A few observations outside this range
Frihagen (1963)	300-500	
Liszka (1964)	120-650	Auroral zone location
Allen et al. (1964)	100-600	Sub-auroral location
Kent and Koster (1964)	250-350	Equatorial location
Beynon and Jones (1964)	250 upwards	Irregularities occur in large patches
Clemesha (1964)	350-450	Elongated in latitudinal direction
Jespersen and Kamas (1964)	250-400	Magnetic latitude variation observed
Barber and Ross (1964)	300-400	Irregularities often occur in thin layers
McClure (1964)	100; 300-400	Patchy; E-region observation definitely established
Frihagen and Liszka (1965)	200-400	Auroral zone observations

Table 2. Irregularity Size

Author	Size (km)	Frequency (MHz)	Remarks
Ross and Bramley (1949)	>5		
Briggs and Phillips (1950)	0.29	2.4; 4.8	Reflections from E- and F-regions
Bramley (1951)	0.34	4.0; 5.0	
Hewish (1952)	5	45	
Spencer (1955)	3	38	Field aligned; ellipticity from 1.1 to >5:1
Vitkevich (1957)	5 - 10	50	Irregularities occur in large patches
Kent (1959)	3	40	Large patches, elongated in latitude
Presnell et al. (1959)	0.0001	216; 398; 780	Auroral backscatter; ellipticity ~ 35:1
Greenhow et al. (1960)	0.16	36	Field aligned; occur in patches
Jones (1960)	2.0 - 7.5	38	Large patches; size, shape vary with elevation
Kent (1960)	>10	20	E-region heights inferred from data
Frihagen and Troim (1960)	0.01	20	Measured ellipticity of 13.5:1
Khastgir and Singh (1960)	0.27	3.8	
Cohen and Bowles (1961)	0.01	50	Field aligned; ellipticity 10:1
Lawrence et al. (1961)	200	53; 108	Often appear as large lens-side patches
Aarons et al. (1961)	<1	54	Subauroral location
Lyon and Forsyth (1962)	0.02	40 - 104	Subauroral location
Titheridge (1963)	5 - 500	40	Irregularities often wavelike, with wavelength of 100 km; total electron content perturbation is typically 0.25 percent
Warwick (1964)	17	7 - 41	Often wavelike, displaying finer structure
Dyson (1967a)			100-km latitude extent, located near F-peak
Little et al. (1962)	0.3	223; 456	Auroral zone location
Calvert et al. (1961)	1	1.9 - 11.5	Topside sounder data

Table 2. Irregularity Size (Contd)

Author	Size (km)	Frequency (MHz)	Remarks
Blevis et al. (1963)	0.0001	488; 944	Subauroral location; auroral backscatter
Al'pert et al. (1963)	2 - 6	20; 90	Patches; large horizontal ionization gradients
Koster (1963)	0.5	45; 108	Field-aligned; ellipticity 7.5:1 and greater
Yeh and Swenson (1964)	2 - 6	20	High latitude location
Kent and Koster (1964)	>0.3	136	Equatorial; field-aligned; ellipticity > 20:1
De Barber and Ross	0.5 - 4	54; 150	
Jespersen and Kamas (1964)	1	54	Field-aligned; ellipticity 10:1
Koster (1965)	0.232	136	Field-aligned; ellipticity exceeds 30:1
Aarons and Guidice (1966)	7	30	
Vitkevich (1960)	3 - 5		Total electron discontinuity 0.3 - 0.4 percent

Table 3. Geographic Variations

Author	Observation
Low Latitudes	
Lyon et al. (1960)	Belt between ±30° from magnetic dip equator (concentrated between ±20°) where equatorial spread-F occurs
Rastogi (1960)	Strong transport mechanisms near sunset
Cohen and Bowles (1961)	East-West extensions up to 1000 km; patch thickness ~ 50 km
Kent (1961)	Patches of order 100 km extent
Skinner and Wright (1957)	Belt between ±30° (concentrated between ±20° dip latitude) for spread-F
Singleton (1963)	Unique spread-F equator, which differs from the magnetic dip equator
Clemesha (1964)	30-400 km extent in East-West vertical plane
Clemesha and Wright (1966)	Approximately 100 km horizontal extent
Millman and Moyceyunas (1965)	Patches of 100-500 km extent
Bol'shoi (1966)	Satellite scintillations maximize in range 0°-20° latitude
Singleton (1968)	Width of low latitude region is ±20° at sunspot maximum, and ±40° at sunspot minimum
Medium Latitudes	
Maxwell and Dagg (1954)	F-region drifts correlated at points separated by 200 km
McNicol and Webster (1956)	Large steps and troughs separated 100-200 km
Drachev and Berezin (1957)	Patches 50-500 km extent
Vitkevich and Kokurin (1957)	~ 200 km extent
Vitkevich (1958)	300-400 km extent
Briggs (1958a)	Spread-F increases towards auroral zone
Briggs (1958b)	Extensions: N-S; ~ 500 km; E-W; > 500 km
Gusev et al. (1958)	Irregularity size ~ 100 km (day); ~ 200 km (night); ellipticity 1.5-2.0 with major axis in N-S direction; lifetime ~ 20 minutes
Kent (1959)	Patches elongated several hundred kilometers in latitude
Greenhow et al. (1960)	Latitude extent 500 km; longitude extent 50 km; horizontal stratification noted
Little and Lawrence (1960)	300 km or greater extent
Renau (1960)	Spread-F frequency dispersion is maximum at high and low latitudes, with minimum near 40° latitude

Table 3. Geographic Variations: Medium Latitudes (Contd)

Author	Observation
Jones (1960)	Large patches elongated in latitude; drifts uncorrelated at points separated in latitude by 400-850 km
Lawrence et al. (1961)	200 km extent
Aarons et al. (1961)	Extensions: N-S; 400-600 km; E-W; 300-500 km
Kokurin et al. (1961)	Wavelike structure with amplitude 0.5 km and wavelength 200 km
Chan and Villard (1962)	Traveling disturbances with fronts having extensions 1300-2000 km
Jespersen and Kamas (1964)	Extent from one km to several hundred km
Al'pert et al. (1963)	100-130 km extent; horizontal gradients in excess of 1000 cm^{-3} km^{-1}
Chidsey (1966)	160 km spacing; direct rocket experiment
Beynon and Jones (1964)	400-700 km horizontal extent
Aarons et al. (1964)	Equator and auroral zone maxima, with medium latitude minimum
Allen et al. (1964)	200-400 km extent
Joint Satellite Studies Group (1965)	Scintillations increase in amplitude and occurrence towards high latitudes
Beynon and Jones (1964)	Scintillations increase towards high latitude
Singleton (1968)	Zone of enhanced spread-F appears at about 50° magnetic latitude at sunspot minimum
High Latitudes	
Brenan (1960)	Scintillations correlated at magnetic conjugate points
Forsyth and Paulson (1961)	Boundary of zone moves in North-South direction with sunspot variation
Beynon and Jones (1964)	Scintillations decrease with decreasing geomagnetic latitude; especially sharp decrease at 2° South of the auroral zone
Schmelkovsky (1963)	Satellite scintillations increase over range 45°-65° geomagnetic latitude, with sharp increase at 55°
Bol'shoi (1966)	Satellite scintillations show sharp increase beyond 55° geomagnetic latitude
Joint Satellite Studies Group (1968)	Satellite scintillations show rapid increase above 55° geomagnetic latitude

Table 4. Magnetic and Solar Activity Dependences

Low Latitudes	
Author	Observation
Koster and Wright (1960)	Negative magnetic correlation at sunspot maximum
Skinner and Wright (1957)	Negative correlation with K-index
Lyon et al. (1960)	Negative magnetic activity correlation
Shimazaki (1959)	Negative magnetic activity correlation
Bowman (1960)	Negative correlation between spread-F and sunspot activity
Marasigan (1960)	Spread-F maximizes in summer at sunspot minimum, but in equinoxes at sunspot maximum
Davies and Barghausen (1966)	Negative magnetic, positive sunspot correlation
Rangaswami and Kapasi (1963)	Positive magnetic, negative sunspot correlation
Singleton (1968)	Low latitude zone expands towards mid-latitudes with declining solar activity
Medium Latitudes	
Dagg (1957)	Drift velocities correlated with K-index
Aarons et al. (1963)	Irregularity structure moves South as K-index increases
Chivers (1960)	Strong positive sunspot correlation
Shimazaki (1959)	Positive magnetic activity correlation
Ryan and Harrower (1960)	27 day solar periodicity in scintillation
Bowman (1960)	Negative correlation with sunspot activity
Lyon et al. (1960)	Positive correlation with K-index
Ko (1960)	Scintillation rate correlated with K-index
Briggs (1964)	Scintillations correlated with solar activity
Briggs (1965)	Spread-F correlated with K-index, with a time lag of $\frac{1}{2}$ to 2 days
Jespersen and Kamas (1964)	Geographic distribution alters with change in sunspot number
Briggs (1965)	K-index but not spread-F exhibits 27 day periodicity
Singleton (1968)	Peak in spread-F appears at 50°-55° geomagnetic latitude at sunspot minimum, but exhibits a seasonal dependence

Table 4. Magnetic and Solar Activity Dependences (Contd)

High Latitudes	
Author	Observation
Forsyth and Paulson (1961)	No sunspot variation in scintillation rate or amplitude
Watkins (1960)	Scintillations, K-index, auroral echoes, all show a similar storm-time dependence
Beynon and Jones (1964)	Scintillations correlate with magnetic activity
Aarons et al. (1963)	Irregularity structure moves South as K-index increases
Shimazaki (1959)	Negative correlation with magnetic activity
Bowman (1960)	Positive correlation with sunspot activity
Owren et al. (1966)	Positive correlation with sunspot activity
Allen et al. (1964)	Positive correlation with magnetic activity; region moves South as magnetic activity increases
Katsenelson (1966)	Spread-F has positive sunspot correlation
Singleton (1968)	High latitude peak in spread-F shows positive sunspot correlation
Stuart and Titheridge (1969)	Strong positive sunspot correlation; scintillation maximum precedes magnetic activity maximum by 12 hours, and scintillation minimum then follows after another day, with a return to normal after 3 days

Table 5. Movements of Irregularities

Author	Velocity Observed
Chapman (1953)	100 m/sec; proportional to K-index
Rao and Rao (1957)	84 m/sec; South-West direction
Hagg and Hanson (1954)	High vertical and E-region velocities
Rao and Murty (1956)	40-90 m/sec; North-East
McNicol and Webster (1956)	55 m/sec
Skinner and Wright (1957)	Spread-F correlated with upward movement
Proshkin and Kashcheev (1957)	Random velocities 0.5-1.5 m/sec (rms)
Rao and Rao (1957)	84 m/sec
Gusev et al. (1958)	130-170 m/sec; direction rotates diurnally
Skinner et al. (1958)	110 m/sec East

Table 5. Movements of Irregularities (Contd)

Author	Velocity Observed
Leadabrand et al. (1959)	550 m/sec East-West (auroral reflection)
Kusnerevski and Zajarnaja (1959)	80 m/sec
Rao et al. (1959)	80-90 m/sec; decreases as K-index increases
Jones (1960)	90 m/sec
Rao et al. (1960)	Spread-F correlated with upward movements
Bowman (1960)	Velocity related to magnetic field direction
Knecht (1960)	135 m/sec, East
Harang and Malmjord (1961)	400-600 m/sec West (auroral zone)
Awe (1961)	13 m/sec rms velocity in E-region
Calvert and Cohen (1961)	100-200 m/sec
Chan and Villard (1962)	400-800 m/sec from North to South (TID)
Koster (1963)	75 m/sec, East
Calvert et al. (1963)	100 m/sec, East
Clemesha (1964)	100 m/sec East; sporadic vertical velocities
Koster (1965)	78 m/sec
Rao (1966)	Equatorial spread-F occurs during both upward and downward F-layer movements
Zelenkov and Rudneva (1967)	Eastward drifts at low latitudes; Westward at high latitudes; variable at mid-latitudes

Table 6. Diurnal Variations

Author	Observation
Kotadia (1956)	Maximum equatorial spread-F at 0300
Briggs (1958)	Spread-F maximizes at 0100 (broad peak)
Bateman et al. (1959)	Equatorial F-scatter maximizes at about 0100
Shimazaki (1959)	Low latitude peak before midnight; elsewhere, maximum occurs after midnight
Marasigan (1960)	Maximum at 2100 (equinox); 0100 (summer)
Lyon et al.(1960)	Spread-F maximum at 1900-0500 and correlated with upward layer movement
Rao et al. (1960)	Spread-F correlated with upward layer motion with maximum occurrence at 1800-1900
Clemesha (1964)	Scintillation maximum at 0400 (rate), and at midnight (amplitude), at subauroral location

Table 6. Diurnal Variations (Contd)

Author	Observation
Koster (1965)	Maximum in occurrence frequency and intensity at 0100, in equatorial zone
Rao (1966)	Equatorial spread-F maximizes at 2100, then falls off slowly until 0400
Stuart and Titheridge (1969)	Polar cap scintillation maximizes at 1800-2200

Table 7. Seasonal Variations

Author	Observation
Shimazaki (1959)	Maximum spread-F in winter (high latitudes); in summer (low latitudes); varies with longitude (middle latitudes)
Marasigan (1960)	Spread-F maximum in summer at sunspot minimum, and at equinoxes at sunspot maximum, in the equatorial zone
Olesen and Bak Jepson (1966)	Winter maximum at sunspot maximum, in high latitudes
Dueno (1961)	Transequatorial scatter maximizes in equinoxes
Southwork (1960)	Transequatorial scatter maximizes in equinoxes
Carman et al. (1963)	Transequatorial scatter maximizes in equinoxes
Koster (1963)	Equinoctial maximum in equatorial zone
Briggs (1964)	Scintillations show no seasonal variation, but spread-F does show such a variation
Aarons et al. (1964)	Weak seasonal variation in scintillations
Munro (1966)	Daytime scintillations maximize in summer and equinoxes, at midlatitude location; diurnal variation itself has seasonal and sunspot dependences
Katsenelson (1966)	Winter maximum in spread-F at high latitudes
Singleton (1968)	Seasonal variation depends on phase of sunspot cycle, and varies differently with sunspot number in different latitude zones
Stuart and Titheridge (1969)	Seasonal dependence of average diurnal variation observed inside polar cap; diurnal irregularity maximum near sunset (summer and winter), but not at the equinoxes

Table 8. Summary of Irregularity Observations

Parameter	Low Latitudes	Medium Latitudes	High Latitudes
Height	F-region	F-region	E- and F-regions
Irregularity size	$\lesssim$ 1 km	1-10 km	$\lesssim$ 1 km
Patch size	100-1000 km	100-1000 km	(?)
Patch alignment	North-South (?)	East-West	(?)
Magnetic activity correlation	Negative	Positive	Positive, with possible time delay
Sunspot variation	Positive	Positive	Positive
Seasonal variation	Summer or equinox peak	Complex and variable	Winter maximum (?)
Drifts*	Towards East	Variable	Towards West
Diurnal variation	Pre-midnight maximum	Post-midnight maximum	Pre-midnight maximum
Additional notes	Correlated with vertical F-layer movements Permanent ducts or sheets of ionization appear to exist above F-layer peak	Patches of size several hundred km may be identified with large traveling disturbances Minimum probability of irregularity occurrence	Associated with visible aurora Rapid increase in activity above 55° magnetic latitude Irregularity boundary moves N-S with variations in magnetic and solar activity

*That is, steady component of drift

References

Aarons, J. et al. (1961) Plan. Spa. Sci. 5:169.

Aarons, J., Mullen, J., and Basu, S. (1963) J. Geophys. Research 68:3159.

Aarons, J., Mullen, J., and Basu, S. (1964) J. Geophys. Research 69:1785.

Aarons, J., and Guidice, D.A. (1966) J. Geophys. Research 71:3277.

Aarons, J., Mullen, J.R., and Whitney, H.E. (1969) J. Geophys. Research 74:884.

Allen, R.S., Aarons, J., and Whitney, H. (1964) IEEE Trans. Mil. Electronics, MIL-8:146.

Al'pert, Ia, Belianski, V.B., and Mitiakov, N.A. (1963) Geomag. and Aeronomy 3:10.

Appleton, E.V. (1946) Nature 157:691.

Awe, O. (1961) J. Atmos. Terr. Phys. 21:142.

Barrington, R.E., Belrose, J.S., and Nelms, G.L. (1966) Electron Density Profiles in Ionosphere and Exosphere, F. Frihagen, Ed., North-Holland, Amsterdam, p. 387.

Barrington, R.E., and McEwan, D.J. (1967) Space Research VII, North-Holland, Amsterdam, p. 624.

Basler, R.P., and DeWitt, R.N. (1962) J. Geophys. Research 67:587.

Bateman, R., Finney, J.W., Smith, E.K., Tveten, L.H., and Watts, J.M. (1959) J. Geophys. Research 64:403.

Bates, H.F., Albec, P.R., and Hunsaker, R.D. (1966) J. Geophys. Research 71:1413.

Benson, R.F. (1960) J. Geophys. Research 65:1981.

Beynon, W.J.G., and Jones, E.S.O. (1964) J. Atmos. Terr. Phys. 26:1175.

Bischoff, K. (1967) Geomag. and Aeronomy 7:533.

Blevis, B.C., Day, J.W.B., and Roscoe, O.S. (1963) Can. J. Phys. 41:1359.

Bol'shoi, A.A. (1966) Cosmic Research 4:502.

Bolton, J.G., Slee, O.B., and Stanley, J.G. (1953) Australian J. Phys. 6:434.

Bowman, G.G. (1960a) Plan. Spa. Sci. 2:133.

Bowman, G.G. (1960b) Plan. Spa. Sci. 2:150.

Bowman, G.G. (1968) J. Atmos. Terr. Phys. 30:721.

Bramley, E.N. (1951) Proc. IEE 98(II):19.

Bramley, E.N. (1953) Proc. Roy. Soc. (London) 220:39.

Bramley, E.N., and Peart, M. (1965) J. Atmos. Terr. Phys. 27:1201.

Brenan, P.M. (1960) J. Atmos. Terr. Phys. 19:287.

Briggs, B.H. (1958a) J. Atmos. Terr. Phys. 12:89.

Briggs, B.H. (1958b) J. Atmos. Terr. Phys. 12:34.

Briggs, B.H. (1964) J. Atmos. Terr. Phys. 26:1.

Briggs, B.H. (1965) J. Atmos. Terr. Phys. 27:991.

Briggs, B.H., and Parkin, I.A. (1963) J. Atmos. Terr. Phys. 25:339.

Briggs, B.H., and Phillips, G.J. (1950) Proc. Phys. Soc. (London) 63:907.

Calvert, W., and Cohen, R. (1961) J. Geophys. Research 66:3125.

References

Calvert, W., and Schmid, C.W. (1964) J. Geophys. Research 69:1839.

Calvert, W., VanZandt, T.E., Knecht, R.W., and Goe, G.B. (1961) Proc. Internat. Conf. on Ionosphere (London), Inst. of Phys. and Phys. Soc.

Carman, E.H., and Kilfoyle, B.P. (1963) J. Geophys. Research 68:5605.

Carman, E.H., Gibson-Wilde, B.C., and Conway, R.J. (1963) Australian J. Phys. 16:171.

Carpenter, D.G. (1966) J. Geophys. Research 71:693.

Carpenter, D.G. (1967) J. Geophys. Research 72:2969.

Catchpoole, J.R. (1967) J. Atmos. Terr. Phys. 29:819.

Chan, K.L., and Villard, O.G. (1962) J. Geophys. Research 67:973.

Chapman, J.H. (1953) Can. J. Phys. 31:120.

Chidsey, I. (1966) Proc. 9th AGARD Symposium, Copenhagen, 1964, in AGARDograph 95, Spread-F and its Effects upon Radiowave Propagation and Communication, P. Newman, Ed., Technavision, London.

Chivers, H.J.A. (1960) J. Atmos. Terr. Phys. 19:54.

Chivers, H.J.A., and Davies, R.D. (1962) J. Atmos. Terr. Phys. 24:573.

Chivers, H.J.A., and Greenhow, J. (1959) J. Atmos. Terr. Phys. 17:1.

Clemesha, B.R. (1964) J. Atmos. Terr. Phys. 26:91.

Clemesha, B.R., and Wright, R.W. (1966) Proc. 9th AGARD Symposium, Copenhagen, 1964, in AGARDograph 95, Spread-F and its Effects upon Radiowave Propagation Communication, P. Newman, Ed., Technavision, London.

Clemmow, P.C., and Johnson, M.A. (1959) J. Atmos. Terr. Phys. 10:21.

Cohen, R., and Bowles, K.L. (1961) J. Geophys. Research 66:1081.

Cole, K.D. (1962) Australian J. Phys. 15:223.

Cummings, W.D., LaQuey, R.E., O'Brien, B.J., and Walt, M. (1966) J. Geophys. Research 71:1319.

Dagg, M. (1957) J. Atmos. Terr. Phys. 11:118.

Dalgarno, A., and Walker, C.G. (1964) J. Atmos. Sci. 21:463.

Davies, K., and Barghausen, A.F. (1966) Proc. 9th AGARD Symposium, Copenhagen, 1964, in AGARDograph 95, Spread-F and its Effects upon Radiowave Propagation Communication, P. Newman, Ed., Technavision, London.

Davis, T.N., and Smith, L.L. (1965) J. Geophys. Research 70:1127.

DeBarber, J.P., and Ross, W.J. (1966) Proc. 9th AGARD Symposium, Copenhagen, 1964, in AGARDograph 95, Spread-F and its Effects upon Radiowave Propagation Communication, P. Newman, Ed., Technavision, London.

Drachev, L.A., and Berezin, Yu. V. (1957) Radiotek. i Elektron. 2:1234.

Dueno, B. (1955) Cornell Technical Report No. 37.

Dueno, B. (1961) J. Geophys. Research 66:2355.

Duncan, R.A. (1960) J. Atmos. Terr. Phys. 18:89.

Dyce, R.B., Dolphin, L.T., Leadabrand, R.L., and Long, R.A. (1959) J. Geophys. Research 64:1815.

References

Dyson, P.L. (1967a) Australian J. Phys. 20:467.

Dyson, P.L. (1967b) J. Atmos. Terr. Phys. 29:857.

Egeland, A. (1964) Arkiv Geophys. 4:103.

Eyfrig, R.W. (1963) J. Geophys. Research 68:2529.

Feldshtein, Ya, Shevnina, N.F., and Lukina, L.V. (1966) Geomag. and Aeronomy 6:247.

Flood, W.A. (1966) Proc. 9th AGARD Symposium, Copenhagen, 1964, in AGARDograph 95, Spread-F and its Effects upon Radiowave Propagation and Communication, P. Newman, Ed., Technavision, London.

Forsyth, P.A., and Paulson, K.V. (1961) Can. J. Phys. 39:502.

Frank, L.A., Van Allen, J.A., and Graven, J.D. (1964) J. Geophys. Research 69:3155.

Frihagen, J. (1963) Radio Astronomical and Satellite Studies of the Ionosphere, North-Holland, Amsterdam.

Frihagen, J., and Liszka, L. (1965) J. Atmos. Terr. Phys. 27:513.

Frihagen, J., and Troim, J. (1960) J. Atmos. Terr. Phys. 18:75.

Frihagen, J., and Troim, J. (1961) J. Atmos. Terr. Phys. 20:215.

Georges, T.M. (1967) J. Geophys. Research 64:1225.

Goldberg, R.A., Kendall, P.C., and Schmerling, E.R. (1963) J. Geophys. Research 68:417.

Greenhow, J.S. (1959) J. Geophys. Research 64:2208.

Greenhow, J.S., Neufeld, E.L., and Watkins, C.D. (1960) J. Atmos. Terr. Phys. 25:121.

Greenspan, J.A. (1966) J. Atmos. Terr. Phys. 28:739.

Gusev, V.D. et al. (1958) Doklady Akad. Nauk S.S.S.R. 123:817.

Gustaffson, G. (1967) Plan. Spa. Sci. 15:277.

Hagg, E.L. (1967) Can. J. Phys. 32:790.

Hagg, E.L., and Hanson, G.H. (1954) Can. J. Phys. 32:790.

Harang, L., and Malmjord, K. (1961) Geophys. Publikasjoner 23:No. 3.

Hartz, T.R. (1955) Can. J. Phys. 33:476.

Hartz, T.R. (1959) Can. J. Phys. 37:1137.

Hartz, T.R., and Brice, N.M. (1967) Plan. Spa. Sci. 15:301.

Heritage, J.L., and Fay, W.J. (1968) J. Geophys. Research 73:2469.

Herman, J.R. (1966) Rev. Geophys. 4:255.

Hewish, A. (1951) Proc. Roy. Soc. (London) 209A:81.

Hewish, A. (1952) Proc. Roy. Soc. (London) 214A:494.

Hines, C.O. (1960) Can. J. Phys. 38:1441.

Hook, J.L., and Owren, L. (1962) J. Geophys. Research 67:5353.

Jespersen, J.L., and Kamas, G. (1964) J. Atmos. Terr. Phys. 26:457.

Joint Satellite Studies Group (1965) Plan. Spa. Sci. 13:51.

References

Joint Satellite Studies Group (1968) Plan. Spa. Sci. 16:775.

Jones, I.L. (1960) J. Atmos. Terr. Phys. 19:26.

Kashin, A.A., Klimanov, F.P., Kushnerevskiy, Yu.V., Mirkotan, S.F., and Nerovnya, L.K. (1966) Geomag. and Aeronomy 6:876.

Katsenelson, I.B. (1966) Geomag. and Aeronomy 6:805.

Kent, G.S. (1959) J. Atmos. Terr. Phys. 16:10.

Kent, G.S. (1960) J. Atmos. Terr. Phys. 19:272.

Kent, G.S. (1961) J. Atmos. Terr. Phys. 20:255.

Kent, G.S., and Koster, J.R. (1966) Proc. 9th AGARD Symposium, Copenhagen, 1964, in AGARDograph 95, Spread-F and its Effects upon Radiowave Propagation and Communication, P. Newman, Ed., Technavision, London.

Kent, G.S., and Koster, J.R. (1961) Nature 191:1083.

Khastgir, S.R., and Singh, R.N. (1960) J. Atmos. Terr. Phys. 18:75.

Kidd, W., Silverman, H., Whitney, H., and Aarons, J. (1962) Nature 193:1246.

Kim, J.S., and Wang, C.S. (1967) J. Atmos. Terr. Phys. 29:829.

King, J.W. (1968) J. Atmos. Terr. Phys. 30:391.

King, J.W., Smith, P.A., Read, K.C., and Seabrook, C. (1967) J. Atmos. Terr. Phys. 29:1237.

Klemperer, W.K. (1963) J. Geophys. Research 68:3191.

Knecht, R.W. (1960) Nature 187:927.

Knudsen, W.C., and Sharp, G.W. (1968) J. Geophys. Research 73:6275.

Ko, H.C. (1960) Proc. IRE 48:1871.

Kokurin, Yu. L. et al. (1961) Radio Eng. and Electron. Phys. 6:653.

Koster, J.R. (1958) J. Atmos. Terr. Phys. 12:100.

Koster, J.R. (1963) J. Geophys. Research 68:2579.

Koster, J.R. (1965) Private communication.

Koster, J.R., and Wright, R.W. (1960) J. Geophys. Research 65:2303.

Kotadia, K.M. (1956) J. Sci. Ind. Research (India) 15:543.

Kotadia, K.M. (1962) J. Atmos. Terr. Phys. 24:659.

Kusnerevski, Iu. V., and Zajarnaja, E.S. (1959) Comm. for IGY (USSR) Acad. of Sci. p. 22.

Lansinger, J.M., and Fremouw, E.J. (1967) J. Atmos. Terr. Phys. 29:1229.

Lawrence, R.S., Jespersen, J.L., and Lamb, R.C. (1961) NBS J. Research 65D:333.

Leadabrand, R.L., Presnell, R.I., Berg, M.R., and Dyce, R.B. (1959) J. Geophys. Research 70:4235.

Liszka, L. (1964) Arkiv. Geofysik 4:211.

Little, C.G. (1951) Mon. Not. Roy. Astron. Soc. 111:289.

Little, C.G., and Lawrence, R.S. (1960) J. Research NBS 64D:335.

Little, C.G., and Maxwell, A. (1952) J. Atmos. Terr. Phys. 2:356.

References

Little, C.G., Reid, G.C., Stiltner, E., and Merritt, R.P. (1962) J. Geophys. Research 67:1763.

Lockwood, G.E.K., and Petrie, L.E. (1963) Plan. Spa. Sci. 11:327.

Lyon, G.F., and Forsyth, P.A. (1962) Can. J. Phys. 40:749.

Lyon, G.F., and Skinner, N.J. (1960) Nature 187:1086.

Lyon, G.F., Skinner, N.J., and Wright, R.W. (1960) J. Atmos. Terr. Phys. 19:145.

Maehlum, B., and O'Brien, B.J. (1963) J. Geophys. Research 68:997.

Malko, L.N. (1966) Geomag. and Aeronomy 6:243.

Marasigan, V. (1960) J. Atmos. Terr. Phys. 18:257.

Mariani, F. (1963) J. Atmos. Sci. 20:479.

Marovich, E., and Roach, F.E. (1963) J. Geophys. Research 68:1885.

Martyn, D.F. (1955) Physics of the Ionosphere, Phys. Soc. (London) p. 254.

Martyn, D.F. (1959) Nature 183:1382.

Mass, J., and Houminer, Z. (1967) J. Geophys. Research 72:4940.

Maxwell, A., and Dagg, M. (1954) Phil. Mag. 45:551.

McClure, J.P. (1964) J. Geophys. Research 69:2775.

McDiarmid, I.B., and Burrows, J.R. (1964) Can. J. Phys. 42:616.

McEwan, D.I., and Barrington, R.E. (1967) Can. J. Phys. 45:13.

McNicol, R.W.E., and Webster, H.C. (1956) Australian J. Phys. 9:272.

Millman, G.H., and Moyceyunas (1965) J. Geophys. Research 70:81.

Mills, B.Y., and Thomas, A.B. (1951) Australian J. Sci. Research A4:158.

Muldrew, D.B. (1965) J. Geophys. Research 70:2635.

Munro, G.H. (1950) Proc. Roy. Soc. (London) A202:208.

Munro, G.H. (1963) J. Geophys. Research 68:1851.

Munro, G.H. (1966) Radio Sci. 1:1186.

Nelms, G.L. (1966) Electron Density Profiles in Ionosphere and Exosphere, F. Frihagen, Ed., North-Holland, Amsterdam, p. 358.

O'Brien, B.J. (1963) J. Geophys. Research 68:989.

Olesen, J.K., and Bak Jepson, S. (1966) Proc. 9th AGARD Symposium, Copenhagen, 1964, in AGARDograph 95, Spread-F and its Effects upon Radiowave Propagation and Communication, P. Newman, Ed., Technavision, London.

Osborne, B.W. (1951) J. Atmos. Terr. Phys. 2:66.

Owren, L., Fremouw, E.J., and Hunsucker, R.D. (1966) Proc. 9th AGARD Symposium, Copenhagen, 1964, in AGARDograph 95, Spread-F and its Effects upon Radiowave Propagation and Communication, P. Newman, Ed., Technavision, London.

Paulikas, S.C., and Freden, G.A. (1964) J. Geophys. Research 69:1239.

Penndorf, R. (1962) J. Geophys. Research 67:2279.

Penndorf, R. (1966) Proc. 9th AGARD Symposium, Copenhagen, 1964, in AGARDograph 95, Spread-F and its Effects upon Radiowave Propagation and Communication, P. Newman, Ed., Technavision, London.

References

Penndorf, R., and Coroniti, S.C. (1958) J. Geophys. Research 63:789.

Piddington, J.H. (1964) Plan. Spa. Sci. 12:127.

Presnell, R.I., Leadabrand, R.L., Petersen, A.M., Dyce, R.B., Schlobohm, J.C., and Berg, N.R. (1959) J. Geophys. Research 64:1179.

Proshkin, E.G., and Kashcheev, B.L. (1957) Radiotek. i Elektron. 2:1.

Rangaswami, S., and Kapasi, K.B. (1963) J. Atmos. Terr. Phys. 25:721.

Rao, B.C.N. (1966) J. Atmos. Terr. Phys. 28:1207.

Rao, B.R., and Murty, D.S. (1956) J. Sci. Ind. Research 13A:462.

Rao, B.R., Rao, E.B., and Murty, Y.V.R. (1959) Nature 183:667.

Rao, M.S., and Rao, B.R. (1957) J. Atmos. Terr. Phys. 10:307.

Rao, M.S., Rao, B.R., and Pant, P.R.R. (1960) J. Atmos. Terr. Phys. 17:345.

Rastogi, R.G. (1959) J. Atmos. Terr. Phys. 14:31.

Rastogi, R.G. (1960) J. Atmos. Terr. Phys. 18:315.

Rastogi, R.G. (1963) J. Atmos. Terr. Phys. 25:393.

Reddy, B.M., Brace, L.H., and Findlay, J.A. (1967) J. Geophys. Research 72:2709.

Rees, M.H. (1964) Plan. Spa. Sci. 12:722.

Renau, J. (1960) J. Geophys. Research 65:3219.

Ross, W., and Bramley, E.N. (1947) Nature 159:132.

Ross. W., and Bramley, E.N. (1949) Nature 164:335.

Ryan, W.D., and Harrower, G.A. (1960) Can. J. Phys. 38:883.

Sayers, J. (1965) Space Research V, North-Holland, Amsterdam, p. 165.

Schmelkovsky, K.K. (1963) Geomag. and Aeronomy 3:907.

Shimazaki, T. (1959) J. Radio Research Labs. (Japan) 6:651.

Singleton, D.G. (1960) J. Geophys. Research 65:3615.

Singleton, D.G. (1961) J. Atmos. Terr. Phys. 23:219.

Singleton, D.G. (1962) J. Atmos. Terr. Phys. 24:871.

Singleton, D.G. (1963) J. Atmos. Terr. Phys. 25:121.

Singleton, D.G. (1968) J. Geophys. Research 73:295.

Skinner, N.J., and Wright, R.W. (1957) Proc. Phys. Soc. (London) B70:833.

Skinner, N.J., Hope, J., and Wright, R.W. (1958) Nature 182:1363.

Somayajulu, Y.V., Rao, B.R., and Rao, E.B. (1953) Nature 172:818.

Southwork, M.P. (1960) J. Geophys. Research 65:601.

Spencer, M. (1955) Proc. Phys. Soc. (London) 68B:493.

Stringer, W.J., and Belon, A.E. (1967) J. Geophys. Research 72:4423.

Stuart, G.F., and Titheridge, J.F. (1969) J. Atmos. Terr. Phys. 31:905.

Taylor, H.E., and Hones, E.W. (1965) J. Geophys. Research 70:3605.

Thome, G.D. (1964) J. Geophys. Research 69:4047.

References

Titheridge, J.F. (1963) J. Geophys. Research 68:3399.

Vaisberg, O.L. (1966) Space Research VII, North-Holland, Amsterdam, p. 369.

Van Zandt, T.E., Steiger, W.R., Roach, F.E., Peterson, V.L., and Norton, R.B. (1965) Report on Equatorial Aeronomy, F. de Mendonca, Ed., Space Physics Laboratory, Brazilian Space Commission, National Council of Research, São Jose dos Campos, São Paulo, Brazil, p. 349.

Vitkevich, V.V. (1958) Radiotek. i Elektronika 3:27.

Vitkevich, V.V. (1960) Soviet Astron. 3:609.

Vitkevich, V.V., and Kokurin, Iu. L. (1957) Radiotek. i Elektronika 2:13.

Wagner, L.S. (1962) J. Geophys. Research 67:4187.

Walters, G.K. (1964) J. Geophys. Research 69:1769.

Warwick, J.W. (1964) Radio Sci. 68D:179.

Watkins, C.D. (1960) J. Atmos. Terr. Phys. 19:289.

Wells, H.W. (1954) J. Geophys. Research 58:284.

Wild, J.P., and Roberts, J.A. (1956) J. Atmos. Terr. Phys. 8:55.

Yeh, K.C., and Swenson, G.W. (1959) J. Geophys. Research 64:2281.

Yeh, K.C., and Swenson, G.W. (1966) Proc. 9th AGARD Symposium, Copenhagen, 1964, in AGARDograph 95, Spread-F and its Effects upon Radiowave Propagation and Communication, P. Newman, Ed., Technavision, London.

Yeh, K.C. et al. (1963) Private communication.

Yeroukhimov, L.M. et al. (1968) Geomag. and Aeronomy 8:138.

Zelenkov, V.E., and Rudneva, N.M. (1967) Geomag. and Aeronomy 7:737.

Application of the Statistics of Ionospheric Scintillation to VHF and UHF Systems

Richard S. Allen

1. INTRODUCTION

A great amount of data on the effects of ionospheric irregularities exists from scintillation studies made since 1949. Most of this is in the form of indices for the depth or rate of fluctuation of the intensity of radio waves. However, specific organizations need evidence that is not explicitly contained in the reports of these studies. Systems now in use, as well as those being developed, require statistical summaries and reliable techniques for predicting the effects of ionospheric irregularities at remote locations, on new radio frequencies, and during extremes of geophysical conditions.

It is not practical to rescale existing data to meet these new requirements, nor is it practical to reinstrument all of the observatories so that they can measure the critical radio frequencies for the latitude-longitude network needed to collect new data. Rather, enough new measurements can be performed to relate statistically the new requirements, such as depth and duration of deep fading, to the existing indices. To describe the variation of these fluctuations in terms applicable to communication problems, it is convenient to use a morphological approach expressed in terms of three classes of variables that can be isolated in the statistical data: (1) stimulus variables that represent changes in the forces that produce the irregularities; (2) trait variables that characterize the ability of the ionosphere to

respond to stimulation; and (3) experimental variables that affect the amount of fluctuation observed for given irregularities.

1.1 Variation With Magnetic K Index

Magnetic K index is used here to relate the variation in response of irregularities to variation in the solar energy carried by the solar wind.

Individual observatories characterize the degree of disturbance of the local magnetic field during 3-hr periods by indices varying from 0 to 9. Normalized data from a world-wide network are then combined in a planetary index, Kp. Distribution functions for Kp conditional on calendar years are shown in Figure 1. The highest values represent periods when the magnetic field displayed major changes identified with periods of intense solar disturbance. Note that the significant change with solar cycle is a change in the proportion of these high indices.

Just how the depth of scintillation varies with the state of magnetic activity depends on the geographic latitude and longitude of the irregularity region. At high geomagnetic latitudes, the depth of scintillation increases with magnetic K index. Figure 2 contains distributions for sets of observations conditional on local magnetic K index. They represent the ionosphere region 51°N lat. to about 55°N lat., as seen from Hamilton, Massachusetts, using the radio star Cassiopeia A. Effects of the increased thickness of the irregularity region arising from the slant viewing angle, constant within the sample, have not been removed. For any statistic in the data, such as median or decile, there is nearly linear increase with the index of the state of magnetic activity.

The change of this dependence with latitude is summarized (Figure 3) by data from a study of the 54-MHz beacon of satellite Transit 4A, taken at Hamilton, Massachusetts, during regularly scheduled periods each month from January 1962 to February 1965. Conditional samples were based on subionospheric (400 km) ranges of ±10° long. and 5° lat. Mean values were produced for all data in subsets determined by integral values of the local magnetic K index K_{Fr} from Fredericksburg, Virginia. Again, the effects of elevation angle have not been removed; this is unimportant since the effect is constant within each latitude sample.

The results for data pooled in this fashion can be summarized as follows:

1. At high latitude there is an increase in depth of scintillation for increase of magnetic K index. The functional behavior of mean values can be related to the functional behavior of other statistics, such as the medians of Figure 2.
2. There is a progressive change in the functional relationship with decreasing latitude until, at mid-latitudes, the depth of scintillation does not increase with K index until the K index exceeds 4 or 5. Studies of a limited number of magnetic storms indicate that the depth of scintillation at mid-latitudes increases sharply with very high K index.

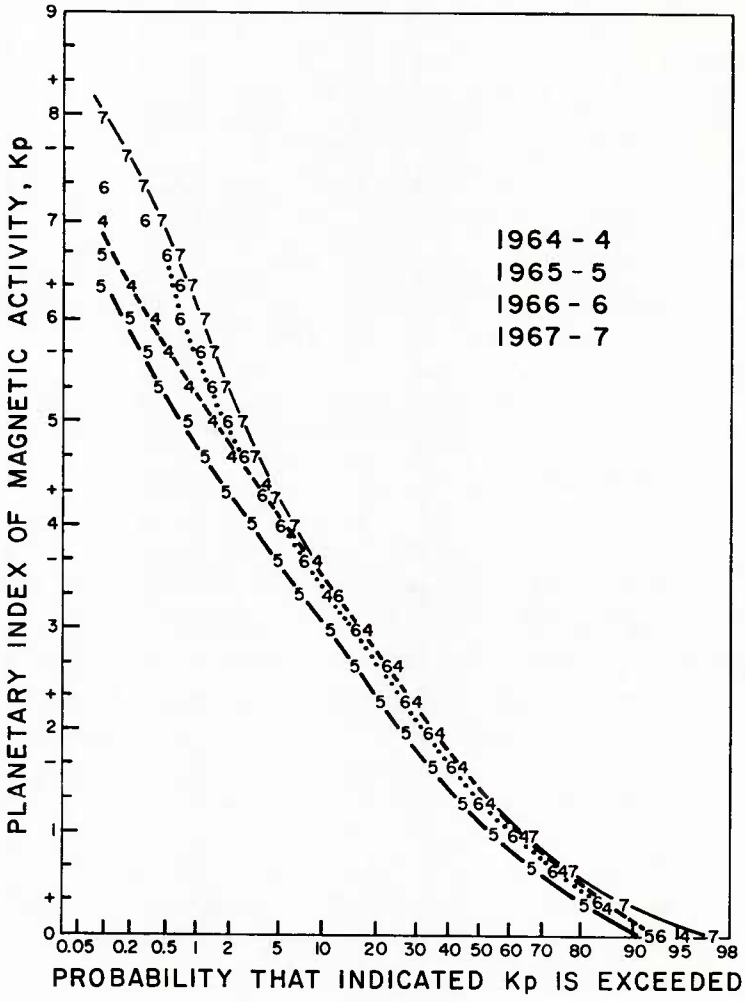

Figure 1. Variation of Magnetic Index, 1964-1967. The planetary index of magnetic activity is not normally distributed. Note the disproportionate increase of high K values for years of increased solar activity over 1964-1965, the period of solar minimum

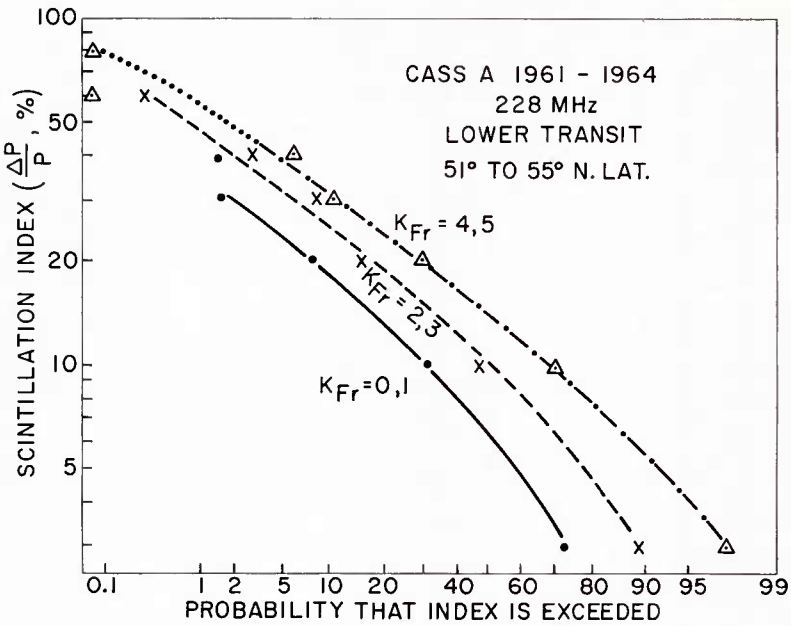

Figure 2. Variation of Scintillation Index with Local Magnetic K Index. The probability that a given depth of scintillation is exceeded increases nearly linearly with local K index for observations at the southern edge of the auroral region

3. As the irregularity region approaches equatorial latitudes, the functional relationship inverts and the depth of scintillation decreases with increasing K index (latitude interval 30° to 35° in Figure 4). Special studies in the equatorial region over Africa (Koster and Wright, 1960) have shown that there is negligible change with K index during the minimum of the solar cycle, but a strong inverse relationship during solar maximum.

1.2 Experimental Variables

For identical conditions in the irregularity region, the fluctuations found by different observers will depend on several experimental variables. These are, principally, the frequency and bandwidth of the radio wave signal and the geometric angle at which the irregularity region is viewed. In some cases the distance of the source from the irregularities and the separation of antennas used for space diversity on the ground can also be treated as experimental variables.

If these variables are independent of the trait and stimulus variables, then some form of an analytic function can be uniquely determined to represent their variation, as is done for radio frequency in the following section. Otherwise a set of functions must be determined, conditional on the other variables that influence their behavior.

1.3 Variation With Radio Frequency

The theoretical prediction of the frequency variation of scintillation depends on several parameters of the irregularity region. Although these are generally unknown, limits can be derived. If the irregularity region can be represented by a thin screen, then close to the irregularity region the depth of scintillation is almost inversely related to the square of the frequency; far from the region it is inversely related to the first power of the radio frequency (Briggs and Parkin, 1963). As the thickness of the layer becomes more significant, the exponent decreases toward zero.

Empirical studies of this variation were made by AFCRL at Hamilton, Massachusetts (Aarons et al., 1967). Simultaneous observations were taken at 30, 63, 113, and 228, using the 84-ft antenna, for the overhead and northern regions covered by the daily motion of the radio star Cassiopeia A. Figure 4 shows cumulative distributions for observations made through the auroral region. When the irregularities are weak, the depth of scintillation and, hence, the scintillation indices are low. The depth of fluctuation then depends inversely on the square of the radio frequency. As the irregularities are enhanced, the indices increase and the exponent of frequency dependence decreases.

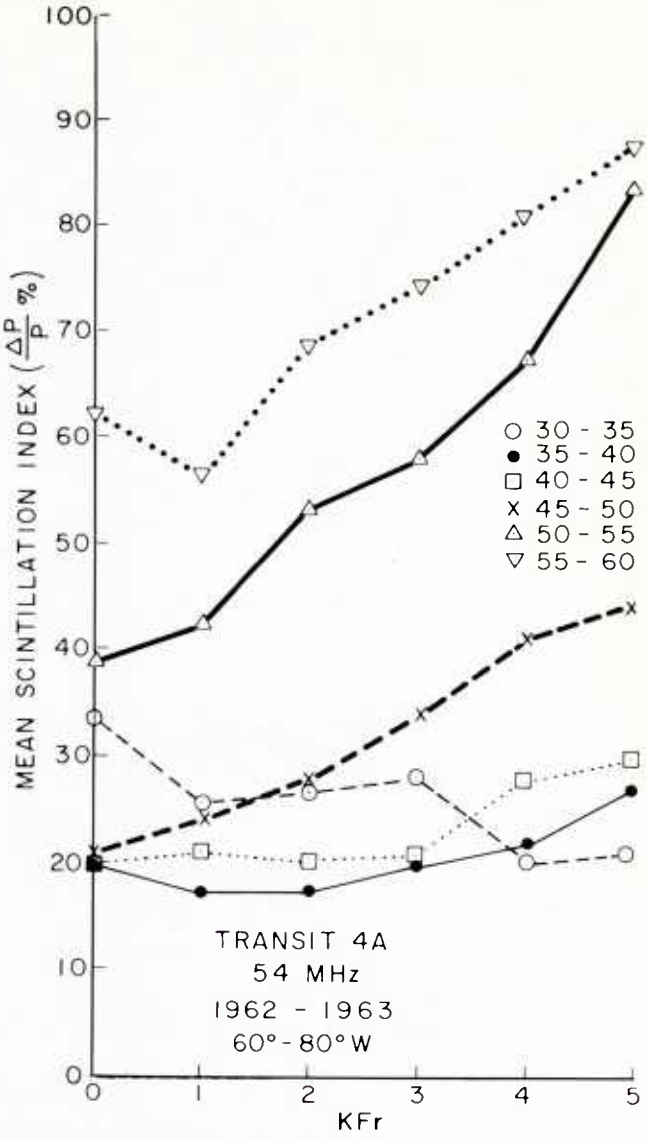

Figure 3. Latitude Change of the Magnetic K Dependence. At high latitudes above Hamilton, Massachusetts, the mean depth of scintillation increases nearly linearly with local magnetic K index. Overhead, in the region 40° to 45° geographic, there is no change until K is greater than about 5. Southward, 30° to 35°, the mean depth of scintillation decreases with increasing K index

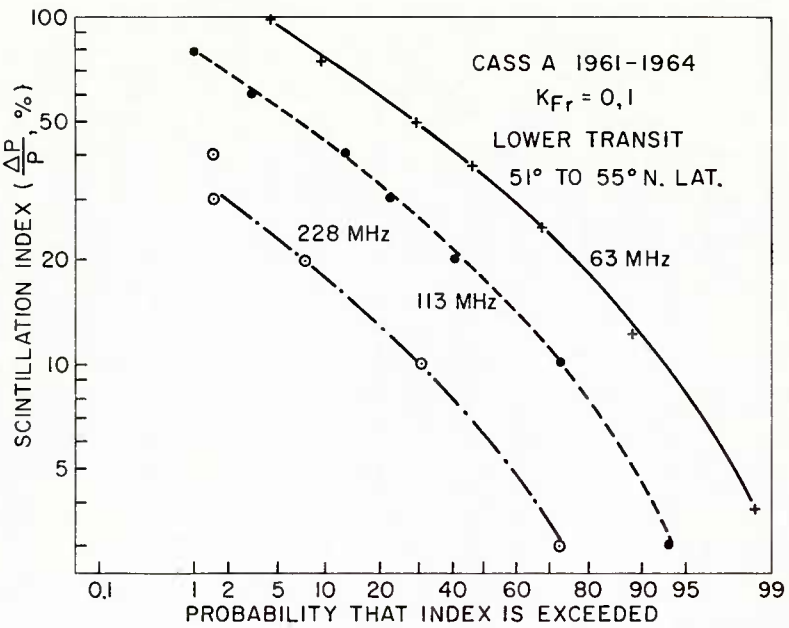

Figure 4. Variation of the Depth of Scintillation with Radio Frequency. At low depths of scintillation there is a nearly inverse square-law-dependence on radio frequencies for low depth of scintillation. As the intensity of the irregularity region increases, the exponent of dependence decreases

Results for the auroral (51° to 55° N lat) and for the overhead regions (43° to 45° N lat) are summarized in Figure 5. The frequency variation seems to depend only on the effective strength of the irregularities. No appreciable change was noted between the latitude samples. Further, no systematic difference was found for samples conditional on the state of the local magnetic field, an indicator of disturbance on the ionosphere. It is not known if these results will also apply to low latitudes and the equatorial region.

1.4 Geometric Variation

If the distribution of irregularities of the ionosphere were similar to a reasonably thin screen, the depth of fluctuation would be expected to vary with elevation angle to the source in the same manner as the apparent thickness of the screen varied. It is now known that this is not valid at all latitudes.

When a statistical latitude variation can be derived from mutually consistent observations, as in the JSSG study to be discussed in Section 1.6, the nonoverhead observations at a particular site can be examined for geometric effects. Data from the JSSG study shown in Figure 6 were restricted to common periods of observations for which the magnetic K index was less than 3 and, therefore, represent the main

geometric features during quiet geomagnetic conditions. At midlatitudes where the average depth of scintillation was low, the nonoverhead indices increase toward the horizon more or less as the secant of the zenith angle times the expected subionospheric depths of scintillations. At subauroral latitudes where the overhead depth of scintillation increased somewhat, observations southward still increase with the slant thickness of the irregularity region but northward the increase is less than expected. This is probably the result of several factors: a thickening of the irregularity region; a reduction of slant range to the irregularity; and perhaps also a decrease in the size of the irregularities.

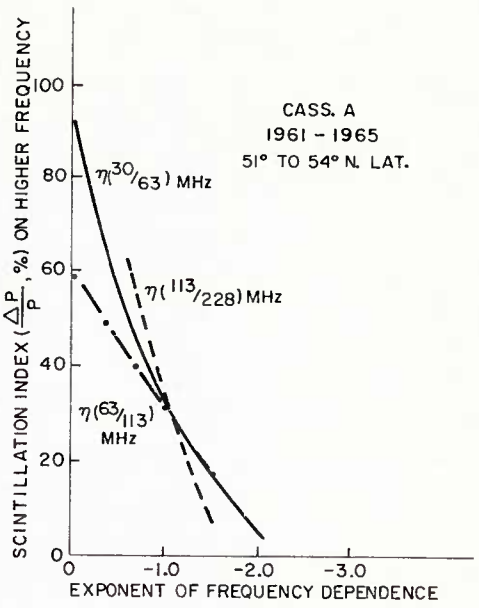

Figure 5. Variation of Frequency Dependence with Scintillation Index. Observation of Cassiopeia A at 30, 63, 113, and 228 MHz indicates that the mean frequency dependence can be specified in terms of the depth of scintillation on one of the frequencies

1.5 Trait Variables

Trait variables (t_i) characterize the ability of the ionosphere to respond to a given stimulus. For example, a difference in response on two different occasions may be due to a difference in the recombination rates of ions and electrons and, hence, a difference in the lifetime for initially identical irregularities. Physical parameters, such as recombination rates, change because of undetected changes in the energy sources that affect the ionosphere. The changes in the irregularity behavior caused by integrated changes in physical parameters can be characterized by trait variables, such as the cyclic changes over the day, solar month, year, and sunspot period. Each of these most likely combine the effects of several parameters, such as electron temperature, neutral gas density, ionospheric wind systems, and so on. Less easy to identify in the data are changes in these trait variables caused by a sudden change in a single parameter, such as a sudden change in composition ratio or in temperature.

Use of trait variables to determine the degree to which the ionosphere responds to physical changes indicates the need for a more reliable way to determine physical parameters and a better theory of irregularity formation and behavior.

Since trait variables are averages over time or space, they represent the integrated effects of a number of undetected, unknown, or sporadic stimuli. An understanding of the physical process at work within the irregularity regions is lost in such a characterization.

For just that reason, trait variables are desirable for a study such as this. By submerging the response of individual events, they establish over-all systematic trends in the response of the whole irregularity region without depending on a complete physical understanding of individual processes.

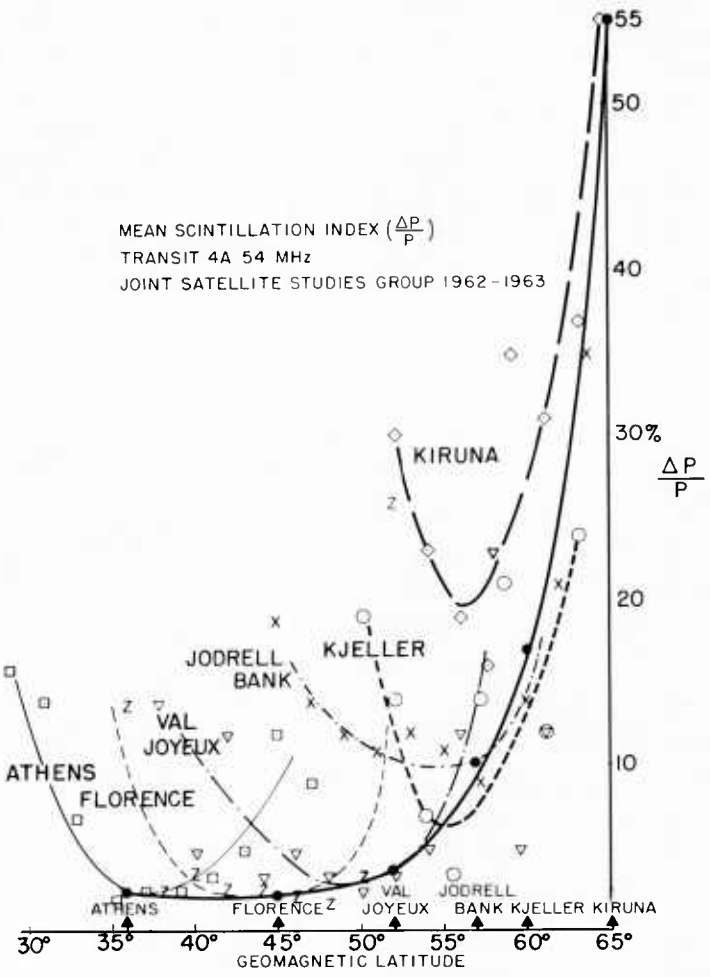

Figure 6. Geometric Variation of the Depth of Scintillation. Derived from simultaneous measurements by members of the Joint Satellite Studies Group. Mean overhead values are linked by a smooth curve representing the latitude variation. Off-vertical observations show the effect of elevation angle

1.6 Latitudinal Variation

Early reports of the scintillation of radio stars (Little, 1951) and beacon satellites (Kent, 1959) noted that the depth of scintillation increased toward the polar region faster than would be expected from purely geometric effects. In a recent study (JSSG, 1968), observations from several stations were combined to establish the quantitative aspects of this variation. Figure 7 summarizes the results from two sets of data.

The first set is from simultaneous observations of the 54-MHz beacon of satellite Transit 4A. The resultant smooth variation with geomagnetic latitude is conditional on nearly identical geometric factors over each JSSG station and on periods of magnetic activity with K index less than 3. The individual observations were spaced from June 1962 to March 1963 by cooperative observational periods selected without meaningful bias.

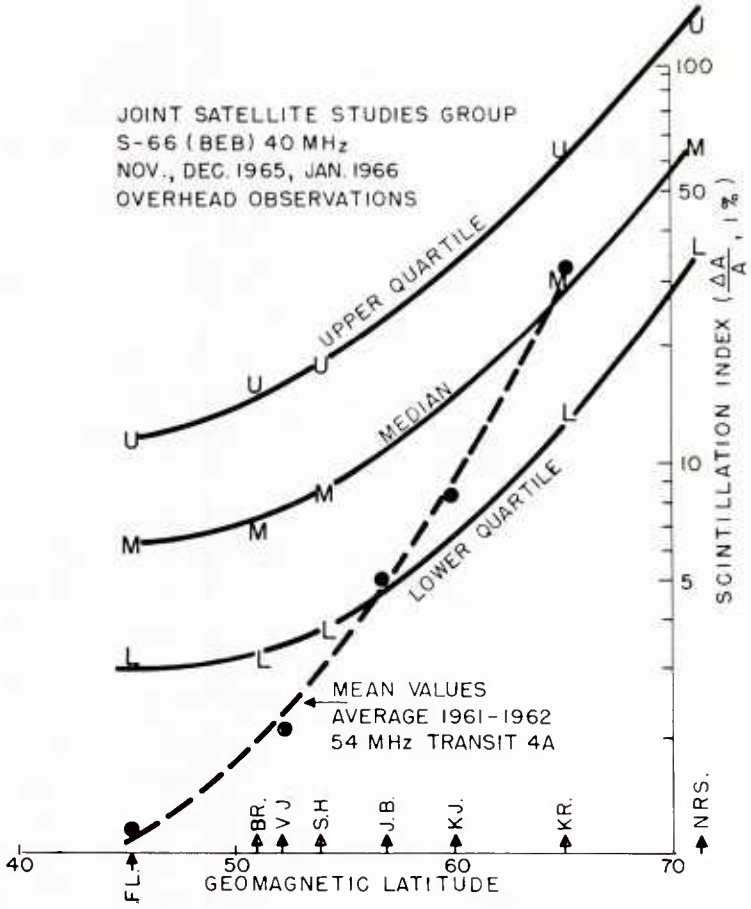

Figure 7. Latitude Variation of the Depth of Scintillation. Derived from simultaneous overhead observations of the Joint Satellite Studies Group. The 1965-1966 results may indicate a change of the latitude variation with solar cycle

The second set of data is the result of simultaneous observations of the 40-MHz beacon of satellite BE-B (S-66). In this case, statistics were produced for all overhead observations during the period 1 November 1965 to 21 January 1966. The resultant latitude variation is flatter than that in the first set, but further study is needed to determine whether the difference is in the prime distribution of irregularities changing with solar cycle or caused by some other factor.

Records of scintillation of the radio beacons on BE-B and the synchronous satellite ATS-3 taken at the AFCRL station at Thule, Greenland, indicate that the latitude function does not dip over the polar region, as do certain auroral phenomena,

but, as yet, there is insufficient data for a quantitative statement.

A second peak of the latitude variation over the equatorial region has been suggested by unpublished JSSG observations of BEB scintillations. It is expected that the quantitative features will be determined from current studies made by JSSG using the 136-MHz beacons of ATS-3 and Canary Bird.

As a final note, the latitudinal variation is a reactive variable, depending on the state of magnetic activity, the time of day, and probably the longitude of observation, as well as other variables. Observations from Hamilton, Massachusetts, in Figure 3 show this for incremental changes in the local index of magnetic activity; the other qualifications follow from evidence on other sections.

1.7 Diurnal—Seasonal Variation

From the early observations of radio star sources it was apparent that there was a nighttime peak in the occurrence and mean intensity of the irregularity regions causing scintillation. A controversy on the existence of a secondary peak during the daytime and the nature of the seasonal variation has only begun to be resolved by recent observations of the beacons of stationary satellites.

Unfortunately, for observations made with either radio stars or low-altitude satellites, the effects of seasonal change cannot be uniquely separated from the effects of diurnal change. For a fixed geographic position of the irregularity region, the time of day when either type of source can be viewed is fixed by season; therefore, in any set of observations, certain pairs of seasonal-diurnal values are always missing. If complementary sets of data are normalized and combined, such as data from several radio stars or satellites, some aspects of the resultant diurnal seasonal variation may be caused by unintentional bias in the normalization process.

Since synchronous satellites remain at fixed positions, analysis of their data does not have this limitation, and seasonal and diurnal effects can be studied separately. Reduced data for observations of the 136-MHz beacon of commercial communication satellite Canary Bird are shown in Figure 8. There is a persistent nighttime peak throughout the year.

The secondary daytime maximum of the scintillations of the Canary Bird beacon during the months of May, June, July, and August 1967 was a principal feature of observations made with the commercial satellite Early Bird during the same period of 1965. The daytime maximum is not significant in similar observations for 1968 made with Canary Bird and with the 137-MHz beacon of the ATS-3 communication satellite.

Comparable daytime scintillations of the Canary Bird 136-MHz beacon were observed at a midlatitude station in Florence, Italy, but they were not found in observations taken at Kiruna, Sweden, near the auroral zone, nor in observations taken at Accra, Ghana, at the magnetic equator.

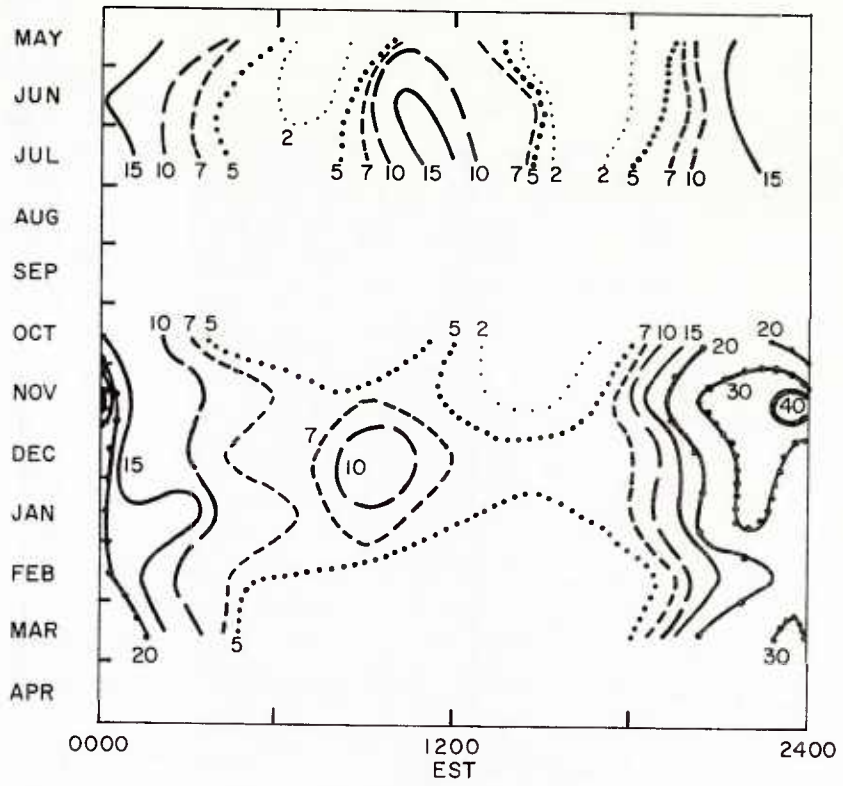

DIURNAL SEASON CONTOURS OF CANARY BIRD 136 MHz SCINTILLATION, HAMILTON, MASS., 1967, 1968.

Figure 8. Diurnal-Seasonal Variation of Scintillation. Continuous observation of the 137-MHz beacon of a synchronous satellite shows that the diurnal and seasonal variations are interrelated. Note the secondary maximums during the day hours.

Like the latitude variation, the diurnal-seasonal variation is also a reactive variable. There is a dependence on the latitude of observation, the state of magnetic activity, and the phase of the sunspot cycle. Details of the dependence of the diurnal-seasonal variation on these other variables are still being determined.

1.8 Variation With Phase of the Solar Cycle

Briggs (1964) has shown that the depth of scintillation of 38-MHz signals of Cassiopeia A received at Cambridge, England, varied systematically with the solar cycle from 1950 to 1961. Since his data were classified by semilogarithmic indices ranging from 0 to 5 and averaged over each period, it is difficult to extend his results to other frequencies, times, or latitudes.

In order to compare the mean values of his semilogarithmic class intervals with statistics derived from linear indices, as in the present study, a conversion is necessary. From the sample records that defined the Cambridge class intervals,

linear indices can be established using the arbitrary rules defined above. The Cambridge index is then a translated logarithm of the AFCRL index. Since the studies of the Hamilton observations have shown that the logarithm of the depth of scintillation is almost normally distributed (Figures 2, 4, and 7), the mean value of the data reduced by Briggs is nearly the median value of the distribution function of the depth of scintillation for each observation period. Therefore, Briggs' data can be transformed as in Figure 9. The logarithm of the depth of scintillation depends almost linearly on the yearly average of the sunspot number.

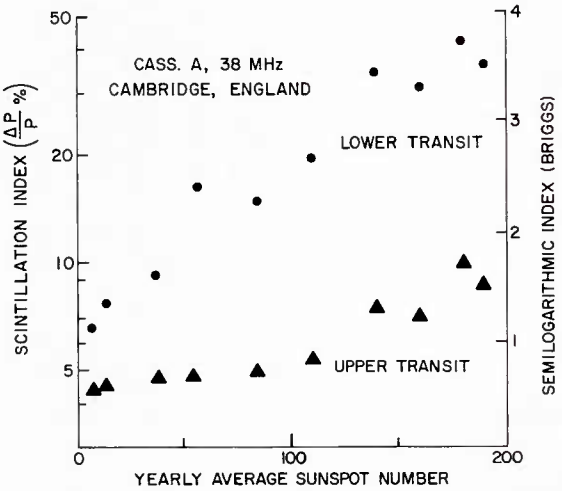

Figure 9. Variation of Scintillation with Solar Cycle. There is a linear dependence of the logarithm of scintillation index with the yearly mean sunspot number. The proportionate increase is the same in the auroral zone as near overhead at Cambridge, England [after Briggs (1964) J. Atmos. Terr. Phys. 26:1]

This variation with sunspot number (or with the phase of the sunspot cycle) can be extended to other frequencies by using the empirical frequency dependence discussed in Section 1.3.

The differences between the behavior for the overhead and lower transit observations indicate that this variation is dependent on the latitude of the irregularity regions and requires further study.

2. APPLICATION TO SYSTEM PROBLEMS

A current example will demonstrate how the morphological data can be applied to a system requirement. Consider an aircraft over the North Atlantic depending on FM voice communication and pulsed navigation system, where VHF signals are relayed between the aircraft and a synchronous satellite. What prediction can be made for fading greater than 3, 6, and 10 dB below normal signal level?

In a special study at AFCRL, the 228-MHz beacon of experimental communication satellite LES-5 was used to establish a link between the empirical scintillation indices and the duration of fading. For observations between 1 August and 31 December 1967, each 15-min sample was scaled for a scintillation index of from 0 to 100, as defined in Section 3. In addition, the duration of fading 3, 6, 10, and 20 dB below normal level was measured for each sample showing intense scintillation.

Table 1 compares the duration of deep fading with scintillation index. The 228-MHz beacon faded 3 dB below its expected intensity only about 0.15 percent of the 1100-hr observation.

Table 1. Minutes of Fading Below Set Levels

Fading Level (dB)	Range of Scintillation Index			
	40-56	57-79	80-100	Total
$\geq$ 3	5.0	21.1	66.2	92.3
$\geq$ 6	0.9	5.5	29.3	35.7
$\geq$ 10	-	0.8	9.5	10.3
$\geq$ 20	-	0.1	2.0	2.1
Observation Time	480	195	240	915

Although the data in Table 1 represent results for a particular set of conditions, they can be used for comparative analysis. For instance, when the scintillation index of a sample period is greater than about 57, the signal will be below the 3-dB level about 20 percent of the time, or below the 10-dB level about 2.5 percent of the time.

The morphological results can be used with Table 1 to predict fading, for example, an aircraft flying over the North Atlantic somewhere between the southern tip of Greenland and Iceland. This flight path is at the edge of the region of maximum auroral disturbance, say at 60° N geomagnetic latitude. The raypath to a synchronous satellite, however, is low to the south. The geometric analysis of the JSSG data, Figure 6, suggests that the median depth of the slant southern path is about four to five times the median depth observed overhead at the penetration point, near 50°N geometric latitude. Since the best data at hand for a VHF comparison are the Canary Bird or ATS-3 observations made at Hamilton, Massachusetts, it is preferable to use the smooth latitude variation to estimate the depth at the penetration point. From Figure 7 it can be seen that the depth of scintillation would be twice that measured on ATS-3 signals at the Hamilton Observatory, which represent the behavior between 50° and 52°N geomagnetic.

The estimated cumulative distribution representing this case is shown in Figure 10. For about 7 percent of the time the scintillation index for 137-MHz signals would be greater than 57, so that an aircraft at 60°N geomagnetic transmitting at 137 MHz to a synchronous satellite would experience fading greater than 3 dB only about 1.4 percent of the total time. Since the diurnal study of signals at this latitude, Figure 8, shows that the occurrence of strong scintillation in the daytime is rare, this estimate can be doubled to represent the night hours.

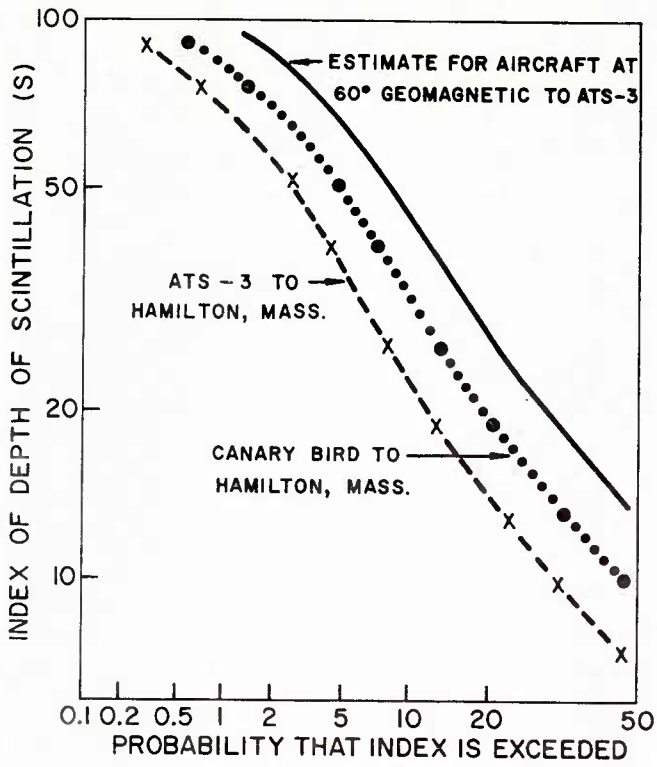

Figure 10. Estimated Scintillation for an Air to Satellite Relay. For a mid-Atlantic synchronous satellite and an aircraft over Southern Greeland, the cumulative distribution of depth of scintillation at 136 MHz is estimated from scaled data taken with Canary Bird at Hamilton, Massachusetts

Other details can be estimated by using the variations established in the figures of Section 1. About 90 to 95 percent of the time, K index of magnetic activity is less than 5 (Figure 1). Therefore, the effects of geomagnetic variability will not be noticed at this latitude. Again, while moderate magnetic activity will degrade local HF and VHF communication, it should not degrade the VHF satellite link. The occurrence of deep scintillations does increase for K indices greater than 5, but the statistics are not yet established.

The estimated cumulative distributions of Figure 10 can be translated for changes in the radio frequency by using the empirical dependence on radio frequency; changes in solar activity can be translated by using the dependence on mean annual sunspot number discussed in Section 1.8.

3. EFFECTS OF IONOSPHERIC SCINTILLATIONS ON TELECOMMUNICATION SYSTEMS

There has been very little direct measurement of the effects of ionospheric scintillations on communication systems that would enable a determination of the reliability factor for systems using space, frequency, or polarization diversity. Measurements have been sporadic, usually involving a few hours of communications to aircraft not instrumented with systems having diversity features.

However, specific measurements of scintillations on radio star signals and on satellite VHF beacons have provided information that can be used to evaluate the effectiveness of diversity systems. Figure 11 shows the simultaneous reception of both linear polarizations of the 136-MHz signal from the Early Bird synchronous

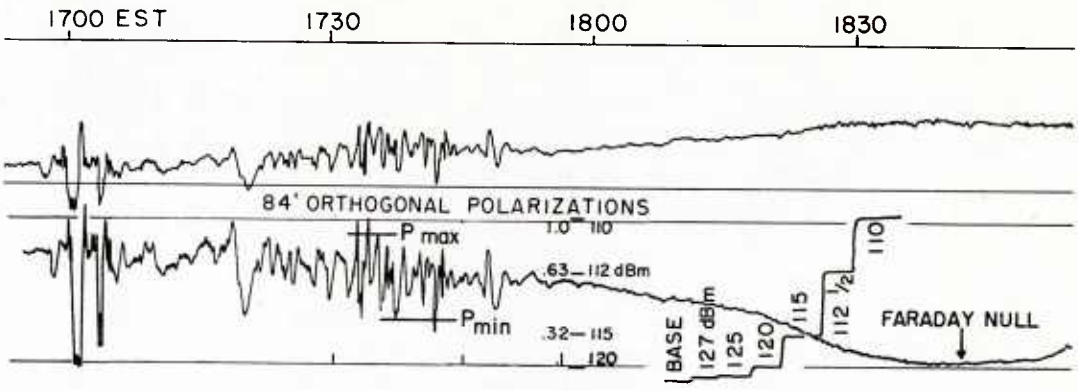

Figure 11. 136 MHz Scintillations from the Early Bird Synchronous Satellite 7 August 1965

satellite. The slow fading that results in a null on the lower channel at approximately 1840 EST is caused by Faraday rotation of the plane of polarization of the linear component of the elliptically polarized signal which had an axial ratio of approximately 10:1. Slow deep fades (up to 10 dB) occurred over a one-hr period. Focusing of the signals can result in a rise above the mean value. The important point is that the fading is coherent on both polarizations, indicating that polarization diversity would be ineffective for reducing the effects of the ionospheric irregularities.

The scintillations on VHF satellite transmissions are of the same origin as those observed on radio star source data. Correlation functions for multi-frequency scintillation have been determined for radio star data over a frequency range of 40 to 228 MHz. The results of this analysis are shown in Figures 12 and 13. As shown in Figure 12, analog processing of Cassiopeia A scintillations resulted in a correlation coefficient of 0.75 obtained between scintillations at 63 and 113 and 113 and 228 MHz. Figure 13 shows that the correlation coefficient decreases very slowly with frequency separation. A frequency ratio of 2 still results in a coefficient greater than 0.5 as read at 0 time lag. Since a relatively high correlation between widely spaced frequencies is normally experienced with the conventional narrow frequency separation used, frequency diversity would not be effective in eliminating the fading effects.

The size of the ionospheric irregularities that produce the scintillations have been measured and found to vary from a few hundred meters to several kilometers in their shortest dimension. These irregularities are elongated along magnetic field lines with measured ellipticities ranging from 5 to 35:1. The large size of irregularities would limit the effectiveness of space diversity, particularly for aircraft communication systems.

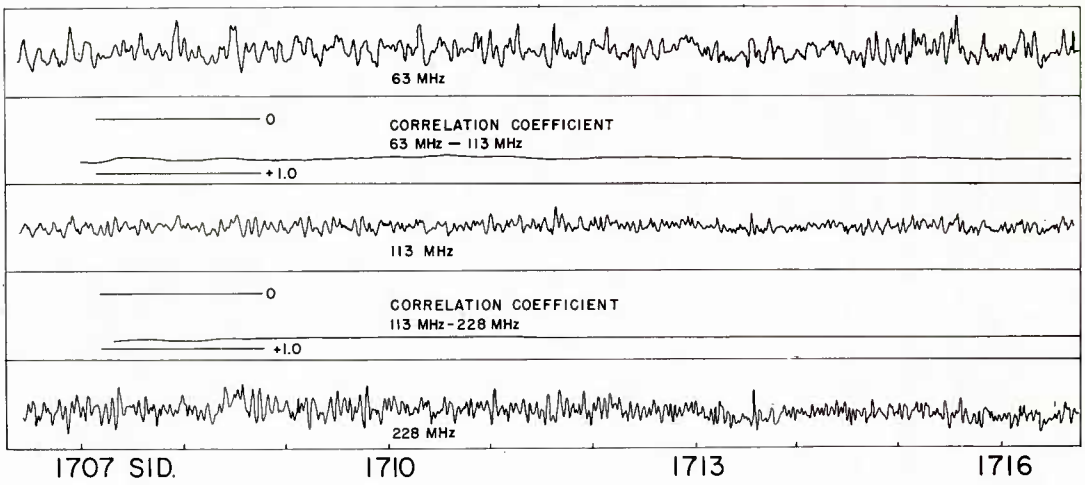

Figure 12. Tracings of the Variable Component of Cass. A Scintillations at an Elevation of 35°, Azimuth 40° (1722 Sidereal Time). Correlation coefficient for the ten minutes analyzed was approximately .75 for both channels. $K_{Fr} = 4$, 12 September 1962

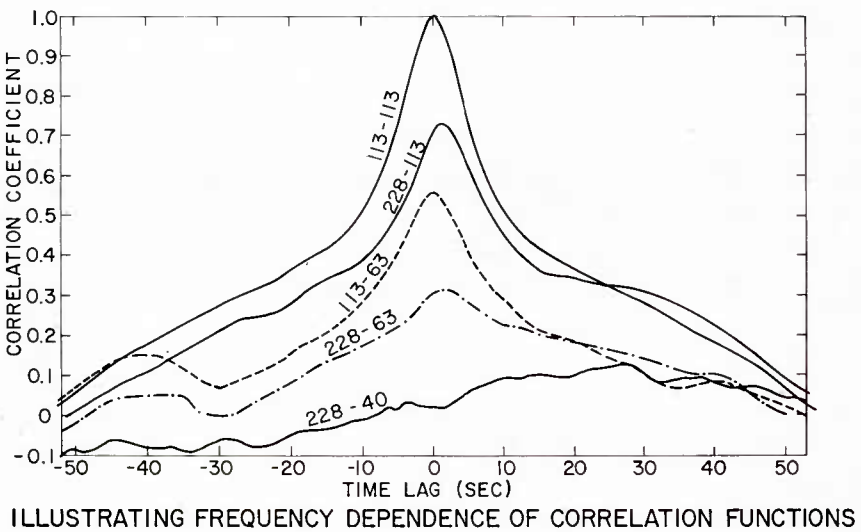

ILLUSTRATING FREQUENCY DEPENDENCE OF CORRELATION FUNCTIONS

Figure 13. Multi-frequency Correlations for Scintillations of Cassiopeia, at a Single Location

References

Aarons, J., and Allen, R.S. (1966) Scintillation of a radio star at a subauroral latitude, Radio Sci. 1(No. 10):1180-1186.

Aarons, J., Allen, R.S., and Elkins, T.J. (1967) Frequency dependence of radio star scintillation, J. Geophys. Research 72(No. 11):2891-2902.

Aarons, J., Mullen, J.P., and Basu, Sunanda (1964) The statistics of satellite scintillation at a subauroral latitude, J. Geophys. Research 69(No. 9):1785-1794.

Allen, R.S., Aarons, J., and Whitney, H.E. (1964) Measurements of radio star and satellite scintillations at a subauroral latitude, IEE Trans. Ant. Prop. AP-12(No. 7):812-822.

Briggs, B.H. (1964) Observations of radio star scintillations and spread-F echoes over a solar cycle, J. Atmos. Terr. Phys. 26:1-23.

Briggs, B.H., and Parkin, I.A. (1963) On the variation of radio star and satellite scintillations with zenith angle, J. Atmos. Terr. Phys. 25:339-350.

Joint Satellite Studies Group (1965) A synoptic study of scintillations of ionospheric origin in satellite signals, Planet. Space Sci. 13:51-62.

Joint Satellite Studies Group (1968) On the latitude variation of scintillations of ionospheric origin in satellite signals, Planet. Space Sci. 16:775-781.

Kent, G.S. (1959) High frequency fading observed on the 40 Mc/s wave radiated from artificial satellite 1957a, J. Atmos. Terr. Phys. 16:10-20.

Koster, J.R., and Wright, R.W. (1960) Scintillation, spread-F and transequatorial scatter, J. Geophys. Research 65:2303-2306.

Little, C.G. (1951) Diffraction theory of the scintillations of stars on optical and radio wavelengths, Monthly Notices Roy. Astron. Soc. 111:289-302.

Mercier, R.P. (1962) Diffraction by a screen causing large random phase fluctuations, Proc. Cambridge Phil. Soc. 58:382-400.

Orhaug, T.A. (1965) Scintillation of discrete radio sources, Chalmers Tak. Hogskol. Handl., p. 229.

Special Problems in Scintillations: Equatorial Scintillations, Polar Cap Scintillations, Lower Atmosphere Scintillations

Equatorial Scintillations

Jules Aarons

1. INTRODUCTION

Scintillations in the equatorial region appear similar to those observed at high latitudes. The heights and short dimensions of the irregularities in the two latitude regions are approximately the same. Equatorial irregularities appear to have great elongation, but they are in general also located in the F-region. There is a distinct falloff of irregularities with distance from the magnetic equator with the latitudinal confinement varying as a function of sunspot cycle. A very distinct seasonal pattern exists, more striking than the high latitude seasonal variation. An abrupt appearance of scintillation on any night and a gradual disappearance of the irregularities are other characteristics of the scintillation phenomena at the equator, quite distinct from those observed at high latitudes.

For the purposes of this review, we have used only stations in Africa and South America. The geographic and geomagnetic coordinates of most of the observatories used are shown in Figure 1. In addition to the observatory placement, we have shown specific subionospheric positions of two synchronous satellites as viewed from Huancayo, Peru. The Huancayo data are from a paper by Bandyopadhyay et al.,(1970).

Figure 1. Sites of Most of the Equatorial Observations Cited in Text. Subionospheric positions of ATS-1 and Canary Bird satellites as observed from Huancayo are also shown

2. APPEARANCE OF SCINTILLATIONS ON AMPLITUDE RECORDS

Two illustrations (Figures 2 and 3), from Huancayo, Peru, on the geomagnetic equator are given to show the appearance of scintillations on synchronous satellite records. Figure 2 illustrates the sudden appearance of scintillations on the propagation path to the two satellites. On the day illustrated, the satellites, ATS-1 and ATS-3, at 136 MHz had subionospheric points separated by approximately one hour. Scintillation on the ATS-1 signal appeared about an hour and a half after those on the more easterly satellite. Starting at 2347, one can see the rapid increase of scintillation on the ATS-3 signal to a completely scintillated signal within a few minutes. The ATS-1 signal takes a few minutes more before it reaches full value.

A fuller expansion of the records is shown in Figure 3 with recordings of two satellites, one on the eastern horizon (Canary Bird) at an elevation angle of 12° and the ATS-1 near the western horizon at an elevation of 7°. Records of a short time period taken during two days in October 1967 are shown, both illustrations having been recorded at the same universal time. The local time of the subionospheric point of the Canary Bird signal was approximately 2220; that of ATS-1 was 2040. On one day (October 25), ATS-1 was fully scintillating with the Canary Bird signal showing low amplitude fluctuations. On another day, both were scintillating fully, but with different rates. This illustration points to an interpretation of the irregularity structure as maintaining an integrity of both size and velocity only within a relatively small area.

The rate illustrated is for synchronous satellites only. Synchronous satellite scintillation rate is determined by irregularity, size, and wind velocity. Low altitude satellites freezing the irregularities in place show high scintillation rates, but these are determined by the angular speed of the satellite to ground propagation path as it is eclipsed by the irregularity.

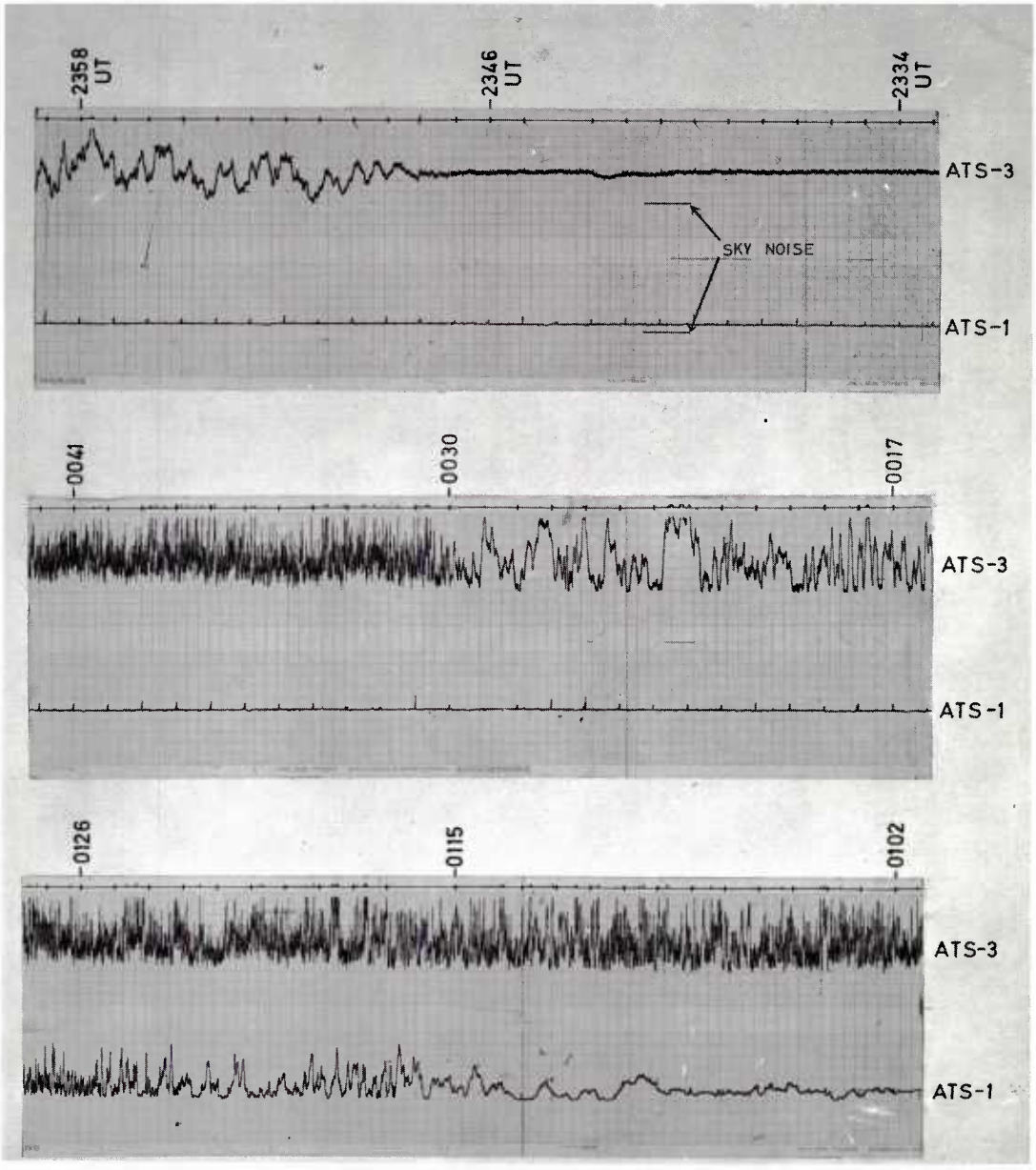

Figure 2. Onset of Scintillation in ATS-3 and ATS-1 Signals Recorded at Huancayo, Peru (Night of October 11-12, 1968)

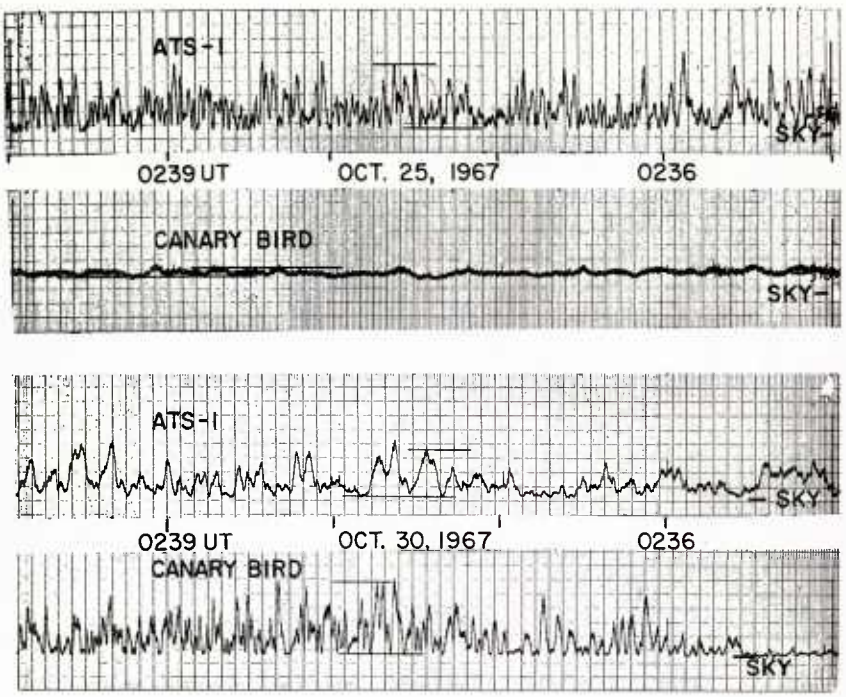

Figure 3. Scintillations on ATS-1 and Canary Bird at the Same Time on Two Days: Huancayo, Peru

3. THE DIURNAL PATTERN

Using summer data at Accra, Ghana (Koster, 1968), one can see the typical diurnal pattern from 15 May to 15 July 1967 (Figure 4). In the equatorial region, peak indices are observed between 2100 and 0200 local time.

Utilizing two synchronous satellites and shifting the axis to reflect subionospheric times, one finds the same results for Huancayo, Peru, for another period, November 1967 (Figure 5). As in many geophysical phenomena, the mean behavior may have a regular pattern but the diurnal values on any one day have great variation. Plotting scintillation indices for any one day may produce a diurnal pattern for two satellites as one would expect (Figure 6), that is, with the time difference of the appearance and disappearance of scintillations for each satellite an effect of local time.

In order to show the individual vagaries of the irregularity structure, the first appearances of high amplitude scintillations in the path of two satellites has been plotted in Figure 7. A scintillation index of 60 percent is used as the starting time. During this period the two subionospheric points were separated by approximately one hour, as illustrated in the diagram. While a large number show the expected length of the "dumbbell," many show shorter or longer time differences.

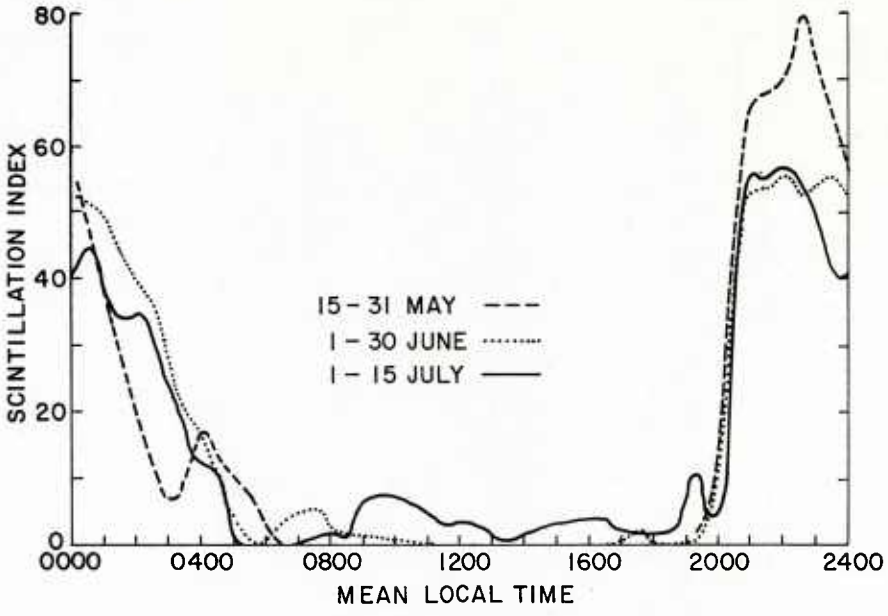

Figure 4. Diurnal Mean for May, June, and July 1967, Canary Bird, 136 MHz Scintillation, Accra, Ghana. 25 min. running mean

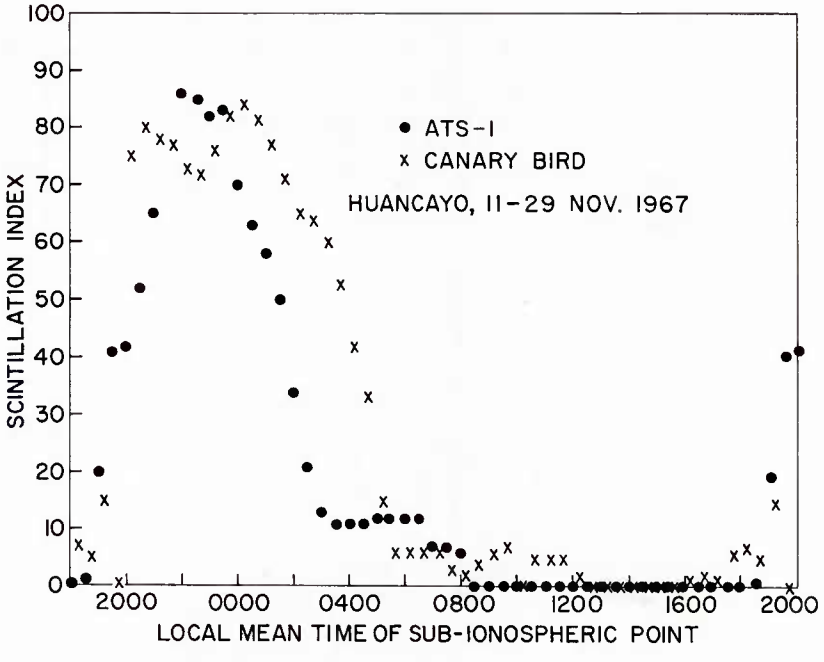

Figure 5. Comparison of Scintillation Indices for Two Satellites for the Same Period (11-29 November 1967)

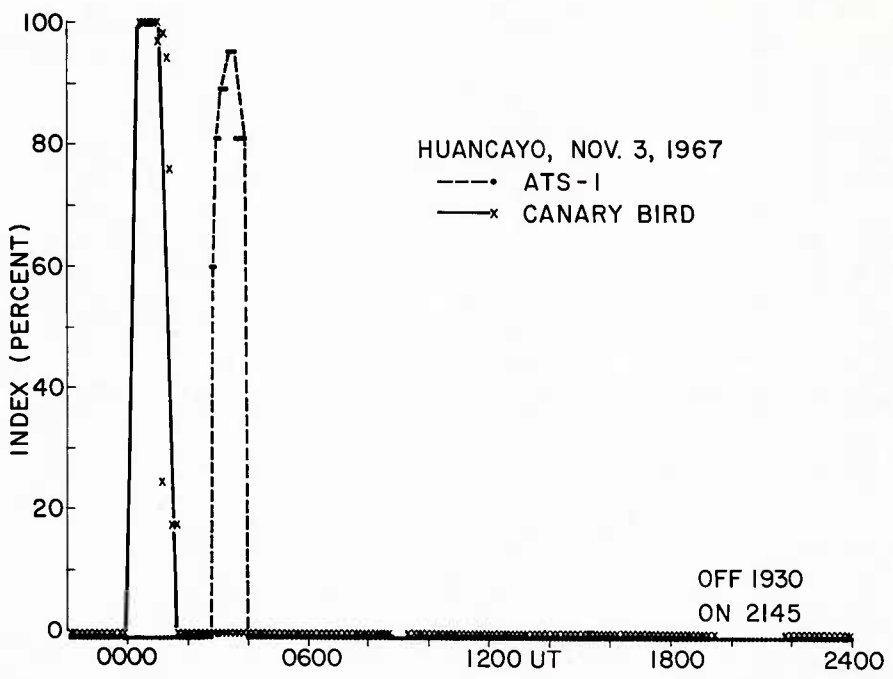

Figure 6. Scintillation Indices on Two Paths. Universal time is used

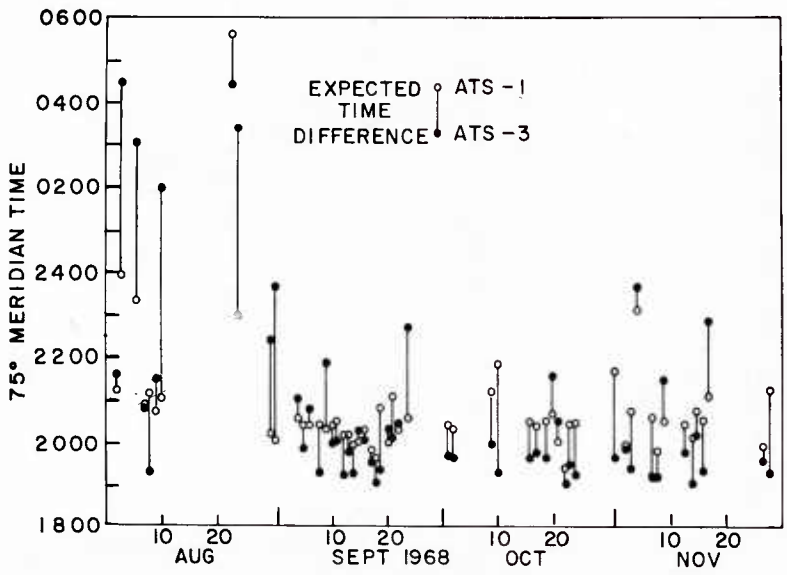

Figure 7. First Appearances of High Amplitude Scintillation (SI > 60%) in ATS-1 and ATS-3 Signals on Different Nights at Huancayo, Peru. Time difference between the 350 subionospheric longitudes was approximately one hour

A few scintillated later than the satellite to the west. It is obvious that the diurnal pattern of Figures 4 and 5 must be used with caution for predicting the pattern of individual days. Equatorial scintillations disappear more gradually than they appear. A great spread of time differences for the disappearance of scintillation on two paths is shown in Figure 8. Both the time of disappearance and differences between the two satellites show great variation.

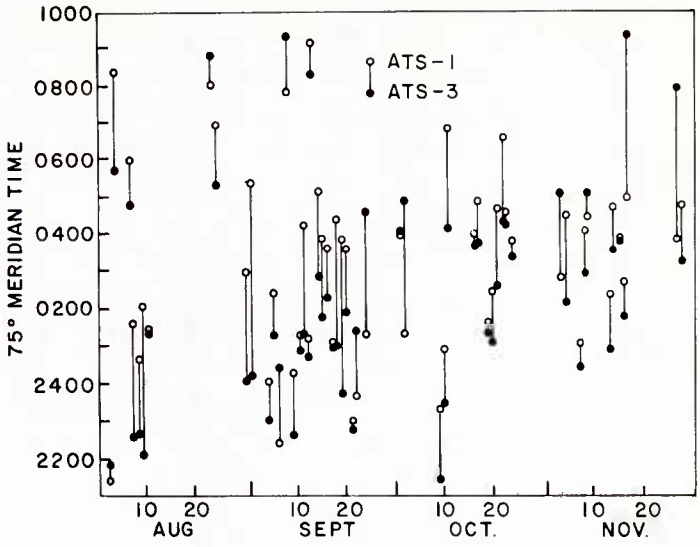

Figure 8. Final Disappearances of High-Amplitude Scintillation (SI > 60%) in ATS-1 and ATS-3 Signals on Different Nights at Huancayo, Peru

4. IRREGULARITY SIZE, HEIGHT, AND ELONGATION

Equatorial measurements of the height of the night irregularities show them to be in the F-layer. The irregularities are elongated along the lines of force of the earth's field with extremely high axial ratios noted. The east-west size of the ground pattern of the irregularities ranges from 100 to 400 meters with the most probable size, 225 meters.

Kent and Koster (1966) took a series of measurements at night in 1962 in Ghana. They found the height of irregularities in the 12 passes analyzed ranged from 244 to 297 km and a mean height of 306 km in close proximity to the electron density maximum. The latter results of data taken in 1965 generally corroborated those taken earlier; both were near sunspot minimum.

The axial ratios measured indicate that the irregularities were highly elongated with axial ratios greater than 60:1 (Koster, Katsriku, and Tete, 1966).

5. RATE

The irregularities are moved by ionospheric winds across the propagation path to the satellite. By spaced receiver methods, the velocity can be measured as a function of time.

The F-layer drift is eastwards at night with velocities varying from 90 m/sec on quiet days to 50 m/sec on disturbed days (Lyon, Skinner, and Wright, 1961). The drift reverses direction at about 0600 in the morning and at 1930 in the evening; daytime drift is westward and about twice as fast as nighttime. Koster (1963) reported that the night F-region drift during times of severe scintillation was eastward with a mean value of 75 m/sec.

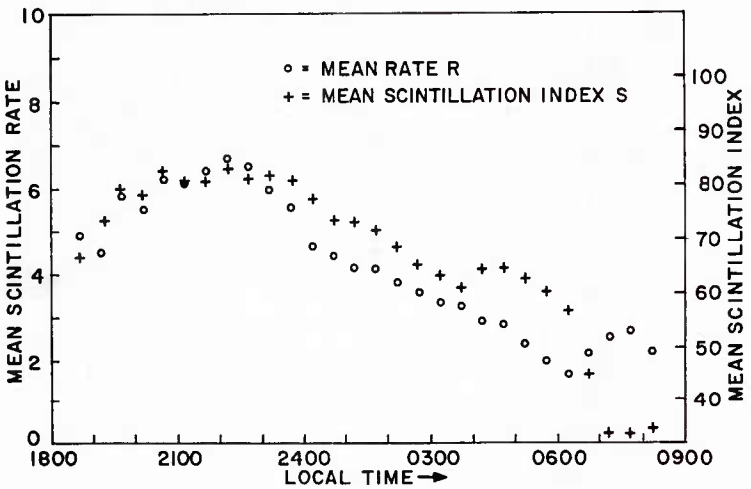

Figure 9. The Diurnal Variation of Mean Rate and Mean Scintillation Index in Ghana (Koster, 1968)

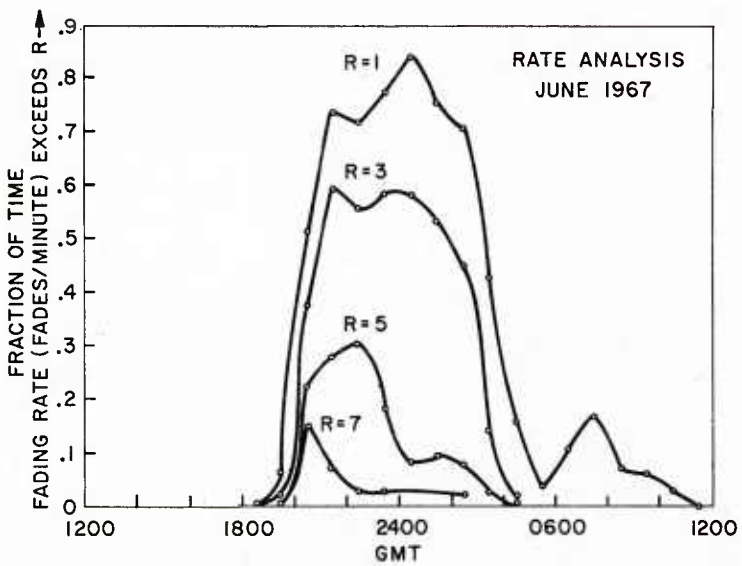

Figure 10. Fraction of Time Fading Rate Exceeds R - June, 1967 in Ghana (Koster, 1968)

On the whole, rate and index are positively correlated. High rate is observed almost wholly during periods of severe scintillation. However, during deeply scintillating periods, the rate can be low. Ghana nighttime records analyzed for predominantly 1967 data are shown in Figure 9. Rate peaks before midnight. Plotting one month in detail, one can see from Figure 10 that the predominant period in June 1967 lies between 10 and 20 seconds.

6. SEASONAL DEPENDENCE

A clear seasonal dependence has been observed in both the African and South American continents. A maximum index is observed during the equinoxes with minima during the solstices. Figure 11 from Ghana shows a year's nighttime observations of Canary Bird. Plotting

additional data from Canary Bird in a different manner, we can see the clear seasonal dependence (Figure 12). The high indices of September and March are in sharp contrast to those of December and June (Figure 13).

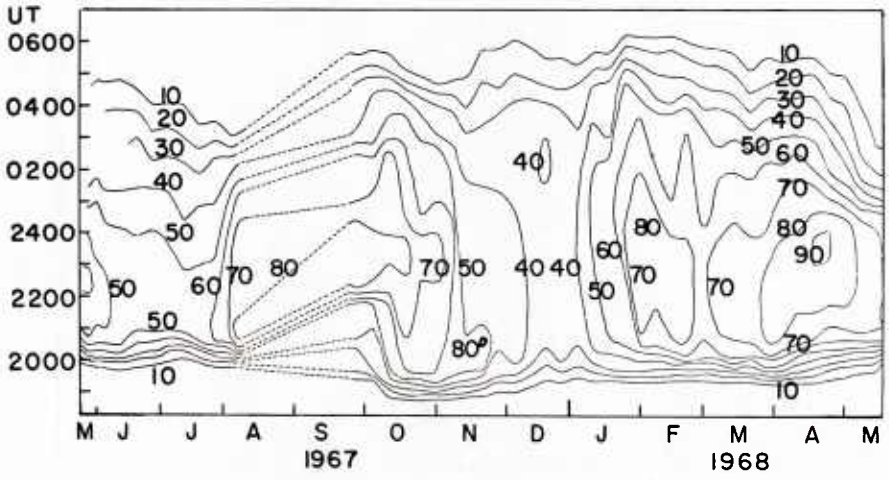

Figure 11. Contours of Time Mean S Exceeds Various Levels (Koster, 1968)

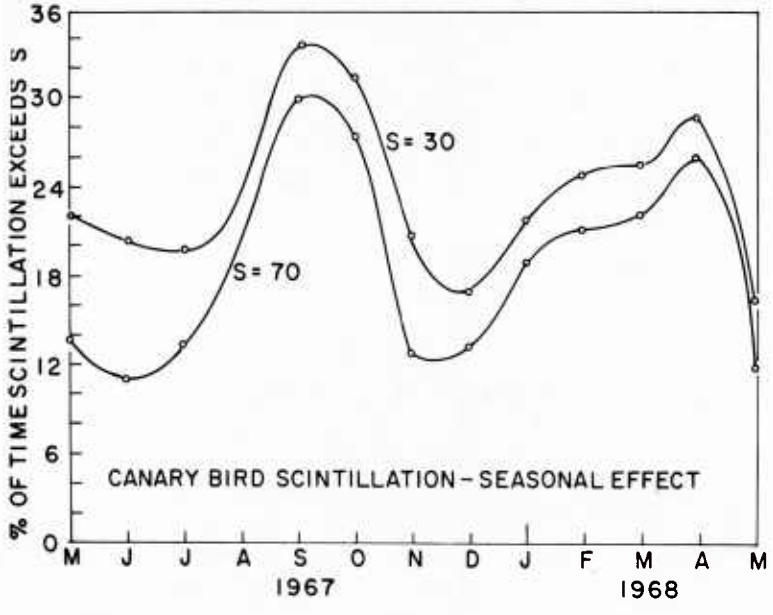

Figure 12. The Seasonal Dependence of Scintillation for Accra, Ghana (Koster, 1968)

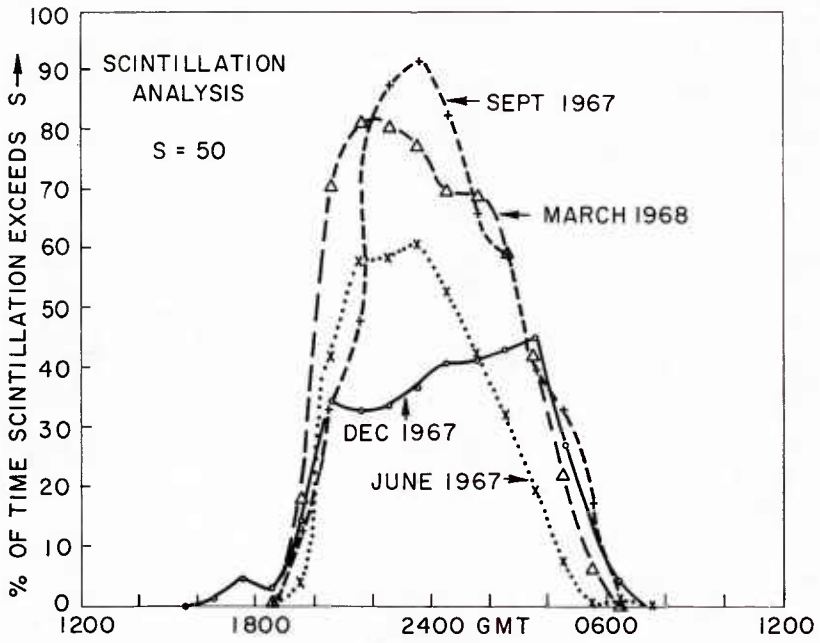

Figure 13. Fraction of Time Scintillation Exceeds 50 percent Index in Ghana (Koster, 1968)

Golden (1968) has shown that the maximum outages due to propagation distortion occurred in October and November 1966 and February, March, and April 1967 (Figure 14). A minimum of propagation outages was noted during December to January and between May and July. A similar pattern is shown in the ATS-1 data from Huancayo (Figure 15) where in five months of observations of ATS-1 a peak was noted in October 1967 and a low in July. Since in all the cases cited a maximum of one year's data is illustrated, the effect of distinctive events in any one month or of changing sunspot number has not been taken into account. With more data (some of which will be discussed later), we shall be able to normalize indices for sunspot number.

7. DEPENDENCE UPON SUNSPOT NUMBER AND K INDEX

The effect of increased solar flux on the irregularity structure is to increase the scintillation index on the geomagnetic equator and to decrease the latitudinal extent of the scintillation region. In a comparison of scintillation during June and July 1965 with that observed in June and July 1967, it was found by Koster (1968) that a sixfold increase in percentage of occurrence was noted at the 50 percent

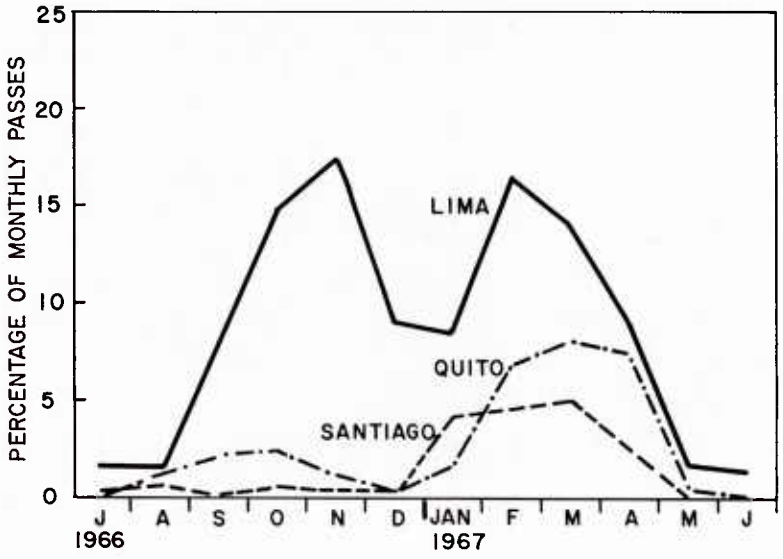

Figure 14. Scheduled Minitrack Passes Missed by Month Due to Propagation Distortion (Golden, 1968)

level and an eightfold increase at the 70 percent index level; 1967 values correspond to near sunspot maximum conditions; 1965 to sunspot minimum.

The extent of the scintillation region will be discussed in the next section, but high sunspot number appears to confine the latitudinal extent. Spread-F studies show a widening of the region during years of low sunspot number (Tao, 1965).

The dependence of scintillation on K index at the equator is not too clear. For the African continent, studies have shown a negative correlation with magnetic index. This has been noted during some intense magnetic storms (Koster, 1968). However, data from Peru (Figure 16) does not corroborate this. Perhaps the difference is due to the relatively small amount of data of

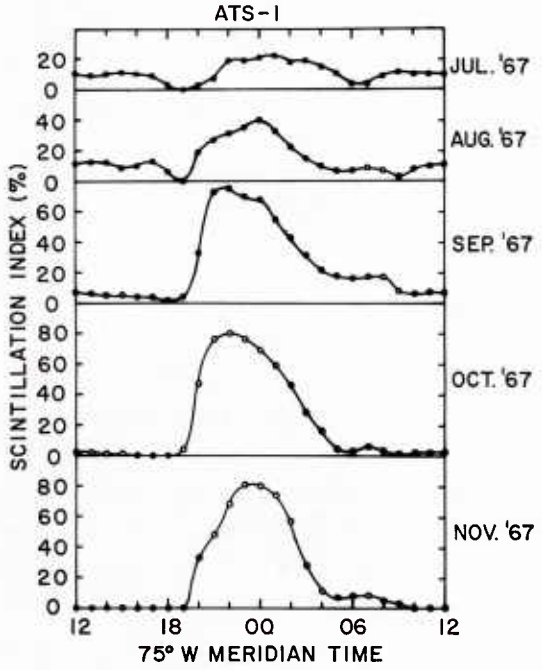

Figure 15. Mean Diurnal Variation of Scintillation Index at Huancayo, Peru

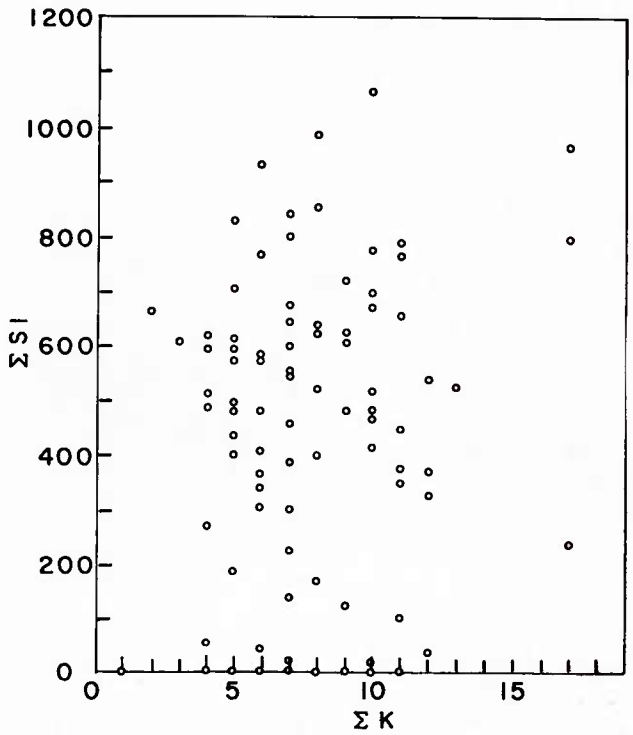

Figure 16. Mass Plot of the Sum of the Three Hourly K Indices (ΣK) Against That of the Mean Hourly Scintillation Indices (ΣSI) for the Daily Interval 00-12 hr UT During July-November 1967 (Huancayo, Peru)

the Peru study. It may also be due to the fact that the before and after midnight indices should be separated prior to a correlation study. As more data are taken and analyzed, the generally accepted anticorrelation is being found to be sensitive to factors such as time of day, season, and sunspot number.

8. THE LATITUDINAL EXTENT OF THE SCINTILLATION REGION

Sinclair and Kelliher (1968), by observing the scintillations of the BE-B 40-MHz beacon, plotted out the boundaries of the equatorial scintillation region. They observed at three stations: Nairobi in Kenya, Addis Ababa in Ethiopia, and Dar Es Salaam in Tanzania. Figure 17 shows the results at the equinoxes in 1967. Premidnight occurrence of scintillation is higher than postmidnight; magnetically disturbed periods for the same hours of the day have a lower occurrence of scintillation. Roughly the occurrence of scintillation dropped to half of its peak level at a distance of 15 geographic degrees from the equator. These data at 40 MHz suffer from "over modulation," that is, strong scattering taking place. The index boundary of 50 percent scintillation index, therefore, is probably somewhat narrower than Sinclair and Kelliher indicate.

Similar indications can be seen in the data on minitrack passes missed (Figure 14) owing to propagation distortion (Golden, 1968). The geomagnetic latitude of Lima is 0°, Quito, Equador is 10° GN. Quito shows less than half of the number of passes missed compared to Lima. Santiago, Chile, 21 geographic degrees south of Lima, shows only half the number of Quito. Further data on the extent of the scintillation region can be noted with the aid of observations of ATS-3 in the Panama Canal Zone. Observing the satellite at high angles of elevation (51°) at a subionospheric intersection of 8.5°N and 77°W, one noted only 31.5 hours of scintillation greater than 10 percent out of a period of 1000 hours. The period of time covered was from

11 July to 1 November 1968. Scintillation is concentrated in the 2000 to midnight local time period, as shown by the diurnal curve (Figure 18). The probability distribution of scintillations is shown in Figure 19. Of the 31.5 hours, approximately 11 hours of scintillations occurred on 31 October 1968. The intersection point was at approximately 19° Geomagnetic North; the data show that except for rare periods low indices are recorded at this latitude during this period of high sunspot number.

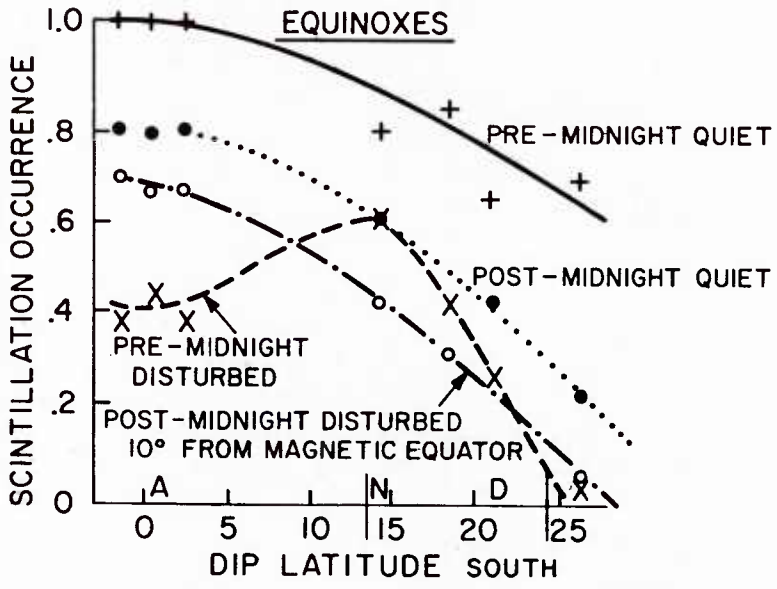

Figure 17. Scintillation Occurrence for Magnetically Quiet and Disturbed Conditions, Pre- and Post-midnight, for Each Season. Continuous line + pre-midnight, quiet; dashed line x pre-midnight, disturbed; dotted line • post-midnight, quiet; dashed/dotted line o post-midnight, disturbed. (Sinclair and Kelliher, 1968)

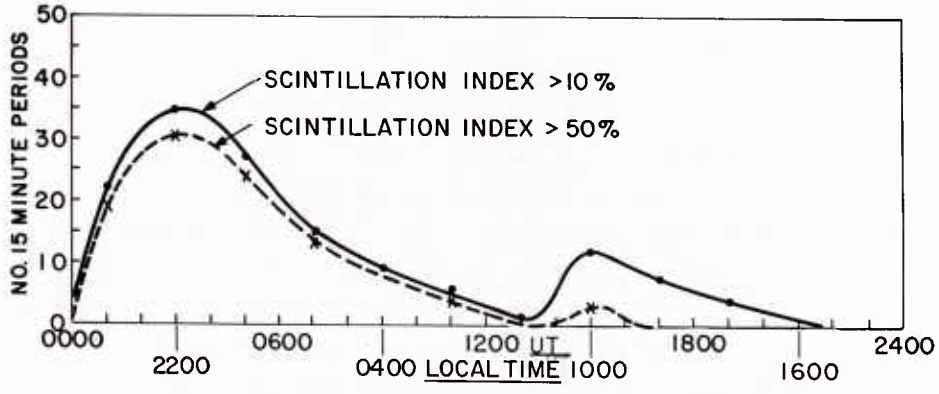

Figure 18. Diurnal Variation of Scintillations Occurring on ATS-3 Signal Received at Panama. Total period = 1000 hours from 11 July to 1 November 1968

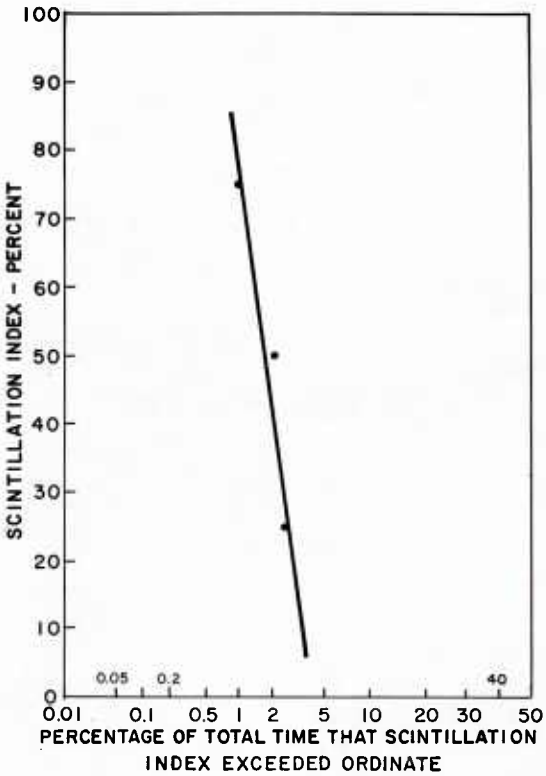

Figure 19. Probability Distribution of Scintillations Occurring on ATS-3 Signal Received at Panama. Total period = 1000 hours from 11 July to 1 November 1968

Farther from the equatorial region, the scintillation diurnal pattern remains, but an increase in daytime scintillation is noted. Figure 20 shows 40-MHz data from Nairobi, Kenya, and Haifa, Israel. The top graph shows scintillations greater than 10 percent; the bottom graph compares intense scintillations.

In a study of IGY Spread-F data, Tao (1965) found a region of plus or minus 15° from the geomagnetic equator where the occurrence of Spread-F decreases to half its maximum value. This was true in the equinox periods and from November to January, but a somewhat narrower confinement was noted from May to July.

The evidence is that during periods of high sunspot number the extent of the high scintillation region near midnight is plus and minus 10° to 15° from the geomagnetic equator, coinciding with the occurrence region of equatorial Spread-F.

9. COMPARISON OF SCINTILLATION DATA FROM GHANA AND PERU

Simultaneous observations have been taken from two widely separated sites on the geomagnetic equator. The comparison in this note is limited to a small amount of data. In May 1967, Koster took records at Ghana on the scintillations of Canary Bird at 137 MHz. In general, the data show high scintillation indices throughout the month, as well as in June. Investigating station activities of minitrack observatories, Golden (1968) found a minimum number of passes spoiled by scintillation during May and June (Figure 14). Our detailed study of Lima Minitrack records verified that very low indices were seen throughout the entire month on the pre- and postmidnight passes.

A day by day comparison of 137-MHz scintillations from Canary Bird was made for data taken in November 1967 in Huancayo, Peru, and Accra, Ghana. Five days showed high amplitude scintillations at both observatories. Five days showed medium

level scintillations at Ghana and severe scintillations at Huancayo. Low indices at both sites were noted only during one day. From these data there appears to be an indication of different occurrence patterns at the two sites on a day to day basis.

The data are too sparse to interpret. In particular, since there is approximately four hours of time difference between the subionospheric points of the two intersections, a slow change in the geophysical conditions producing the irregularities may account for the differing indices; one would expect the time difference to disappear from a larger sampling.

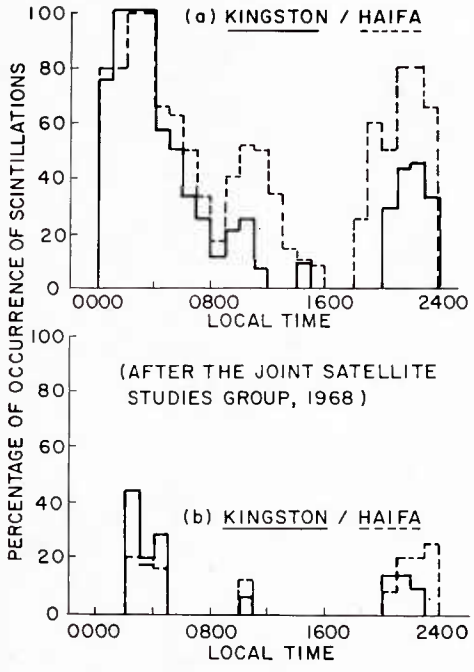

Figure 20. Percentage of Occurrence of (a) All Scintillations and (b) Severe Scintillations at Two Stations at a Similar Magnetic Latitude, for the Period March to June 1965

10. SCINTILLATION AND SPREAD-F

The Spread-F correlation with scintillation has already been referred to. One can note similarities in pattern by comparing Figures 21 and 22 (both for Huancayo, Peru). However, the Spread-F data are taken of the overhead ionosphere and the ATS-1 observations of the ionosphere 14° to the west. The general correlation of Spread-F and the severe scintillations are readily seen.

The detailed day to day data are shown in Figure 23. Again a general correlation is seen but there are days with scintillation and no Spread-F (September 29 and October 8). In general, the occurrence of scintillations and Spread-F are correlated if one compensates for the time difference.

It is clear that scintillations are a more precise measure of the electron density of the irregularities than Spread-F which is basically a qualitative description of an ionospheric condition. If multi-frequency scintillation observations are available, the exact deviation of the electron density from ambient might be determined. This could lead to a quantitative recording of irregularity electron density when the sunspot number decreases.

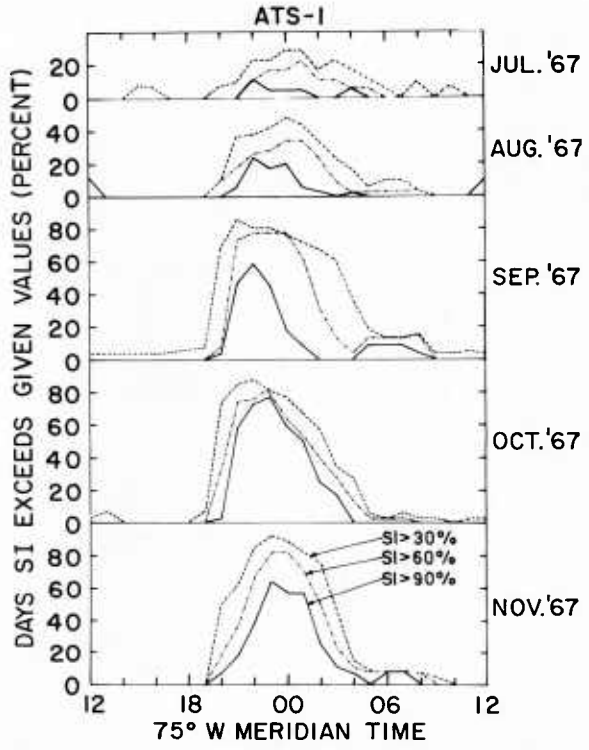

Figure 21. Mean Diurnal Variation of Scintillation Occurrences at Huancayo, Peru

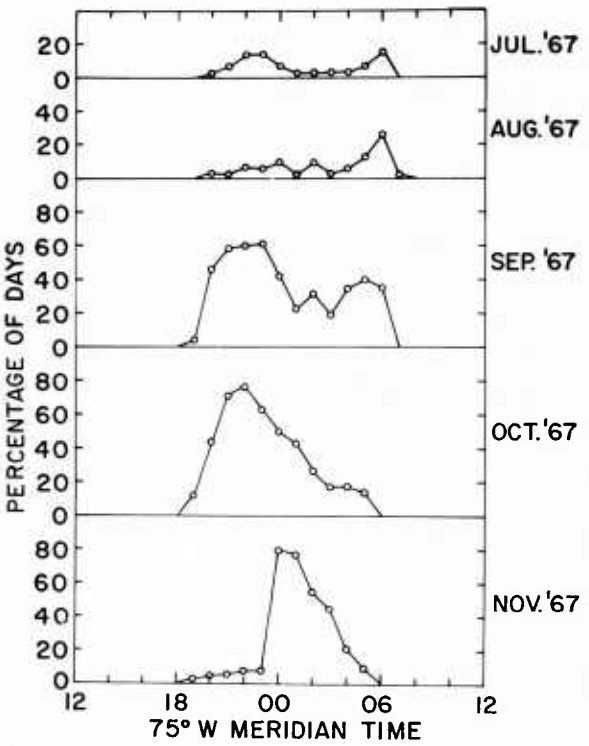

Figure 22. Mean Diurnal Variation of Spread-F Occurrences at Huancayo, Peru

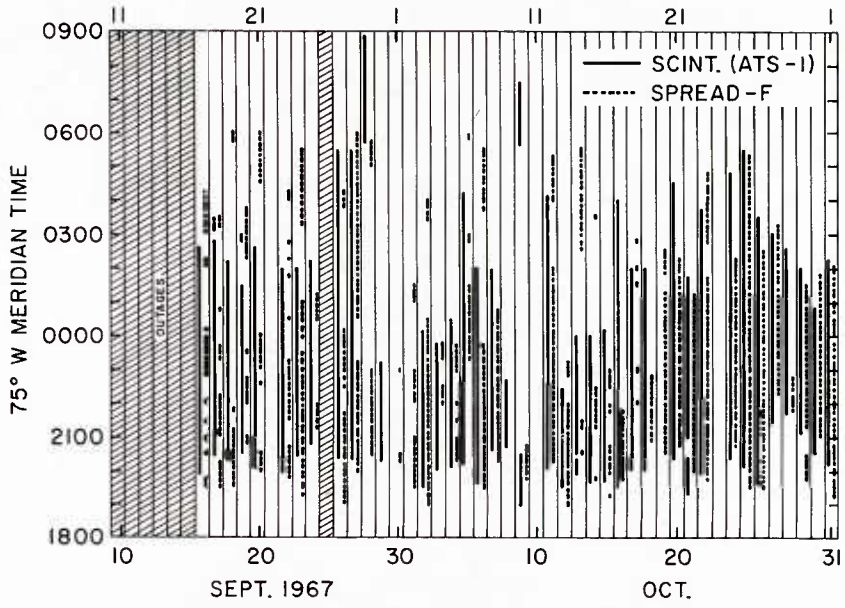

Figure 23. Day to Day Occurrence of High Amplitude Scintillation (SI > 50%) and Spread-F at Huancayo, Peru

11. CONCLUSIONS

As the midnight time sector moves along the geomagnetic equator, irregularities form. The direction of winds within the irregularity structure is eastward at night even though the large scale excitation of the ionosphere into the irregularity formation mode is westward.

The height of the irregularity structure both by spaced receiver measurements and by large scale movements has been shown to be in the 250 to 400-km region. If one assumes a height of 350 km and adjusts the time difference between two separated synchronous satellites, a correlated pattern results. If E-layer heights or heights greater than 400 km were assumed, this correlation would not be noted.

The causal mechanism is far from known. An important clue must lie in the seasonal dependence of scintillation with its solstice minima and equinoctial maxima.

References

Bandyopadhyay, P., and Aarons, J. (1970) Radio Sci.

Golden, T. (1968) Report No. X-525-68-56, NASA Goddard Space Flight Center, Greenbelt, Maryland.

Kazes, I. (1957) Proc. Acad. Sci. (Paris) 245:636.

Kent, G.S., and Koster, J.R. (1966) Ann. Geophysique 22:3.

Koster, J.R. (1963) J. Geophys. Research 68:2579.

Koster, J.R. (1967) Final Report, Contract AF61(052)-800, AFCRL-68-0020.

Koster, J.R. (1968) Report of the Joint Satellite Studies Group, JSSG Report No.3, Contract No. F61052-67-C-0088, AFCRL-68-0260.

Koster, J.R. (1968) Progress Report No.3, Contract No. F61052-67-C-0027, AFCRL-68-0006.

Koster, J.R., Katsriku, I., and Tete, M. (1966) Annual Summary Report No. 1 Contract No. AF61(052)-800, AFCRL-66-814.

Lyon, J.A., Skinner, N.J., and Wright, R.W.H. (1961) J. Atmos. Terr. Phys. 21:100.

Sinclair, J., and Kelliher, R.F. (1968) J. Atmos. Terr. Phys. 31:201.

Tao, K. (1965) J. Radio Research Lab. 12:317.

Polar Cap Scintillations

1. INTRODUCTION

In order to observe the propagation characteristics of synchronous satellite transmissions at 137 MHz in the polar cap region, a program of observations of ATS-3 has been instituted at Thule, Greenland, at the AFCRL Geopole Station. The Thule data are relevant to both auroral and polar effects.

Thule, located at a latitude of 76.6°N and a longitude of 69°W, is near the geomagnetic pole, at a geomagnetic latitude of 88°. It observes synchronous satellites of very low inclination at longitudes of 19°W and 118°W on its horizon; satellite elevation rises to 1° when the satellite station longitude is 113°W or 25°W. At 90°W the satellite can be observed at 4° of elevation with the highest elevation approximately 4.9° at the station longitude of 69°W.

For the measurement periods, October to November 1968 and May 1969, to be described, we are interested in the latitude of the intersection of the 350-km point with the ionosphere, since irregularities are probably predominantly near the height. In October and November 1968, the sub-ionospheric latitude was 62°N, 55.4°W, or approximately 72° Geomagnetic North. In May the sub-ionospheric points were 62°N, 72°W (approximately 73° Geomagnetic North). The angle of elevation was 3.7° in October to November 1968 and 4.8° in May 1969.

The auroral oval is a region a few degrees wide where the maximum flux of low energy precipitated particles ($\geq$ 40 keV) is noted. Its mean position is generally taken to be approximately ±4° of 68° at night during moderately quiet conditions.

The propagation path from Thule to ATS-3 went through the auroral zone at night and through the lower latitude edge at noon.

2. OBSERVATIONS

2.1 Phase A

During the time period, October 1968 to April 1969, a linearly polarized yagi, low noise converter and a stable receiver were used along with a chart recorder capable of reproducing 100 cps signals; however, the time constant used was 0.1 sec. It was quite difficult to determine the mean signal level since the satellite signal fades were never less than 3 to 5 dB. However, a signal of 10 dB above background noise can be taken to be the mean level. In Figure 1, we have reproduced several signal periods, each approximately 20 minutes in length. Figure 1(a), which encompasses a Faraday peak (lasting approximately 15 minutes), had fast fades with periods of the order of several seconds. The fades were of the order of 12 to 15 dB. In Figure 1(b), faster fades with deeper nulls can be observed. Slow fades with shallow nulls can be seen in Figure 1(c); this minimum fading is of the order of 3 to 6 dB. It might be noted that fades can rise above mean level at least 5 to 6 dB, as well as fall to noise levels [Figure 1(b)].

2.2 Phase B

In order to determine if the optimum time constant was being used and in order to determine polarization characteristics of the signal, another equipment modification was made in May 1969. Two yagis, with E vector planes tilted 60° to one another, were set up on masts. A low noise preamplifier placed at the antennas was incorporated in the system. This increased the signal-to-noise ratio by a factor of approximately 3 to 4 dB. Various time constants were used to determine whether information was being lost by utilizing too long a time constant during periods of intense activity.

Figure 2 illustrates fading from ATS-3 with time constant of 0.02, 0.1, and 3.0 sec (but with different gains on recorder amplifiers). By following this high speed recording, one can see that the time constant of 0.1 sec reproduces all of the larger amplitude peak and nulls while the 3-sec time constant does not reproduce the short period fluctuations. Following these observations, the time constant subsequently used for the measurements was 0.1 sec. The period of the shortest period fluctuations was of the order of 2 sec peak to peak.

In Figure 3, a somewhat different receiver and data configuration is illustrated. Two yagis oriented at angles of 60° were used; 4 min were spent on one polarization and $3\frac{1}{2}$ on the other. A typical record is shown and a calibration is included on the

right. On the high signal level antenna, maximum fades are of the order of 15 dB representing a probable increase of about 5 dB above mean level and negative fades of 10 dB. It can be seen from this recording that the high scintillation does not depolarize the signal; the scintillation is in amplitude, not polarization. Polarization diversity would not,therefore, improve the fading characteristics. We have tested this hypothesis at another site and verified this conclusion.

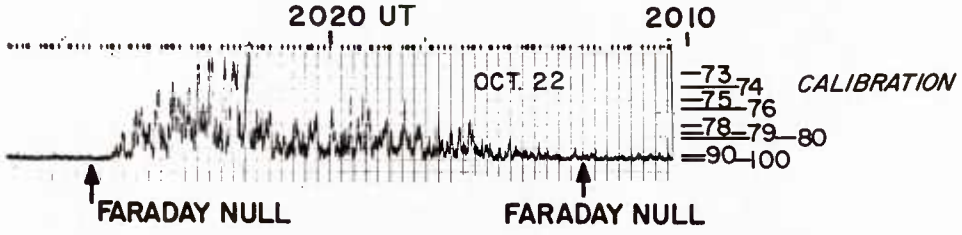

(a) ILLUSTRATES A MEDIUM RATE SCINTILLATION WITH FADES OF THE ORDER OF 12 - 15 dB.

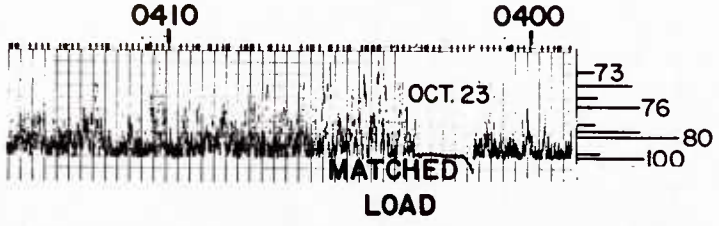

(b) FAST AND DEEP SCINTILLATIONS (TO NOISE). A MATCHED LOAD IS SHOWN AT 0402.

(c) SHOWS SLOW RELATIVELY SHALLOW SCINTILLATIONS CHARACTERISTIC OF THE PERIOD AROUND LOCAL NOON; FADES ARE OF THE ORDER OF 4–9 dB WITH THE PERIOD OF FADING 20–40 SECONDS.

Figure 1. Characteristic Fading Records During the Quiet Period of October 21-23, 1968

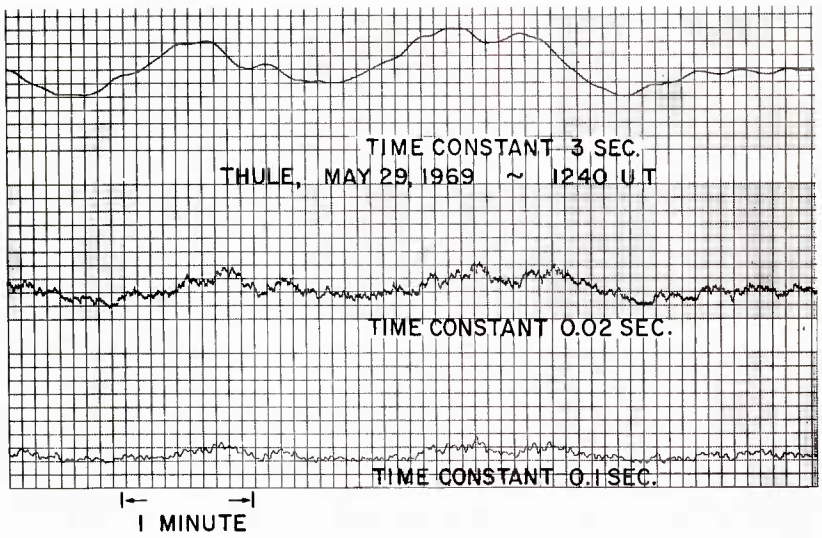

Figure 2. Detailed Recording of 3 Time Constants. Note that 0.1-sec time constant follows fluctuations while 3-sec time constant fails to do so

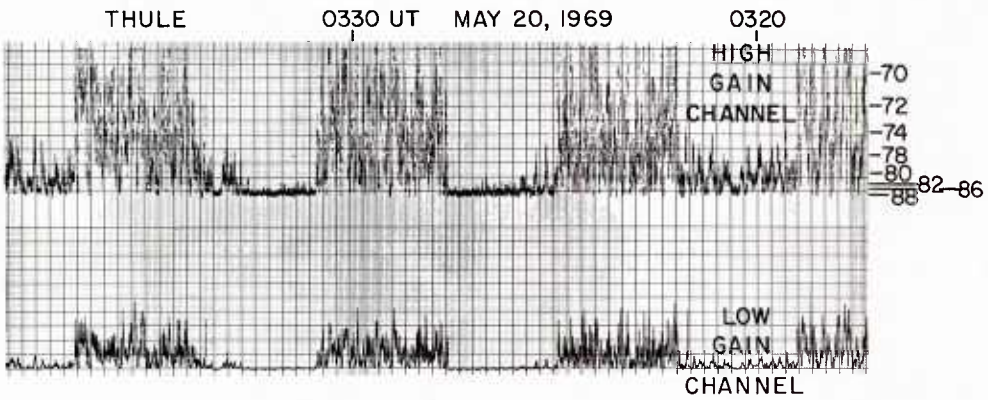

Figure 3. High Amplitude Scintillations on High and Low Gain Amplifiers. Signal peaks are 18 dB above noise but during very intense scintillations fail to show in other channel (~ 0332, ~ 0326)

3. THE MAGNETICALLY QUIET PERIOD OF OCTOBER 21, 22, AND 23, 1968

During three magnetically quiet days in a row, October 21, 22, and 23, continuous observations were made. A_p's were 1, 2, and 3. October 22 was the only day in 1968 when an A_p of 1 was recorded. The satellite's elevation was 3.7°. In an attempt to look at the peak to peak fading for the period, the three days were

analyzed for hourly fading period and fading depth. We assumed maximum fades of 15 dB (to noise level), although this is probably low. The minimum fades noted were of the order of 3 dB. In Figure 4, the results are plotted showing that minimum fading occurs between 0500 and 1400 local time. The fading periods are also shown in Figure 4 for the three days. The longest periods noted were of the order of 60 sec (as shown in Figure 1); the shortest about 2 sec (Figure 2). Between 0700 and 1400 local time, very long period fading was noted on all three days, usually when the fades were not deep.

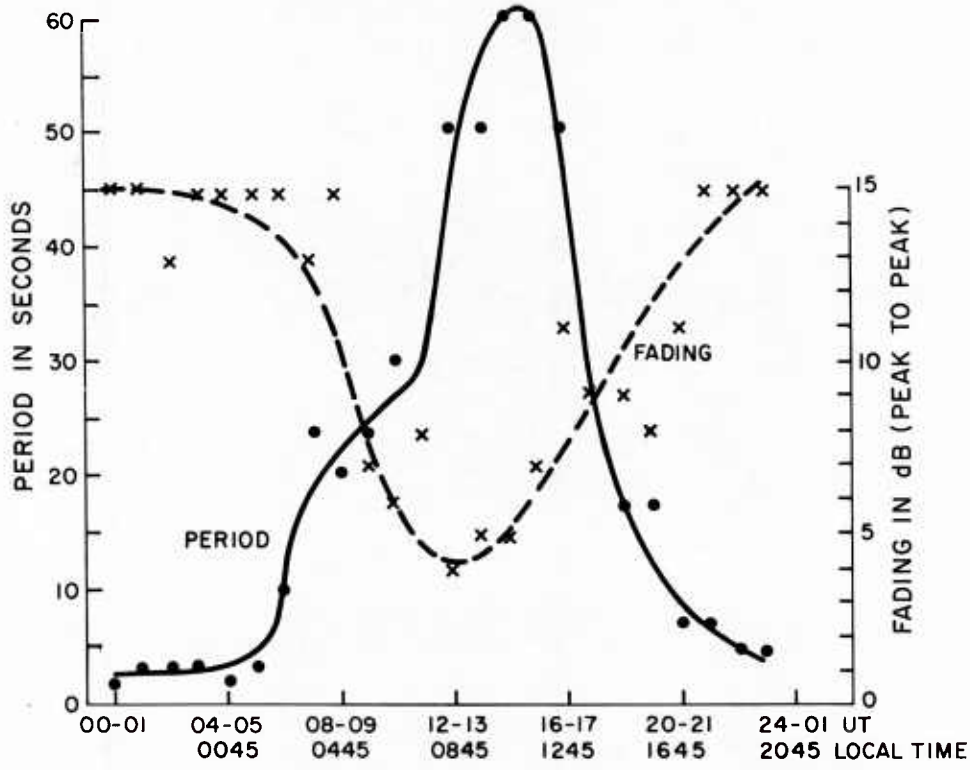

Figure 4. Fading Period and Amplitude for Thule During Quiet Period of October 21, 22, 23, 1968 with A_p's of 2, 1, and 3

4. THE MAGNETIC STORM PERIOD

October 31 to November 2, 1969 contrasted with the quiet days. The observations during the magnetic storm showed consistent fluctuations to noise throughout

each day. A_p's for the period were:

October 31 - 112
November 1 - 122
November 2 - 82

The slower Faraday rotations are not visible as they are in October 21, 22, and 23. Often the polarization changes rapidly over a period of 10 to 20 minutes. Figure 5 illustrates the storm behavior. The combination of fast highly localized intense magnetic variations and the rapid drift of large electron clouds probably produce the relatively fast change in Faraday rotation. During the storm, it was not possible at Thule to distinguish periods of low amplitude fluctuations of the synchronous satellite signal. Observations of S-66 at 40 MHz show that throughout the intense storm (October 30 to November 3) higher amplitude scintillations were observed over the entire polar cap than during quiet days.

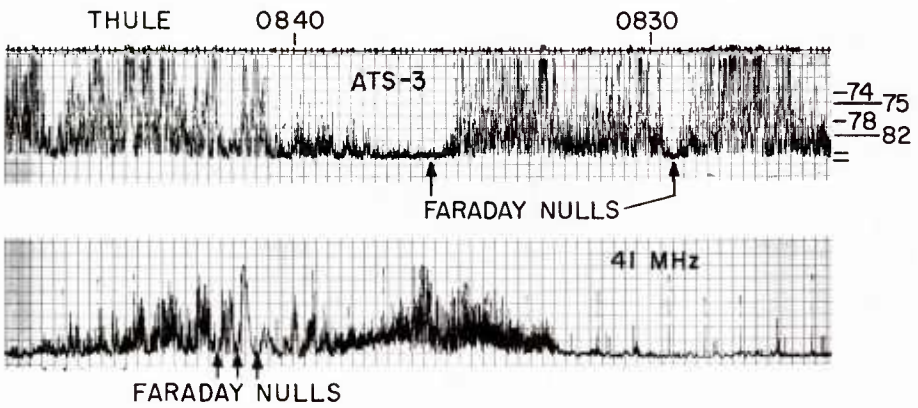

Figure 5. Fast Faraday Rotation During Magnetic Storm of October 31, 1968. High indices were also noted on BEB throughout pass

5. EARLIER OBSERVATIONS

Polar cap observations are meager. One series of measurements taken at 20 MHz was made at Baker Lake [64.3°N, 96.1°W (Yeh and Swenson, 1966)]. Scintillation rate was much faster at Baker Lake than at Urbana, Illinois, but it was not known if strong scattering or the size and height of the irregularities produced the difference in rate.

In studies of the scintillation from S-66 made in 1965, Aarons et al. (1966) reported a permanent high level of scintillations at 40 MHz over the polar cap, including the Geopole. There was some evidence of a lower scintillation rate and lower

amplitudes over the northern polar cap regions than over the auroral oval.

More recent studies (Frihagen, 1969) in Spitzbergen at 40 MHz have revealed several facts. The presence of scintillations over the entire northern polar cap was confirmed. The southern boundary of the region was found to be sensitive to variations in K_p varying from L = 16 at K = 0 to L = 6 (65°G.N.) for K = 2.

In the study of Antarctic scintillations with data obtained at 40 MHz from BE-B, Titheridge and Stuart (1968) found a minimum in scintillation indices during the high sunspot number years near local noon, the same local time we have noted. They found a maximum near 1900 local time.

6. CONCLUSIONS

The data and observations reported in this note were made during the period from October 1968 to May 1969; they are continuing. The fluctuations vary from slow, relatively shallow variations during an extremely quiet period magnetically to fast, deep fluctuations observed during disturbed periods and during portions of a day in magnetically quiet periods. It is not feasible to analyze in great detail the rest of the data since the fades are deep a large portion of the time.

Because of the low elevation angle at which these observations were made, it should not be concluded that overhead satellites would scintillate to this extent. As we have shown, 40-MHz transmissions at times show low amplitude scintillations (Aarons et al., 1966). A recent illustration of the variability of scintillation index as the path of a satellite crosses the polar regions is shown in Figure 6;

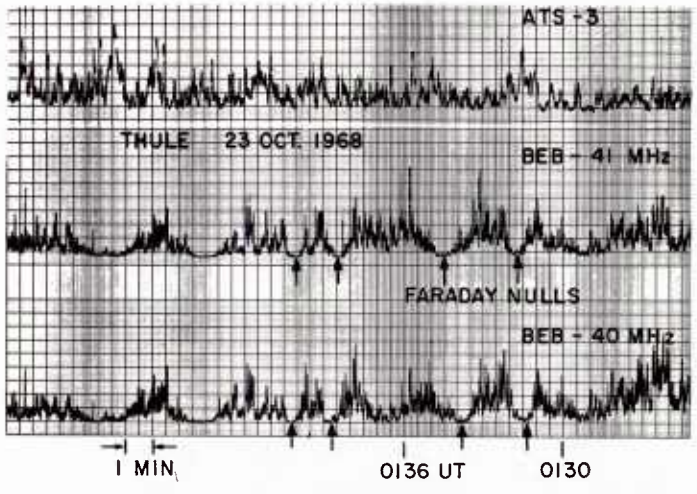

Figure 6. High Amplitude Scintillations on ATS-3 While Faraday Nulls Can Be Observed on BEB 40-41 MHz Signals

ATS-3 at 137 MHz shows deep fades, whereas some of the fades of the BE-B beacon at 40 MHz show only low amplitude scintillations. It is to be expected that with scintillation depth decreasing with frequency (Aarons et al., 1967) overhead satellite transmissions at 136 MHz would show low fading indices at times. This study is now in progress at Thule.

During years of high sunspot number, one should expect deep fades at 137 MHz a great deal of the time when one observes synchronous satellites from polar cap sites in Greenland. Since fades of 10 dB or more are normal daily occurrences, communications and navigation systems must be able to contend with them.

References

Aarons, J., Silverman, H.M., and Ramsey, B.A. (1966) Ann. Geophys. 22:349.

Aarons, J., Allen, R.S., and Elkins, T.J. (1967) J. Geophysics Research 72:2891.

Frihagen, J. (1969) J. Atmos. Terr. Phys. 31:81.

Titheridge, J.E., and Stuart, G.F. (1968) J. Atmos. Terr. Phys. 30:85.

Yeh, K.C., and Swenson, G.W., Jr. (1966) Proc. 9th AGARD Symposium, Copenhagen, 1964, in AGARDograph 95, Spread-F and its Effects upon Radiowave Propagation Communication, P. Newman, Ed., Technavision, London.

Lower Atmosphere Scintillations

1. INTRODUCTION

From the point of view of efficient utilization of satellites, low angle observations are extremely important. The addition of what is often the conventionally "forbidden" 0 to 5 degrees of elevation means a large extension of the effective area of a satellite. In particular, high latitudes are forced to view synchronous satellites at low angles. Low angle viewing of low altitude satellites increases both the time of visibility and range enormously. In the case of a 1000-km satellite viewed from a latitude of 43°, approximately 5° of latitude are added by the 0 to 5° elevation angle segment.

The problem is, therefore, to determine the atmospheric effects on the signal. These are three in number: (1) absorption of signal, of practical importance below 20 MHz and above 10 GHz; (2) refraction, which can be calculated and for which corrections are simple for most systems in the range 100 to 4000 MHz; and (3) amplitude fluctuations or scintillations.

For geomagnetic latitudes less than 60°, tropospheric effects rather than ionospheric predominate above 400 MHz at low angles. Ionospheric scintillations have been noted as high as 1200 MHz, but this type of scintillation is rare and associated with aurora.

2. SUNRISE OBSERVATIONS

The sun is an extended source varying as a function of frequency from 31 to 40 minutes in angular diameter. At microwave frequencies the sun is a narrower source than at meter wavelengths where the corona increases the emitting area. Sources this large do not show scintillation. One can look simply at extended sources as a series of point sources whose diffraction patterns add in such a manner as to cancel the pattern on the ground. However, active centers on the sun have angular diameters ranging from less than one minute of arc to several minutes of arc; these sources frequently show scintillation.

In Figure 1, we have illustrated with a sunrise some of the observational features of tropospheric scintillations. These observations were taken in Manila, Philippines with a single antenna and a multifrequency feed. The scintillation features are as follows:

1. There is a high degree of correlation of peaks and nulls across the microwave band. One can observe from ten minutes to fifteen minutes after sunrise a series of large peaks and nulls whose positions with respect to one another are perfectly correlated at all the observed frequencies.

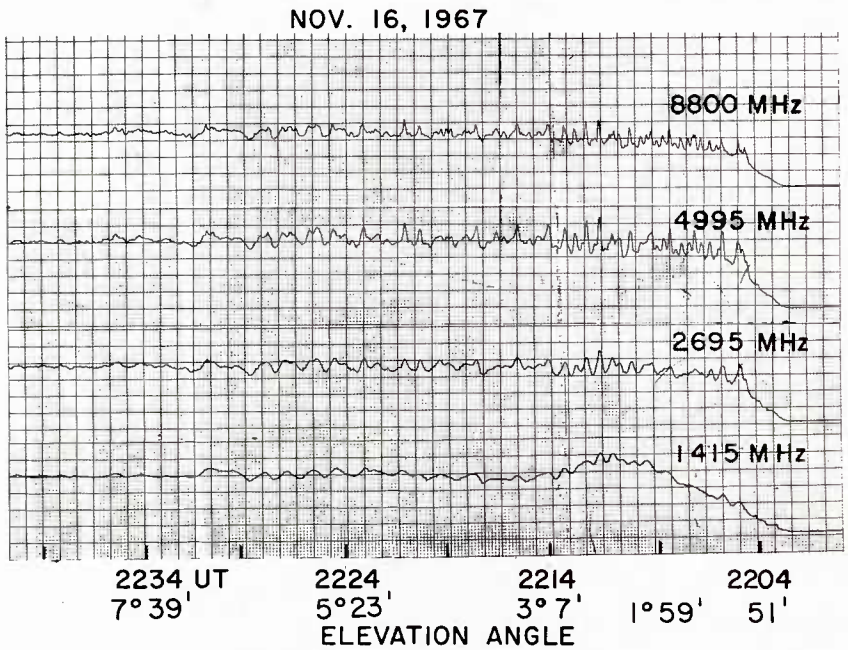

Figure 1. Sunrise at Manila, Philippines. Note the correlation of peaks and nulls at all frequencies (2209-2214 in particular). Higher frequencies have short period fluctuations modulating the long period scintillations

2. The scintillations are of extremely low amplitude after the first few degrees of elevation.

3. The higher frequency observations show more detailed structure (higher frequency components) than the lower frequencies. The period of the lower frequencies is of the order of 30 seconds.

We use the scintillation data on discrete radio star and solar active regions since with these sources scientific studies have accumulated a background of data; however, important differences between true point source rises (such as satellites) and the relatively wide angular diameter sources of solar active regions and some discrete radio star sources should be noted.

3. RADIO STAR OBSERVATIONS

A similar study was carried out earlier with the rise and set of Cygnus. In this case, two frequencies were used, 1200 and 2980 MHz, and the source tracked. In order to obtain effective sky temperature a "mock" rise was also taken and the scintillation index taken from the temperature contributed only by the source. The results are shown in Figure 2. We have included other data utilizing the sun as a source by Kazes (1957) and curves for slant range to the irregularity using 1 km heights. While neither the 1 km nor the 10 km curve shows a good fit, the form of the 1 km is closer to the observations than the higher altitude curve.

4. SYNCHRONOUS SATELLITE RISES AND SETS AT 401 MHz

A series of satellites exists with low powered telemetering beacons on 401 MHz. These synchronous satellite rises and sets have provided us with measurements that indicate fading amplitude as a function of elevation for one site. A tracing of a record is shown in Figure 3. A striking factor is that good signal levels are available after the source has risen to one degree of elevation. The signal is usable if suitable gain is available after 0.3° of elevation. The knowledge of the statistics of fading and fading rates for this satellite allows users to work with communications systems at low angles of elevation.

The very slow type of fading was observed in the elevation angle from 0 to 3° and was characterized by fading periods in the 5 to 30 minute range. In the study done at Sagamore Hill (Elkins et al., 1968) where set took place in the east over water and rise in the west took place over land area, there was a distinctly different pattern to rise and set. Figure 4 shows fading amplitude in dB as a function of angle of elevation. Signal level in the 0 to 1° block may be somewhat different than assumed (and, therefore, fading amplitude in dB) due to either antenna or refraction

effects. The strong elevation angle dependence is seen but the low fading amplitudes should be noted.

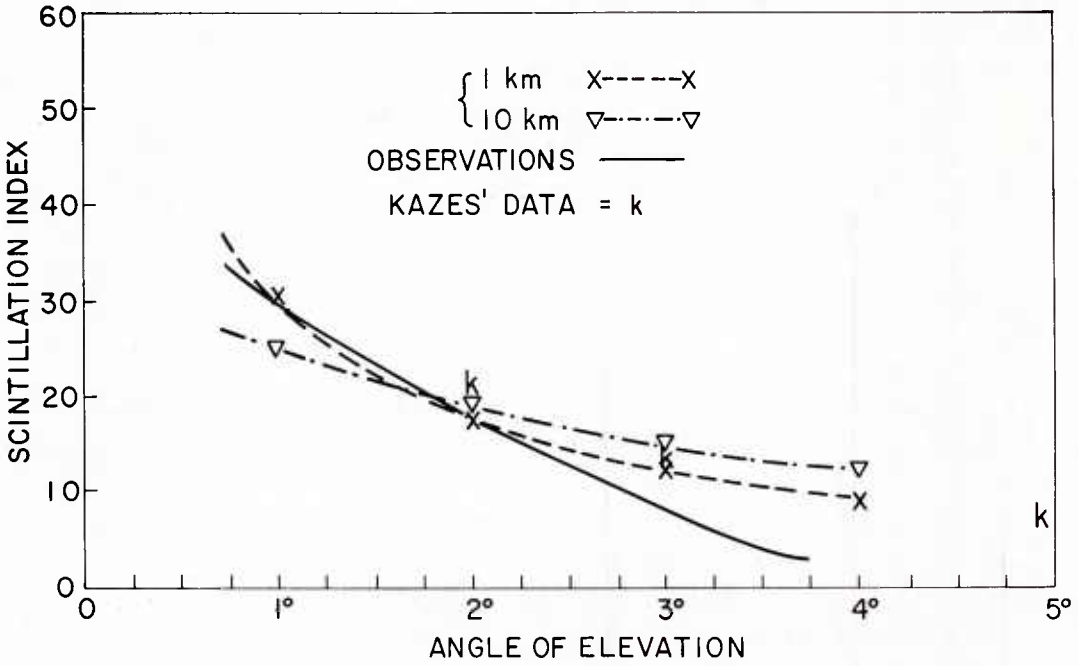

Figure 2. Mean Scintillation Indices at 1200 and 2980 MHz as a Function of Angle of Elevation for Cygnus Rise and Set at the Sagamore Hill Radio Observatory. The Kazes (1957) observations are noted (k) as are normalized curves for Z where Z is the distance to the 1-km and 10-km layers

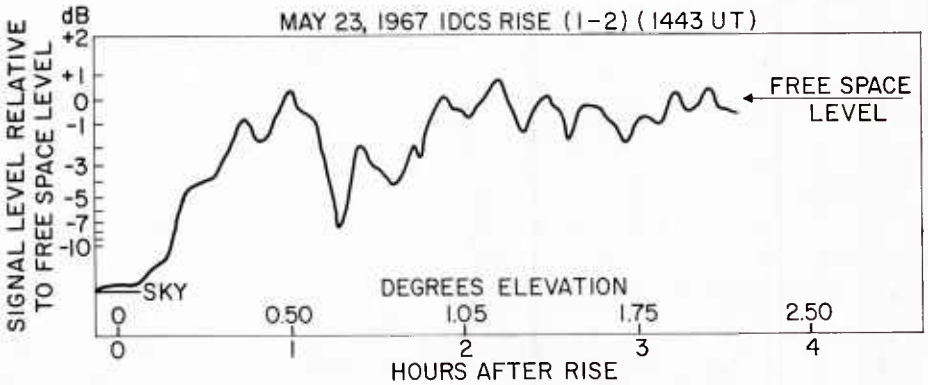

Figure 3. Rise of IDCS Synchronous Satellite Transmitting at 401 MHz. Note long period fluctuations

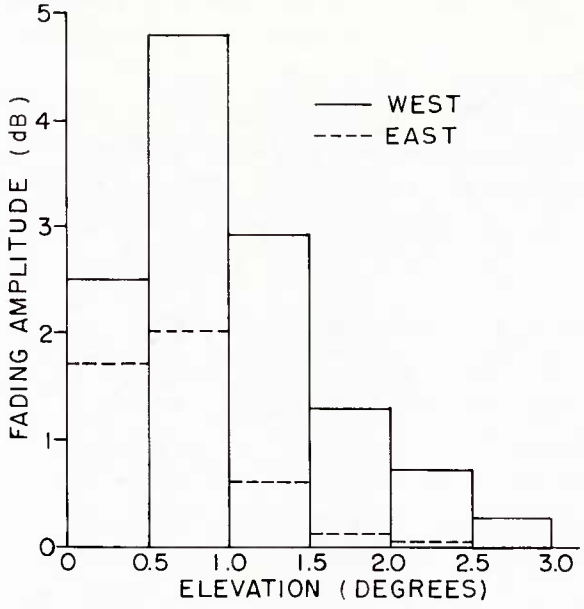

Figure 4(a). Fading Amplitude as a Function of Angle of Elevation for the IDCS Satellites (401 MHz)

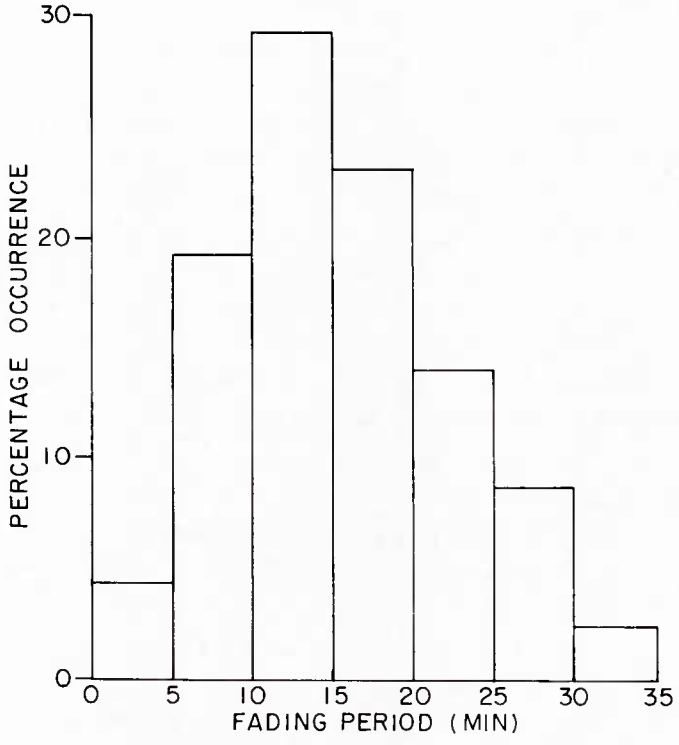

Figure 4(b). Percentage of Occurrence of Fading Periods

The fading period for 40 rises and sets obtained during April and May 1967 is shown in Figure 4(b). Since the fading is a function of (1) the size of the irregularities, (2) the wind velocity, and (3) the motion of the source relative to the ground, it is difficult to separate these variables with only one measurement. It might be noted that the lengthening of the period compared to sunrise indicates that the dominant velocity being measured is the track of the source across the atmospheric irregularities rather than a wind carrying irregularities through the pattern.

5. SYNCHRONOUS SATELLITES AT LOW ELEVATION ANGLES

Some observations have been made of synchronous satellites "hovering" on the horizon. The nonrefracted elevation angle varied in the case of ATS-1 viewed from the Sagamore Hill Radio Observatory, Hamilton, Massachusetts from -.1° to +.75° of elevation. The beacon signal at 136 MHz was affected by both ionospheric and tropospheric irregularities and it is difficult to separate these effects. However, there are times when neither tropospheric nor ionospheric scintillations are observed and the "seeing" is good. An illustration of that condition can be noted in Figure 5(a) on the ATS-1 records, but a second illustration, Figure 5(b), shows extremely high ionospheric scintillations. The conclusion is that the ionospheric and tropospheric irregularity structure is controlled by latitude and temporal factors. Only when irregularities exist does the angle of elevation effect hold.

Similar results of rise and sets with high and low scintillations can be noted in LES-5 observations at 232 MHz. Many rises and sets exist with little scintillation, and long periods were observed at low angles of elevation with no scintillation (Figure 6).

6. DISCUSSION

To explain tropospheric scintillations, several hypotheses have been advanced. Elkins et al. (1968) state that tropospheric gravity waves are being observed as they have been by other radio techniques and by meteorological methods. An irregularity with a wavelength of several hundred meters to a few kilometers would be the diffracting source. The ground level variations would then be the projection of a moving shadow pattern of the irregularity on the ground. Refractive effects brought about by internal gravity waves in the low troposphere would produce the fading. These waves which can introduce a relative change in refractive index of 10^{-4} may produce focusing effects at very low incidence angles as illustrated in Figure 7, where the vertical scale has been greatly exaggerated for clarity. The conclusion is supported by the elevation dependence of fading amplitudes.

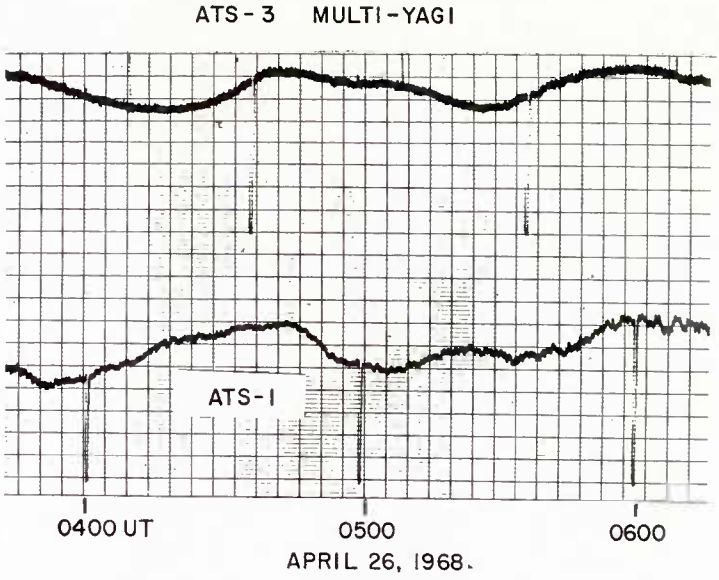

Figure 5(a). Low Amplitude Scintillations of Both ATS-3 (Elevation Angle 38°) and ATS-1 (Elevation Angle 0.5°) Both at 136 MHz. Hour markers are matched load calibrations. Slow wavelike structure is Faraday rotation

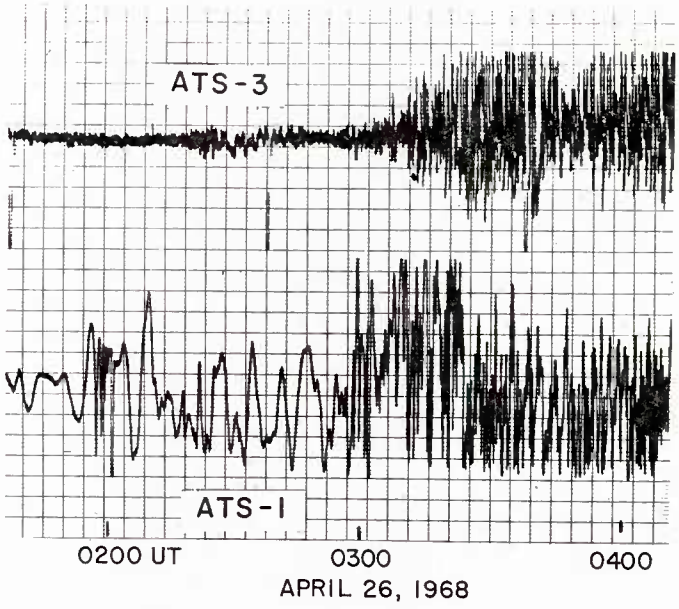

Figure 5(b). High Amplitude Scintillations of the Two Satellites on Another Night. Both satellites are at about the same elevation angle as in Figure 5(a)

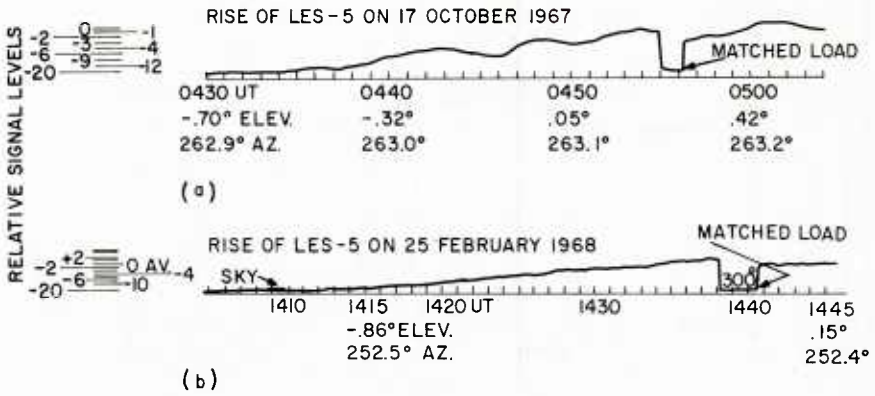

Figure 6 (a&b). Rise of LES-5 on 17 October 1967 and 25 February 1968

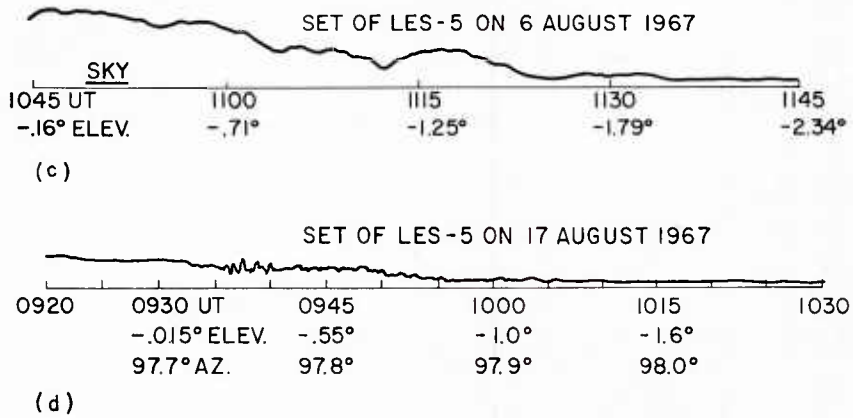

Figure 6 (c&d). Set of LES-5 on 6 August and 17 August 1967

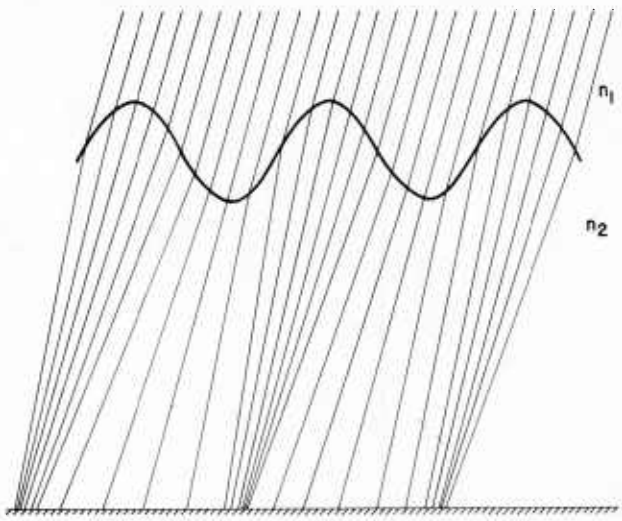

Figure 7. A Simplified Graphical Representation of Focusing Effects

Another hypothesis makes use of the sharp discontinuities noted in refractive index measurements of the vertical structure of the lower 5 km. These measurements are performed by aircraft refractometer studies in situ and by meteorological balloons. At low angles of elevation the radio sources are observed near grazing incidence relative to the irregularities. The sharp discontinuities in refractive index act alternately to focus and defocus the source, similar to the glinting phenomenon. For the first few degrees of elevation the propagation path is nearly parallel to the horizontal jump in refractive index. After the angle becomes too large the "glint" effect disappears and the scintillations cease.

References

Castelli, J.P., Aarons, J., and Silverman, H.M. (1964) J. Atmos. Terr. Phys. 26:1197-1213.

Elkins, T.J., and Papagiannis, M. (1968) Space Research VIII, North-Holland, Amsterdam.

Kazes, I. (1957) Proc. Acad. Sci. Paris 245:636.

Propagation Delays of UHF Waves

John A. Klobuchar

1. INTRODUCTION

Interest has been expressed by designers of proposed satellite ranging systems in predicting the additional time delay of a VHF radio wave that travels through the ionosphere. The ionosphere retards the free space travel time of VHF radio waves which traverse it by measurable and sometimes significant amounts. It is the purpose of this section of the report to present data showing how the delay varies as a function of several parameters and to discuss the problems in making predictions of the time delay.

Ideally, a system designer would like to have an analytic function or set of tabulated values to enable him to correct for this additional time delay on a routine basis, and he would like to know the accuracy of his corrected values. There are several ways to attempt to satisfy this requirement. First, perhaps one can take real time calibrated measurements of the ionospheric time delay at VHF along or near the desired path to correct for ranging errors. This is the most exact range error correction method, though, in practice, such measurements usually cannot be made, owing to equipment design considerations, or the remote areas for which these data are required. Second, lacking real time measurements, and measurements at a specific required location, data from other stations can be used to construct an analytic model of the time delay along a required path. Third, perhaps

the time delay can be related to some other ionospheric parameter that is presently measured and predicted on a world-wide basis. Each of these methods of determining the time delay of a VHF radio wave will be discussed.

2. PROPAGATION DELAY

The additional time delay of a VHF radio wave traveling from a satellite to a ground station is due to the group retardation of the wave in the ionosphere. This additional time delay of the information or modulation of the VHF signal can be expressed as

$$\Delta T = T - T_o = \frac{1}{c}\int \mu_g \, dl - \frac{1}{c}\int dl \ ,$$

where c is the velocity of light, $\int dl$ the ray path, and μ_g the group refractive index of the ionosphere.

At the frequency of interest for a VHF satellite ranging system, say, 120 MHz, the group refractive index may be expressed as

$$\mu_g = \frac{1}{\mu_p} \approx 1 + \frac{X}{2} \ .$$

Therefore,

$$\Delta T = \frac{1}{2c}\int X dl = \frac{40.3}{cf^2}\int N dl$$

or since

$$\Delta r = c\,\Delta T$$

$$\Delta r = \frac{40.3}{f^2}\int N dl$$

It can be seen that the additional time delay is inversely proportional to the square of the frequency and directly proportional to the integrated number of electrons along the radio wave ray path. For a frequency of 120 MHz, a 1-μ sec delay will be pro duced by an integrated number of approximately 10^{17} (actually 1.07×10^{17}) electrons in a unit area column of ionosphere.

3. FARADAY EFFECT

The integrated number of electrons, more commonly called total electron content (TEC) is one of the more often and most easily measured ionospheric parameters.

Measurements have been made of the TEC of the ionosphere since 1956 by using the well-known Faraday effect. The TEC as measured by the Faraday effect is not the "true" number of electrons along the path from, say, a geostationary satellite to a ground station, but only those electrons within the first couple of thousand kilometers above the earth's surface. However, the region below this height contains perhaps 90 percent of the electrons along the path, at least in the daytime. Hence, the Faraday measurements provide a good, but slightly underestimated measure of the total time delay for a VHF signal traveling through the ionosphere.

4. TOTAL ELECTRON CONTENT VERSUS PARAMETERS

The TEC of the ionosphere is dependent upon many parameters; the more obvious include time of day, season, solar activity, magnetic activity, geographic location, and elevation angle. Figure 1 contains a year's TEC data, showing the large day to day and seasonal variability.

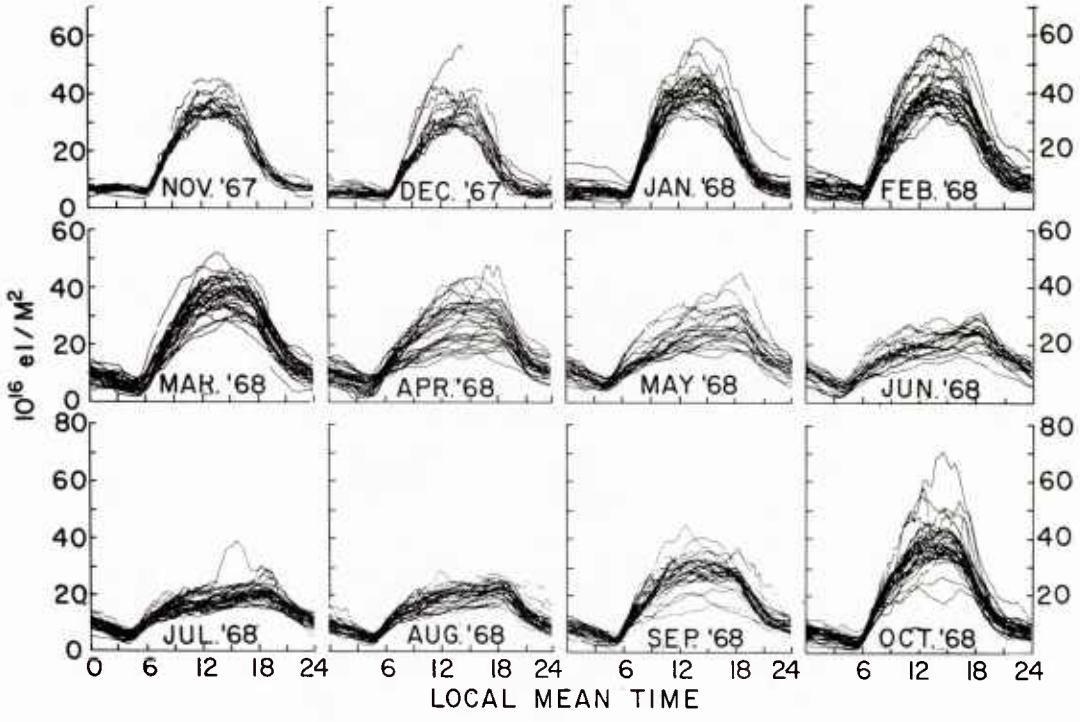

Figure 1. Total Equivalent Vertical Electron Content From Hamilton, Mass. (Looking towards ATS-3)

5. ELEVATION ANGLE

Since satellites are rarely viewed precisely at the zenith, the TEC or time delay must be computed for a slant range path in the direction of the satellite. For elevation angles at the ground above 10° a simple trigonometric secant of the zenith angle of the mean subionospheric point times the vertical TEC will usually suffice to compute the time delay along the slant range path. The mean subionospheric point is that geographic location on the earth's surface above which the ray from the satellite to the earth station intersects a certain mean ionospheric height, usually 350 to 400 kilometers. This mean ionospheric height is then the reference point for latitude and longitude (that is, local time) for the TEC along the slant path. The relationship between satellite elevation angle measured at the ground and the zenith angle at the mean ionospheric height is:

$$\cos(\text{el}) = \frac{r + h}{r} \sin(\text{zen}) ,$$

where r is radius of earth, and h is mean ionospheric height.

As an example, a single ground station viewing two geostationary satellites in different directions simultaneously could easily have a one-hour time difference in the local time at the mean subionospheric points. When determining TEC values for time delay, care must be taken to use the local time and latitude at the subionospheric point rather than the time at the earth station. Figure 2 shows TEC data taken from Hamilton, Massachusetts, using signals from two geostationary satellites. Note the apparent time shift between the two curves due to the approximate one-hour difference in local time at their subionospheric points. When plotted versus local time at their respective subionospheric locations, the agreement between the two curves is much better.

6. TOTAL ELECTRON CONTENT VERSUS LONGITUDE

While the TEC is a function of local mean time, it is also a function of longitude. That is, two stations at the same geographic latitude but at different longitudes have different diurnal changes in TEC. A preliminary examination of data recorded at Sagamore Hill, Hamilton, Massachusetts, and Florence, Italy, both at approximately the same geographic latitudes, shows this difference. While the TEC values differ, the slab thickness agrees quite well at the two locations. Slab thickness is defined as the ratio of TEC divided by density at the peak of the F-region. Further study will be made into this comparison to see if N_{max}, the density at the peak, is a useful parameter in the prediction of TEC time delay.

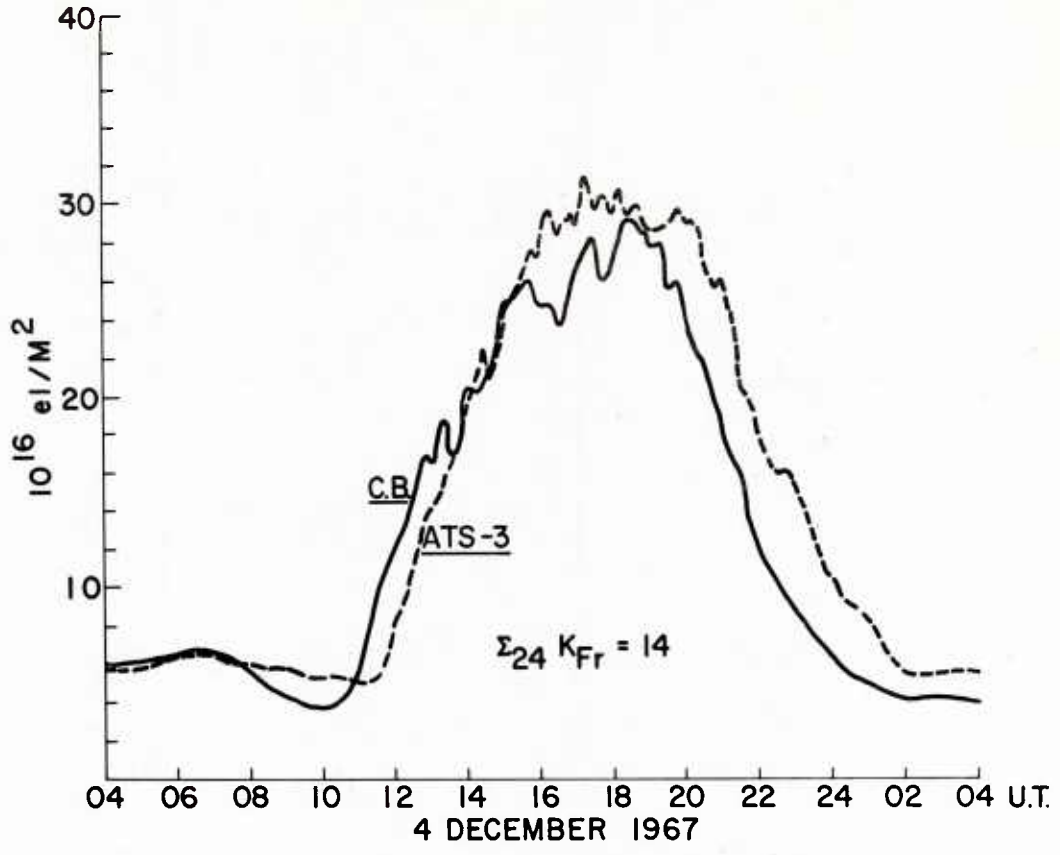

Figure 2. Total Equivalent Vertical Electron Content From Hamilton, Mass. (Looking towards satellites Canary Bird and ATS-3)

7. DAY TO DAY TOTAL ELECTRON CONTENT VARIATIONS

In an attempt to determine more about the longitude behavior of TEC, the data from Hamilton, Massachusetts were compared with data from Aberystwyth, Wales. Hamilton and Wales are at approximately the same geomagnetic latitude though at quite different geographic latitudes. In the course of this comparison, a preliminary look was taken at the variation of TEC from the median values on a day to day basis of comparison between the two sets of data. Only two months, February and May 1968, were completed. TEC data were available on a continuous basis from the two locations both viewing the polarization received from VHF signals radiated from geostationary satellites. Figures 3(a) and (b) show the results of this comparison for the two months. Note that the winter month shown in Figure 3(a) shows a higher correlation of changes in TEC at the two locations than does the summer data.

Note also that the spread in TEC value is considerably greater for the Hamilton data than for the Wales.

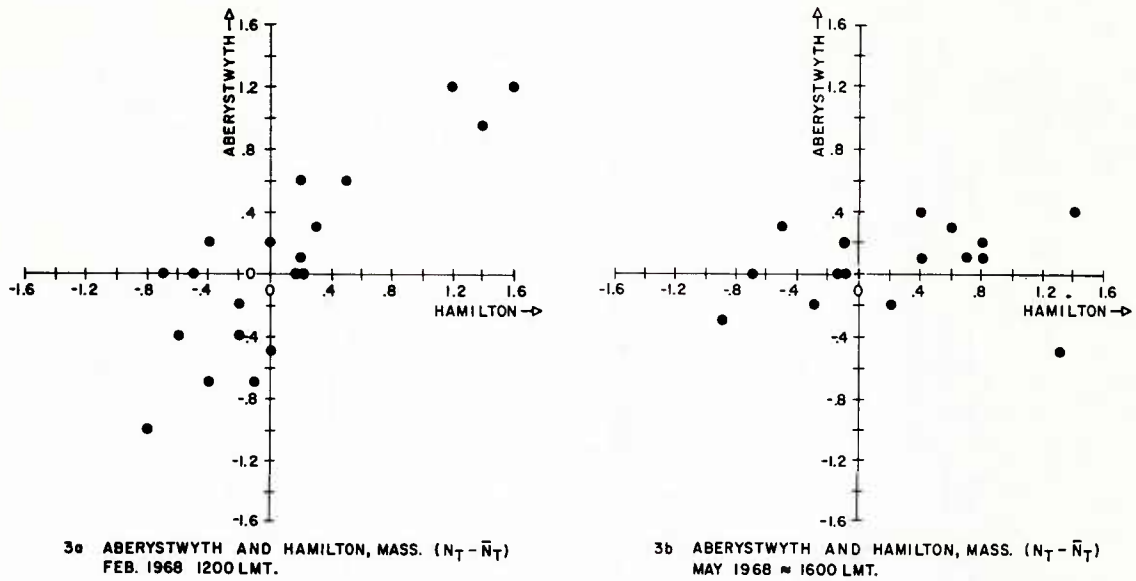

3a ABERYSTWYTH AND HAMILTON, MASS. $(N_T - \bar{N}_T)$ FEB. 1968 1200 LMT.

3b ABERYSTWYTH AND HAMILTON, MASS. $(N_T - \bar{N}_T)$ MAY 1968 ≈ 1600 LMT.

Figure 3. Daily Deviation From the Monthly Mean Electron Content at Hamilton, Mass. and Aberystwyth, Wales

8. ADDITIONAL FACTOR TO BE DISCUSSED

In the final report, additional comparisons of TEC data taken from both sides of the North Atlantic will be shown. Attempts will be made to determine if the existing ESSA predictions of f_0F_2 can be related to time delay measurement with any degree of accuracy. Also an attempt will be made to derive an analytic function that will adequately describe the existing TEC data and that can be used for an error correction function.